Characterization of pathogenesis of and immune response to *Burkholderia pseudomallei* K9243 using both inhalational and intraperitoneal infection models in BALB/c and C57BL/6 mice

J. J. Bearss[1], M. Hunter[2], J. L. Dankmeyer[2], K. A. Fritts[2], C. P. Klimko[2], C. Weaver[2], R. G. Toothman[2], W. M. Webster[2], D. Fetterer [3], J. A. Bozue[2], P. L. Worsham[2], S. L. Welkos[2], K. Amemiya[2], and C. K. Cote[2]*

United States Army Medical Research Institute of Infectious Diseases (USAMRIID),

1425 Porter Street, Fort Detrick, Frederick, MD, 21702

[1]Pathology Division

[2]Bacteriology Division

[3]BioStatisitics Division

*Corresponding Author. Christopher.k.cote.civ@mail.mil 301-619-4936

Running title: Comparison of *B. pseudomallei* in different mice challenged by different routes

Key words: *Burkholderia pseudomallei*, melioidosis, intraperitoneal, mouse, infection, inhalational immune response

Disclaimers: Opinions, interpretations, conclusions, and recommendations are those of the authors and are not necessarily endorsed by the U. S. Army. Research was conducted under an IACUC approved protocol in compliance with the Animal Welfare Act, PHS Policy, and other Federal statutes and regulations relating to animals and experiments involving animals. The facility where this research was conducted is accredited by the Association for Assessment and Accreditation of Laboratory Animal Care, International and adheres to principles stated in the Guide for the Care and Use of Laboratory Animals, National Research Council, 2011.

ABSTRACT

Burkholderia pseudomallei, the etiologic agent of melioidosis, is a gram negative bacterium designated as a Tier 1 threat. This bacterium is known to be endemic in Southeast Asia and Northern Australia and can infect humans and animals by several routes. Inhalational melioidosis has been associated with monsoonal rains in endemic areas and is also a significant concern in the biodefense community. There are currently no effective vaccines for *B. pseudomallei* and antibiotic treatment can be hampered by non-specific symptomology and also the high rate of naturally occurring antibiotic resistant strains. Well-characterized animal models will be essential when selecting novel medical countermeasures for evaluation prior to human clinical trials. Here, we further characterize differences between the responses of BALB/c and C57BL/6 mice when challenged with similarly low doses of a low-passage and well-defined stock of *B. pseudomallei* K96243 via either intraperitoneal or aerosol routes of exposure. Before challenge, mice were each implanted with a transponder to collect body temperature readings, and daily body weights were also recorded. Mice were euthanized on select days for pathological analyses and determination of the bacterial burden in selected tissues (blood, lungs, liver, and spleen). Additionally, spleen homogenate and sera samples were analyzed to better characterize the host immune response after infection with aerosolized bacteria. These clinical, pathological, and immunological data highlighted and confirmed important similarities and differences between these murine models and exposure routes.

INTRODUCTION

Burkholderia pseudomallei is the causative agent of melioidosis [1]. It is a gram negative bacillus that is commonly found in soil and water in Northern Australia and Thailand and is a known cause of sepsis [2-7]. There is significant recent evidence to support the concept that *B. pseudomallei* may be distributed in tropical locations located throughout the world [8-18]. Melioidosis is commonly initiated from the introduction of the bacterium into a subcutaneous injury. The Center for Disease Control and Prevention has categorized this bacterium as a Tier One biological select agent. An infection of *B. pseudomallei* can cause either acute sepsis or a chronic infection [9, 19-22]. Acute sepsis generally manifests within 1 to 21 days, while a chronic infections with *B. pseudomallei* is characterized by symptoms that last substantially longer (i.e. greater than two months). There are currently no effective vaccines for melioidosis [23], and treatment can be hampered by non-specific symptomology, high frequencies of naturally occurring antibiotic resistance, and the propensity of the bacterium to cause a chronic infection that reemerges years (to decades) later [24, 25]. Several factors, including occupational exposure (i.e. rice farmer in Thailand) alcoholism, or diabetic mellitus have been shown to be important risk factors for presenting with melioidosis [2, 26, 27]. Of specific concern to the biodefense research community is the fact that *B. pseudomallei* is known to be transmitted to humans via inhalation, most often associated with strong rains and winds in geographic areas where the bacterium is endemic [7, 28, 29].

There has been significant effort invested in developing appropriate animal models of melioidosis (i.e. mice, rats, hamsters, goats, and non-human primates) [30-34]. Small animal models, specifically the BALB/c and C57BL/6 mouse models, have been used to mimic both the

acute and chronic stages of *B. pseudomallei* infection [27, 30, 35-43]. The BALB/c mouse model results in an acute infection after either intraperitoneal injection or aerosol exposure [30, 40, 41, 44]; while C57BL/6 mice are considerably more resistant to infection and hypothesized to be a suitable model for chronic infection in both intraperitoneal injection and aerosol exposure [30, 41, 44, 45]. The BALB/c mouse model is a useful tool in identifying the mechanisms of virulence of *B. pseudomallei*, as well as for preliminary screening for vaccine or therapeutic efficacy [30, 35, 39, 46-50]. The disease model is of course dependent upon the different routes of infection used in these studies (i.e. intraperitoneal or intranasal/inhalation) and may be dependent upon the *B. pseudomallei* strain used for challenges [46, 50, 51]. These routes of exposure within the BALB/c mice result in an acutely disseminated infection that mimics some of the features of human melioidosis. The mice develop numerous abscesses and/or pyogranulomatous masses in various organs or locations throughout the body (i.e. spleen, liver, lungs) [46]. Depending upon the dose administered, BALB/c mice can succumb to infection within 2 to 3 days. The C57BL/6 mice generally clear the bacteria (unless large doses are delivered) to below the limits of detection in both the spleen and liver within days to weeks of being inoculated with the bacterium [37, 38]. It has been reported that C57BL/6 mice may remain asymptomatic for months before spontaneous reactivation of the disease occurs [37]. The spontaneous reactivation appears in the form of localized lesions (i.e. lesions on the ear, tail, liver and spleen). The long term latency of the infection in C57BL/6 mice potentially mimics that of the chronic human illness, although these mice may still succumb to disease within a few months of infection.

The formation of multinucleated giant cells (MNGCs) by infected cells has been well documented using in vitro assays with macrophage-like cell culture lines infected with

Burkholderia species [46, 52-56], primary mouse macrophages [57], and nonphagocytic cell lines [55, 56] MNGCs, referred to as a "hallmark" of *B. pseudomallei* infection [58], have been reported in other studies of chronic melioidosis in mice [37, 58], Madagascar hissing cockroaches [59], and in human autopsies [60]. Surprisingly, there are very few descriptions of MNGCs in mice infected with *B. pseudomallei* [37, 58]. Mouse models will be essential for preliminary prescreening and subsequent down selection of novel medical countermeasures (i.e. therapeutics, vaccines, or combination regimens), accordingly; better characterization of the extent and significance of this phenomenon in mice is warranted.

This report adds to the growing body of literature characterizing the murine experimental models of melioidosis. We show data collected from a head to head comparison between BALB/c and C57BL/6 mice challenged with either an intraperitoneal injection or by exposure to aerosolized bacteria using the well-documented *B. pseudomallei* strain K96243. In both cases, the challenge doses were purposefully low to more fully characterize the disease progression and to look for signs of chronic infection. Weight and temperatures were recorded daily, bacterial burdens were determined, and immunological and histological analyses are reported, to depict a more complete disease model.

MATERIALS AND METHODS

Animal challenges. Groups of BALB/c mice (Charles River-Frederick, MD; female 7-10 weeks of age at time of exposure to bacteria) were challenged by the intraperitoneal (IP) or inhalational route with *B. pseudomallei* K96243 grown in 4% glycerol (Sigma Aldrich, St. Louis, MO)-1% tryptone (Difco, Becton Dickinson, Sparks, MD) and 5% NaCl (Sigma Aldrich, St. Louis, MO) broth (GTB). The bacteria used for challenge were harvested from a late log phase culture

grown in GTB medium at 37°C with shaking at 200 rpm. The bacteria were resuspended in GTB and quantified via OD_{620} estimations. The actual delivered doses of bacteria were then verified by plate counts on blood agar (Trypticase soy agar with sheep blood) plates (Remel™, ThermoFisher Scientific, Waltham, MA). Each IP dose was delivered in 200 µl of GTB medium. The IP challenge groups doses were as follows: BALB/c mice received approximately $3.0x10^4$ colony forming units (CFU) (approximately 0.49 LD_{50} equivalent) and C57BL/6 mice received approximately $9.2x10^5$ CFU (approximately 0.42 LD_{50} equivalents) [45, 46]. Exposure to aerosolized bacteria was accomplished as previously described [61]. Briefly, mice were transferred to wire mesh cages (up to 10 mice per cage) and up to four wire mesh cages were placed in a whole-body aerosol chamber within a class three biological safety cabinet located inside a BSL-3 laboratory. Mice were exposed to aerosolized *B. pseudomallei* strain K96243 created by a three-jet collision nebulizer. Samples were collected from the all-glass impinger (AGI) and analyzed by performing CFU calculations to determine the inhaled dose of *B. pseudomallei*. The inhalational challenge doses were as follows: BALB/c mice received approximately 5 CFU (approximately 0.2 LD_{50} equivalents) and C57BL/6 mice received approximately 18 CFU (approximately 0.05 LD_{50} equivalents) (Waag and Soffler, personal communication).

Prior to challenge BALB/c and C57BL/6 female mice were implanted with Electronic ID Transponder –IPTT 300 (Bio Medic Data Systems-BMDS, Seaford Delaware). Mice were scanned for daily temperatures via Smart Probe SP-6005 (BMDS, Seaford, Delaware) and daily weights were determined on Adventurer Pro Balance (Ohaus, Pasippany, NJ). These data were recorded by host DAS-8001 Data Acquisition System (BMDS, Seaford, Delaware) and stored in Excel format. Mice were monitored for clinical signs and symptoms for 60 days for the IP

challenge group and 91 days for the inhalational challenge group. Early endpoint euthanasia was employed by CO_2 exposure in a uniform manner to limit pain and distress of the mice. For dissemination studies, mice were euthanized by exsanguination under deep anesthesia on days 0 (approximately 4-6 hours post exposure to *B. pseudomallei*), 2, 4, 7, 15, 22, and 59 post-infection and lungs, spleen, and liver samples were collected. Tissues were harvested, weighed, homogenized, and then CFU were enumerated on SBA plates. The limit of detection for spleen, liver, and lungs was approximately 10 CFU/ml. Due to blood volume constrains, the limit of detection for blood was approximately 100 CFU/ml. Confirmatory bacterial identification was also performed using *Burkholderia cepacia* selective agar plates (Remel™, ThermoFisher Scientific, Waltham, MA). The surviving C57BL/6 mice in the inhalational challenge group were retained through day 91 in an attempt to identify any signs of chronicity (i.e. clinical signs such as weight loss, temperature increase, altered appearance, or bacterial burden in tissues after euthanasia).

Research was conducted under an Institutional Animal Care and Use Committee (IACUC) approved protocol in compliance with the Animal Welfare Act, Public Health Service (PHS) Policy, and other federal statutes and regulations relating to animals and experiments involving animals. The facility where this research was conducted is accredited by the Association for Assessment and Accreditation of Laboratory Animal Care, International and adheres to principles stated in the 8th Edition of the Guide for the Care and Use of Laboratory Animals, National Research Council, 2011.

Histological pathology. Post-mortem tissues were collected from euthanized mice and fixed in 10% neutral buffered formalin for $\geq$ 21 days. Samples were embedded in paraffin and sectioned

for hematoxylin and eosin (HE) staining, as previously described [40, 62]. Immunohistochemistry was performed on selected samples as previously described (REF). We define a multi-nucleated giant cell (MNGC) as a large (>20μm diameter), round to irregular cell with abundant clear to eosinophilic cytoplasm and having two or more eccentric reniform nuclei. N = 3 mice for most time points.

Spleen cell preparation. Splenocytes were prepared essentially as previously described [63]. Briefly, spleens were excised from mice (N = 5 mice for most time points), weighed, and disaggregated in RPMI 1640 medium (Life Technology, Grand Island, NY) containing 25 mM HEPES, 2 mM glutamine (wash medium) to make the spleen extract. Aliquots of the spleen homogenate were saved for cytokine/chemokine determination and stored at -70° C. Samples were irradiated and confirmed sterile before use. CFU in non-irradiated aliquots of the homogenate were determined on sheep blood agar plates (BD Diagnostics, Franklin Lake, NJ) with undiluted extract or 10-fold dilutions in sterile phosphate-buffered saline (PBS). Plates were incubated at 37° C for two days before counting CFU. Red cells in the spleen homogenate were lysed with ACK (Ammonium-Chloride-Potassium) Lysing Buffer (BioWhittaker, Walkersville, MD) after the extract was diluted with wash medium and cells pelleted by centrifugation at 1200 rpm for 10 min. Splenocytes were then washed once and suspended in complete medium [wash medium containing 10% heat-inactivated fetal calf serum (Life Technology), 1 mM sodium pyruvate, 0.1 mM non-essential amino acids, 100 U/ml of penicillin, 100 μg/ml streptomycin, and 50 μM 2-mercaptoethanol and cells counted.

Cytokine/chemokine expression. Cytokines and chemokines in mouse sera and spleen homogenates (N = 5 for most time points) were measured by Luminex Mag Pix (Life Technology, Grand Island, NY) as per manufacturer directions. Spleen homogenates and sera from uninfected mice were used as normal, uninfected controls (N = 10 BALB/c; N = 4 C57BL/6). The levels (pg/ml) of the following 20 cytokines/chemokines were measured: FGFb, GM-CSF, IFN-γ, IL-1α, IL-1β, IL-2, IL-4, IL-5, IL-6, IL-10, IL-12 (p40/p70), IL-13, IL-17, IP-10, KC, MCP-1, MIG, MIP-1α, TNF-α, and VEGF. We did not report all the cytokines/chemokines because some did not show any change during the study.

Splenocyte composition. Approximately $1x10^7$ splenocytes from each mouse were washed in FACS staining buffer (FSB) (1XPBS, 3% fetal calf serum, Life Technologies), and fixed in FSB containing 4% formaldehyde (Pierce, Rockford, IL) at 4° C. The cells were washed in FSB and then distributed into a microtiter plate ($5x10^5$ cells/well), and nonspecific binding was inhibited by the addition of Fc Block (BD Biosciences, San Jose, CA). Cells were labeled with the following specific antibodies (BD Biosciences): CD4 T cells, CD4-PE/CD44-FITC; CD8 T cells, CD8-PE/CD44-FITC; B cells, B220-PE/CD86-FITC; monocytes/macrophages, CD11b-PE/CD44-FITC; NK cells, CD49b-PE/CD44-FITC; and granulocytes, Ly6G-PE/CD44-FITC. Corresponding isotype controls were used and all were incubated for 60 min on ice. All samples were fixed in FSB with 4% formaldehyde and stored at 4° C until analysis. Cells were identified with a BD FACSCalibur using CellQuestPro software (BD Biosciences). Splenocytes from uninfected BALB/c mice were prepared as described above and used as normal, uninfected controls.

Ethics statement- Animal research at the United States Army Medical Research Institute of Infectious Diseases (USAMRIID) was conducted under an animal use protocol approved by the USAMRIID Institutional Animal Care and Use Committee (IACUC) in compliance with the Animal Welfare Act, PHS Policy, and other Federal statutes and regulations relating to animals and experiments involving animals. The facility where this research was conducted is accredited by the Association for Assessment and Accreditation of Laboratory Animal Care International (AAALAC) and adheres to principles stated in the Guide for the Care and Use of Laboratory Animals (National Research Council, 2011). Challenged mice were observed at least daily for up to 90 days for clinical signs of illness. Early interventions endpoints were used during all studies, and mice were humanely euthanized when moribund, according to an endpoint score sheet. Animals were scored on a scale of 0–11: 0–2 = no significant clinical signs (e.g., slightly ruffled fur); 3–7 = significant clinical symptoms such as subdued behavior, hunched appearance, absence of grooming, hind limb issues of varying severity and/or pyogranulomatous swelling of varying severity (increased monitoring was warranted); 8–11 = distress. Those animals receiving a score of 8–11 were humanely euthanized. However, even with multiple observations per day, some animals died as a direct result of the infection.

Statistical analyses. Individual daily temperatures and weights were analyzed. The 5 day lagged, moving average was computed for each individual daily temperature and weight profile by taking the average of each daily measure and the measures obtained on the 4 preceding days. The definition is extended to study days preceding the fifth by including all days available. For example the day 2 lagged average includes days 0, 1 and 2. Our motivation in using these running averages is to reduce the impact of fluctuations apparent in the individual weight and

temperature profiles. The resulting lagged averages were entered into the linear mixed effect repeated measures model for analysis. Our model utilized a moving average correlation structure to accommodate the inherent correlation among the lagged averages, successive averages being computed from sets of observations which are not mutually exclusive. The analysis is implemented in SAS® Proc Mixed. *P*-values are not adjusted for multiple comparisons.

We also considered the correlation coefficient between the body temperature observed on a particular day, and the change in temperature between that day and the day following, a quantity hereafter referred to as the lag 1 autocorrelation. We estimated this correlation coefficient separately for each mouse, with comparison between groups of mice were made by standard ANOVA procedures for means. Analysis of this correlation was restricted to the first 15 days of study, before significant animal mortality was observed. Bacterial burdens are depicted as CFU per gram of tissue. The geometric means of the calculated values are included as horizontal bars. Spleen weights were analyzed by T-test and geometric means are depicted.

RESULTS

The impact of intraperitoneal bacterial challenge on body temperature and weight of mice.

Individual temperatures and body weights were recorded daily following IP challenge with *B. pseudomallei* K96243.. Regarding temperature, the BALB/c mice had a greater body temperature compared to C57BL/6 mice starting at day 10 and continuing through day 20, but differences were not statistically significant thereafter (Figure 1A). Notably, BALB/c mice showed a 0.3^{o} C increase in body temperature when compared to the C57BL/6 mice at these early time points, an observation which closely mirrors that obtained in mice exposed to aerosolized bacteria (discussed later). The time by strain interaction was statistically significant

(P<0.01), confirming that an overall difference in the temperature profiles between the two strains existed. The BALB/c and C57BL/6 strains were roughly equivalent in lag1 autocorrelation (ρ =-0.71 vs -0.68; P = 0.51), suggesting that the two mouse strains had a similar tendency to return to a normal body temperature following challenge.

The mouse weights for BALB/c and C57BL/6 mice were statistically distinguishable starting at day 5 and at every time point thereafter (Figure 2B). At day 0 the mouse strains differed by 0.5 grams, an amount which was not statistically significant (P = 0.71). The C57BL/6 mice exhibited a greater average weight gain relative to the BALB/c mice, leading to a statistically significant time by strain interaction (P <0.01).

Bacterial burden observed in mice receiving an intraperitoneal injection of bacteria

Figure 2 illustrates the recovered CFU/gram of organ or CFU/ml of blood following IP challenge. Similar median lethal dose equivalents were administered to either the BALB/c (approximately $3.0x10^4$ CFO or 0.49 LD_{50} equivalents) or C57BL/6 mice (approximately $9.2x10^5$ CFU or 0.42 LD_{50} equivalents); to account for the inherent differences in susceptibility to infection that have been well documented (REF). The dissemination patterns observed in either BALB/c or C57BL/6 mice were similar when approximately equal lethal equivalents were delivered by an intraperitoneal injection (Figure 2). Of interest is the rapid hematogenous spread of bacteria throughout the animal. Bacteria were identified in all organs and blood in most mice on day 0 (within approximately 4-6 hours post injection). As demonstrated in previous reports, spleen weight can be indicative of aspects of both bacterial replication and host immune response. Thus we compared the weights of the spleens obtained in BALB/c mice and C57BL/6 mice. As shown in Figure S1, in the IP challenge experiment, spleen weights and associated

weight increases were statistically indistinguishable, with the exception being day 4 post-infection. Throughout the course of the study, some of the mice were euthanized in accordance with early endpoint criteria or succumbed to infection (19 of 80 BALB/c mice and 13 of 80 C57BL/6 mice).

Histopathology observed in mice receiving an intraperitoneal injection of bacteria.

Consistent with previous studies involving intraperitoneal infection of *B. pseudomallei* in mice [46], the most striking lesions attributed to *B. pseudomallei* infection in 9/36 C57BL/6 and 17/36 BALB/c mice were focally extensive areas of pyogranulomatous inflammation in the rear legs, tail, and spine (Figure 3A). It is unclear why there is an apparent predisposition for the caudal half of the body (rear legs, tail, and caudal vertebral column); however, it may be related to the route of lymphatic drainage from the IP challenge site. Human case reports have documented *B. pseudomallei* infection in muscle, bones, and joints [64, 65]. These lesions were first observed at within a week of each other post exposure in both mouse strains, beginning in BALB/c mice at day 15 and in C57BL/6 mice at day 22. However, lesions in BALB/c mice were seen with more frequency and were more severe. Lesions were composed of large aggregates of viable and degenerate neutrophils and necrotic debris surrounded by low numbers of epithelioid macrophages. The areas of pyogranulomatous inflammation (Figure 3B) were widespread and indiscriminant about the tissue types affected, including skeletal muscle, peripheral nerves, bone, cartilage, adipose tissue, and fibrous connective tissue. This situation made determination of the temporal pathogenesis of these lesions difficult, however, it is likely that these lesions represent persistent niduses of inflammation incited by hematogenous or lymphatic bacterial spread earlier in the course of disease. Other less common but significant sites of pyogranulomatous or

suppurative inflammation included the cerebrum, cerebellum, brainstem, liver, and spleen. Lesions in these tissues illustrate the widely dispersed sites of imflammation resulting from hematogenous spread of *Burkholderia* following intraperitoneal challenge.

Inflammation in the liver, which was the earliest detectable lesion in both mouse strains, began acutely as neutrophilic infiltration of hepatic sinusoids and areas of individual hepatocyte necrosis (Figure 4A) and was present in 6/6 C57BL/6 mice and 5/6 BALB/c mice between days 0 and 4. This progressed chronically to mixed neutrophilic and histiocytic infiltration, and in a few mice, to frank suppurative or pyogranulomatous hepatitis in 18/30 C57BL/6 and 13/30 BALB/c mice from day 7 until day 60. Immunohistochemistry demonstrated large amounts of *B. pseudomallei* capsular antigen in these lesions.

Neutrophilic inflammation was only seen acutely in the spleen of 1/6 BALB/c mice and was not seen acutely in C57BL/6 mice, although the identification of these lesions was often obfuscated by the striking extramedullary hematopoiesis (EMH) seen in these mice. The development of pyogranulomas and abscesses within the spleen (Figure 4C) was only seen in 4/36 BALB/c mice but was not seen in any of the C57BL/6 mice. While EMH in the splenic red pulp and sinusoids of the liver are very commonly seen in normal mice in response to a variety of antigens [66], the degree of EMH in these mice was significantly greater than what is typically encountered and affected 28/36 C57BL/6 and 19/36 BALB/c mice between days 4 and 60. This is consistent with a physiologic response to increased tissue demand for leukocytes secondary to bacterial infections that elicit intense inflammatory reactions. Given the large areas of pyogranulomatous inflammation seen in these mice, this exuberant EMH is most likely related to infection with *B. pseudomallei.* For the same reason, many of these mice had significant myeloid hyperplasia in the bone marrow (Figure 4B), predominantly of the neutrophil lineage. In

some cases, the myeloid hyperplasia was so intense that it extended outside of the marrow cavity of the bones and into adjacent tissues. In the case of the vertebral column, this excessive hyperplasia occasionally resulted in compression and/or disruption of the spinal cord and peripheral nerve ganglia. This may partially explain why some mice, despite a lack of significant pyogranulomatous inflammation in the spine or rear limbs, still exhibited neurologic clinical signs (i.e. paralysis, ataxia). Interstitial neutrophilic inflammation was seen in the lung of 13/36 C57BL/6 and 17/36 BALB/c mice. The pathogenesis of this inflammation in the lung is not clear. There is little histologic evidence that the lung is a primary site of *Burkholderia* infection in these mice by IP challenge, as only 3/36 BALB/c and none of the C57BL/6 mice developed suppurative or pyogranulomatous pneumonia at any time during the study. The increased neutrophils could be confined to the capillaries in the interstitium and represent the relative increase in numbers of circulating neutrophils in the blood as a response to inflammation elsewhere in the body. Other common sites of neutrophilic inflammation were the nasal sinuses and the middle ear, however, because of the timing (as early as day 0 post infection) and sporadic nature of the inflammation seen in the nasal sinuses and middle ears, these could be background lesions and may be unrelated to the challenge agent.

Immunological response observed in mice receiving *B. pseudomallei* K96243 by intraperitoneal (IP) injection

We wanted to further examine the cellular immune response in spleens of the infected mice after IP infection. We used the same spleens that were used in the previous analyses (CFU burdens and weight) to examine the changes in the cellular composition of the spleens after infection over time, and concurrent cytokine/chemokine expression in serum and spleen extracts from the same mice. The histopathology description above of tissue/organs noted the large

316 increase in neutrophils after IP infection in BALB/c mice. We used flow-cytometry to better
317 identify and quantitate the type of cellular infiltrate into the infected spleens after IP infection
318 (Table S1, and Figure 5). We compared the cellular composition of the infected *B. pseudomallei*
319 K96243 mouse spleens to the cellular composition of spleens from normal, naïve mice (Table
320 S1, Figure 5A.). Immediately post-infection (PI) at 0 day (~4-6 h PI), there was a slight increase
321 in monocytes/macrophages (CD11b+/CD44), and NK cells (CD49b+/CD44) ~2-fold-2.8-fold,
322 ($P<0.05$), respectively] followed by granulocytes (Ly6G+/CD44) (4.83-fold, $P\leq0.001$). There
323 was an initial decrease (2 Days PI) in all three cell types before we detected a slight but
324 significant increase (2.94-fold, $P\leq0.001$; 4.74-fold, $P\leq0.001$; and 4.51-fold, $P<0.05$,
325 respectively) at day 4 PI. Between 7 to 15 days PI, we saw a significant increase in the
326 inflammatory granulocytes (35.8-fold, $P\leq0.001$), monocytes/macrophages (8.33-fold, $P\leq0.001$),
327 and NK cells (7.61-fold, $P<0.01$) in spleens of BALB/c mice where the numbers essentially
328 leveled off until day 22 PI. After this period, the amount of the three inflammatory cells dropped
329 close to levels seen at day 0 in the spleens from BALB/c mice that were left in the IP study after
330 28 days PI. After this period, there was a slow but significant increase in the percentage of
331 granulocytes ($P<0.01$), monocytes/macrophages ($P\leq0.001$), and NK cells ($P\leq0.001$) until the end
332 of the study at day 59. During the same period of the study, the three other cell types that we
333 examined, CD4+ and CD8+ T cells, and B cells, we detected only a slight but modest overall
334 increase in CD8+ T cells at days 7 and 59 (1.53-fold, $P\leq0.001$; and 1.25-fold, $P<0.05$),
335 respectively)(Table S1, Figure 5A).

336 In C57BL/6 mice, we detected a slightly different pattern in the increase in the
337 inflammatory granulocytes, monocytes/macrophages, and NK cells in the early part of the
338 infection (Table S1, and Figure 5B). Four days PI, we detected a slight increase in the

inflammatory cells (17.5-fold, $P<0.05$; 5.78-fold, $P<0.05$; and 7.62-fold, $P\leq0.001$, respectively) before they decreased at day 7 PI. Then at day 15 PI, we saw an increase in the amount of granulocytes (29.7-fold, $P\leq0.001$) present in the infected spleens, with a further increase detected at day 22 PI (38.8-fold, $P<0.01$). These mice did not exhibit a leveling off of the amount of granulocytes as we saw in spleens from BALB/c mice in this same period. We detected a lower but significant increase in monocytes/macrophages from 8.23-fold ($P\leq0.001$) to 10.4-fold ($P\leq0.001$) at days 15 and 22 PI, respectively. For the same two days PI, we saw a significant increase in NK cells of 8.21-fold ($P\leq0.001$) and 5.71-fold ($P\leq0.001$), respectively. Similar to what we saw in BALB/c spleens at day 28 PI, we detected lower amounts of granulocytes, monocytes/macrophages, and NK cells (2.62-fold, 2.0-fold, and 3.22-fold, respectively) compared to that found in the normal, naïve C57BL/6 spleens in surviving mice. We then detected a significant increase in granulocytes (12.4-fold, $P\leq0.001$), monocytes/macrophages (16.9-fold, $P\leq0.001$), and NK cells (6.11-fold, $P\leq0.001$) after 59 days PI. Although we saw some small but significant changes in the number of CD4+ and CD8+ T cells and B cells over the same period of the study (Table S1 and Figure 5B), they were not as large as seen in the inflammatory cells. Overall, the pattern of increase in the inflammatory cells (primarily granulocytes, followed by monocytes/macrophages and NK cells) in spleens from infected BALB/c mice was similar to that seen in infected spleens from C57BL/6 mice, except for the early influx in these cells at 4 days PI that we observed in infected spleens from C57BL/6 mice (Figure 5B), and the leveling off of the peak number of granulocytes between day 15 and 22 PI in spleens from infected BALB/c mice. In addition, there was a similar substantial decrease in

the three inflammatory cells in spleens from both species of mice between 22 to 28 days PI before we saw a slow increase of these same cells to the end of the study at 59 days PI.

We also examined the change in cytokine/chemokine levels in sera and spleen extracts in both types of mice after IP infection. The amount of 15 out of 20 cytokines/chemokines (reported as geometric means with geometric standard error of the means) that we detected in sera from infected BALB/c mice is shown in Table S2. Not all showed significant changes after exposure to bacteria when compared to naïve, uninfected mice. We saw immediate [0 day (4-6 h)] changes PI in IL-1α [196.2 (1.16) pg/ml, $P \leq 0.001$], IL-5 [36.7 (1.21) pg/ml, $P < 0.05$], and KC [2668 (1.15) pg/ml, $P \leq 0.001$]. After 2 days PI, we detected a significant increase in sera of IFN-γ[168.3 (1.11) pg/ml, $P \leq 0.001$], IL-1β [113.9 (1.12) pg/ml, $P \leq 0.001$], FGFb [288 (1.05) pg/ml, $P < 0.05$], IP10 [93.3 (1.16) pg/ml, $P \leq 0.001$], MCP-1 [37.2 (1.16) pg/ml, $P < 0.05$], and MIG [4009 (1.11) pg/ml, $P \leq 0.001$]. These increases can be seen more clearly in Figure S4A, which shows the fold-changes in the cytokines/chemokines in serum. After 4 days PI, we saw little change in the levels of the cytokines/chemokines in sera until day 59 PI when we saw small increases in TNFα (2.39-fold, $P < 0.05$), IL-1β (3.76-fold, $P < 0.05$), IL-2 (2.81-fold, $P \leq 0.001$), and IL-10 (2.88-fold, $P \leq 0.001$).

In sera of C57BL/6 mice (Table S2) we saw immediate (0 day) increases over naïve controls of IL-1α [235.3(1.15) pg/ml, $P \leq 0.001$], IL-5 [96.5 (1.19) pg/ml, $P < 0.01$], KC [3848 (1.08) pg/ml, $P \leq 0.001$], MCP-1 [247.5 (1.29) pg/ml, $P \leq 0.001$], and MIG [439.7 (1.33) pg/ml, $P \leq 0.001$] (Table S2). After day 2 PI we detected significant increases in IFN-γ [97.6 (1.11) pg/ml, $P < 0.01$], IL-1α [85.3 (1.33) pg/ml, $P < 0.05$], IL-5 [37.2 (1.20) pg/ml, $P < 0.05$], FGFb [516.9 (1.05) pg/ml, $P < 0.05$], IP-10 [78.0 (1.43) pg/ml, $P < 0.05$], KC [424.4 (1.68) pg/ml,

382 $P<0.05$], MCP-1 [118.0 (1.54) pg/ml, $P<0.05$], and MIG [2107 (1.13) pg/ml, $P\leq0.001$]. At 4
383 days PI we saw only increases in FGFb [464.2 (1.14) pg/ml, $P<0.05$] and MIG [491.8 (1.27)
384 pg/ml, $P\leq0.001$]. The early fold-changes in sera from C57BL/6 mice can be seen in Figure S4B
385 when compared to those in sera from BALB/c mice, except for the fold-changes in the level of
386 MIG because the early responses by this chemokine (0, 2, or 4 days PI) were so high compared
387 to all the other cytokines/chemokines in serum from C57BL/6 mice (see Table S2). For MIG at
388 0, 2, and 4 days PI, there were increases of 54.3-fold ($P\leq0.001$), 231-fold ($P\leq0.001$), and 54.0-
389 fold ($P\leq0.001$), respectively. For the chemokine KC at 0 days PI we saw there was an
390 immediate 52.7-fold increase ($P\leq0.001$), which was high compared to the other
391 cytokines/chemokines except for MIG (Figure 2B). Between days 7 to 28 PI levels of IFN-γ
392 ($P<0.05$), IL-1α ($P<0.01$), and MIG ($P\leq0.001$) were significantly elevated compared to most of
393 the other cytokines/chemokines. Finally, by day 59 PI, we detected significant levels of TNF-α
394 [44.8 (1.11) pg/ml ($P<0.01$)], IL-2 [19.0 (1.03) pg/ml, $P\leq0.001$)], IL-10 [147.9 (1.07) pg/ml,
395 $P\leq0.001$)], KC [225.4 (1.38) pg/ml, $P<0.05$)], and MIG [77.3 (1.15) pg/ml, $P\leq0.001$)].
396 Generally, at the early time points, we saw a few more elevated cytokines/chemokines in the sera
397 of BALB/c mice PI than in sera of C57BL/6, but there were slightly higher levels of
398 inflammatory cytokines/chemokines after the initial peak seen PI in sera from C58BL/6 mice.
399 We also examined the amount of cytokines/chemokines in spleen extracts PI from the
400 same set of mice that we analyzed above (Table S3, Figure 6). In spleen extracts from BALB/c
401 mice at 0 day PI, we detected a significant increase in levels of a majority of the
402 cytokines/chemokines we measured: IL-1α [356.8 (1.09) pg/ml, $P\leq0.001$], IL-1β [256.8 (1.09)
403 pg/ml, $P\leq0.001$], IL-12 [63.8 (1.03) pg/ml, $P\leq0.001$], FGFb [2908 (1.13) pg/ml, $P\leq0.001$], IP-10

[103.8 (1.08) pg/ml, $P \leq 0.001$], KC [1237 (1.21) pg/ml, $P < 0.01$]MCP-1 [41.2 (1.15) pg/ml, $P < 0.01$], MIG [1122 (1.10) pg/ml, $P \leq 0.001$], MIP-1α [108.9 (1.06) pg/ml, $P \leq 0.001$], and VEGF [58.8 (1.06) pg/ml, $P \leq 0.001$]. At day 2 PI we detected a significant increase in the same cytokines/chemokines as 0 day PI with the addition of IFN-γ [171.4 (1.16) pg/ml, $P \leq 0.001$], TNF-α [33.2 (1.06) pg/ml, $P < 0.001$], IL-5 [42.3 (1.14) pg/ml, $P < 0.05$], IL-6 [48.1 (1.08) pg/ml, $P \leq 0.001$], and IL-10 [35.2 (1.07) pg/ml, $P \leq 0.001$]. At days 4 and 7 PI, we saw fewer increases in the cytokines/chemokines levels, but at day 15 PI, we saw the greatest increase in the amount and number of cytokines/chemokines expressed (Table S3, Figure6A). The peak of activity began decreasing after day 15 and further decreased by day 22 PI before we detected a slight but significant increase in the amount and number of cytokines/chemokines expressed in spleen extracts on day 59 PI from BALB/c mice.

When we examined the amount of cytokines/chemokines present in spleen extracts from C57BL/6 mice we saw at least three differences over the course of the study compared to that in BALB/c spleen extracts (Table S3, Figure 6B). First, in most cases there was an greater immediate increase in amounts of the cytokines/chemokines that we examined (compared to that found in spleen extracts from naïve mice) in spleen extracts from C57BL/6 that we detected on day 0 PI, that were higher than found in spleen extracts from BALB/c mice at day 0 PI. Most notable were IP-10 [1221 (1.25) pg/ml, $P \leq 0.001$], IL-1β[672.7 (1.10) pg/ml, $P \leq 0.001$], IL-1α [1237 (1.25) pg/ml. $P \leq 0.001$], MIG [3653 (1.21) pg/ml, $P \leq 0.001$], KC [3320 (1.12) pg/ml, $P \leq 0.001$], MIP-1α [382.4 (1.25) pg/ml, $P \leq 0.001$], and IFN-γ [100.3 (1.35) pg/ml, $P < 0.01$]. Second, we did not see a peak in the change in the level of the cytokines/chemokines that we just mentioned on day 2 PI, as we saw in spleen extracts from BALB/c mice, but there was a modest

peak at day 7 PI (see Figure 6B). The third difference was that the peak change in IL-1β [846.5 (1.67) pg/ml, $P<0.01$] levels, which is an inflammatory cytokine, occurred at day 22 PI in spleen extracts from C57BL/6 infected mice, rather than at day 15 PI in spleen extracts from infected BALB/c mice. However, there was a distinct decrease in the change in the levels of cytokines/chemokines at day 28 PI seen in spleen extracts from both strains of mice. We also detected a similar increase in many of the cytokines/chemokines on day 59 PI in spleen extracts from both mice (Table S3). Hence, we saw an increase in the inflammatory cytokines IL-1α and IL-1β and also MIG was increased in the early part of the infection in extracts from both strains of mice. As we saw in the change in the influx of inflammatory cells in the spleen (Figure 5), there appeared to be a distinct change in cytokines/chemokines levels between 22 and 28 days PI in spleen extracts that may suggest that there was a transition from an early or acute phase of infection to a late or chronic phase of infection (Figure 6AB).

Mice Exposed to Aerosolized *Burkholderia pseudomallei* K96243

The impacts of exposure to aerosolized *B. pseudomallei* on body temperature and weights of mice.

Individual weights and temperatures were recorded daily. When mice were exposed to aerosolized bacteria, the difference in temperature between BALB/c and C57BL/6 mice was appreciable. Statistically significant differences between the BALB/c and C57BL/6 mouse body temperatures were observed for the average of day 1 to day 5 ($P<0.01$), with the BALB/c strain having a temperature 0.33^{o} C greater than that of the C57BL/6 mice (Figure 7A), however differences between the BALB/c and C57BL/6 strains were not statistically significant at later time points. The strain by time interaction was statistically significant ($P<0.01$), which is attributable to the separation at early time points diminishing as the study continued. Consistent with the observed longitudinal temperature trends, we found that the C57BL/6 mice showed a

significantly more negative lag 1 auto correlation (ρ =-0.71 vs -0.38; P <0.01) over the first 15 days of study, indicating that, the BALB/c strain maintained greater body temperature in the short term and the C57BL/6 strain had a greater propensity to return to normal body temperature. Statistically significant differences between the mouse strains in terms of body weight were observed by day 5 and at all subsequent time points (Figure 7B). The strain by time interaction was statistically significant (P<0.01). Absolute differences in mean body weight between strains continued to increase with time, reaching 4.5 grams by day 15.

Bacterial burden observed in mice exposed to aerosolized *Burkholderia pseudomallei*

Unlike the dissemination patterns observed in mice exposed to *B. pseudomallei* via IP injection, the mice that were exposed to aerosolized *B. pseudomallei* had fairly distinct dissemination patterns that differed between BALB/c and C57BL/6 mice. Some of these differences are likely partially related to the different LD_{50} equivalents delivered via each route of exposure. Both strains of mice received low doses of aerosolized bacteria; the BALB/c were exposed to approximately 5 CFU (0.5 LD_{50} equivalents) and the C57BL/6 mice were exposed to approximately 18 CFU (0.02LD_{50} equivalents). The BALB/c were all euthanized or had succumbed to infection by day 28, whereas the C57BL/6 mice survived longer and serial samples were collected at day 91. The dissemination patterns for the BALB/c mice were similar in all organs sampled (Figure 8). While variation existed between animals, the average bacterial burden seemed to peek at day 7 post-exposure and then continue to drop through day 22. The bacterial burden in the lungs was the most pronounced (Figure 8B), followed by the spleens (Figure 8A) and then finally liver samples (Figure 8C). The liver samples indicated that bacterial burden in this organ was approximately 10% of what can be observed in the spleens of the same

mice. Similar observations have been reported by Massey et al. [51]. Some of the BALB/c mice became bacteremic between day 2 and day 4 (Figure 8D).

The dissemination patterns of the C57BL/6 mice were markedly different compared to BALB/c (Figure 8). At time points examined, none of the mice showed signs of bacteremia (limit of detection 100 CFU/1 ml of blood) (Figure 8D). The C57BL/6 mice were seemingly better able to control the ensuing infection, and the bacterial burdens did not reach the magnitude observed in BALB/c mice and appeared to peak 2-4 days post-exposure to aerosolized bacteria. The dissemination data collected from the spleens (Figure 8A) and livers (Figure 8C) of the C57BL/6 mice suggested a predisposition towards a potentially chronic infection as has been previously reported [30, 38]. The spleen samples (Figure 8A), for example, were negative (limit of detection 10 CFU/1 ml of spleen homogenate) for *B. pseudomallei* after day 7 post-exposure, but on day 91 post-exposure 2 out of 12 surviving mice were culture positive for *B. pseudomallei*. These data indicated that at least a subset of C57BL/6 mice retained a low level of bacteria 91 days post exposure to a low dose of aerosolized bacteria. Twelve mice were euthanized and sampled on day 91 of which 2 of 12 mice were culture positive in the spleen sample, 3 of 12 mice were culture positive in the liver sample, and 6 of 12 mice maintained low levels of infection in lung tissue. Spleen weight was also analyzed, and significant differences were noted on days 15 and 22 post-infection ($P = 0.03$ and 0.0007, respectively), indicating that the BALB/c spleens were larger which in this experiment seemed to be associated with bacterial replication (Figure S2). Throughout the course of the study some of the mice were euthanized in accordance with early endpoint criteria or succumbed to the infection (30 of 80 BALB/c mice and 1 of 80 C57BL/6 mice).

Histopathology observed in mice exposed to aerosolized bacteria.

In contrast to the intraperitoneal challenge model, mice in the aerosol challenge model most consistently developed acute lesions in the nasal cavity and lung, and chronic lesions in the lung and spleen. Acute lesions in the nasal cavity were noted in 13/28 C57BL/6 mice as early as day 2 and in 9/29 BALB/c mice as early as day 4 and were characterized by intense neutrophilic inflammation which filled nasal sinuses (Figure 9A) and occasionally caused necrosis of the respiratory/olfactory epithelium and underlying subepithelial connective tissue. These lesions were generally confined to the posterior segment of the nasal cavity and often directly abutted the cribriform plate. In 2 of the BALB/c mice, the inflammation continued along olfactory nerve tracts, penetrating the cribriform plate and involving the meninges and neuropil of the olfactory bulbs and rostral cerebrum (Figure 9B). This was accompanied by a marked to severe neutrophilic exudate in the middle ear (Figure 9C), with necrosis of the respiratory epithelium lining the middle ear in 8/28 C57BL/6 mice and 9/29 BALB/c mice; it is surmised that in these cases the inflammation in the middle ear originated in the nasal cavity and extended along the eustachian tubes into the middle ear. This phase of infection appears to have remained active beyond the acute post-challenge timeframe in at least some of the mice, as evidenced by the persistence of neutrophilic inflammation and the lack of a progression to a more chronic inflammatory cell population in animals as late as 91 days post infection. This nidus of infection and inflammation may be a potential source of dissemination or reinfection for these mice at later time points.

16/28 C57BL/6 mice and 24/29 BALB/c mice had lung lesions attributed to *Burkholderia* infection. Not surprisingly, lesions in the lungs of the aerosolized mice from both strains

occurred much more acutely than in mice challenged via the intraperitoneal route. The earliest lesions consisted of multiple randomly arranged neutrophilic/suppurative foci with variable amounts of pneumocyte and septal necrosis. These foci were often associated with small and medium pulmonary vessels in an apparent embolic pattern (Figure 10A and B).; this pattern of inflammation in the lung is usually associated with infectious agents that arrive via a hematogenous (embolic) route. This is unexpected, as one would expect the aerosolized *Burkholderia* to arrive as inhaled particles and establish lesions more consistent withbronchopneumonia. There are two possible explanations for this pattern of inflammation. The first is that following exposure to aerosolized *B. pseudomallei*; the bacteria quickly enter the circulation via alveolar septa and establish a bacteremia, with subsequent embolic spread to multiple sites throughout the lung and more distant organs. The second is that following aerosol exposure, the bacteria are quickly phagocytized by resident alveolar macrophages, which then traffic the bacteria to these perivascular sites where they incite an intense neutrophilic reaction. Given the short amount of time in which these lesions are established, the latter seems more plausible, particularly since *B. pseudomallei* is hypothesized to evade the immune response by its intrahistiocytic localization [67]. In the BALB/c mice, by day 7 the inflammation progressed to histiocytic or pyogranulomatous inflammation (Figure 10C and D), with higher numbers of histiocytes and epithelioid macrophages. In some cases, these areas of granulomatous inflammation developed into well-organized pyogranulomas, with a core of necrotic debris and viable and degenerate neutrophils surrounded by epithelioid macrophages, further bounded by a fibrous capsule and numerous lymphocytes and neutrophils. Occasionally, there were multinucleated giant cell macrophages admixed with the epithelioid macrophages. Adjacent alveolar septa were often expanded by neutrophils and histiocytes, and alveolar, bronchiolar, and

bronchial lumens were often expanded by a profound neutrophilic exudate. These lesions are similar to those described in melioidosis in man [60]. Severe lung lesions in C57BL/6 mice were far less common, typically consisting only of interstitial inflammation and only rarely developing into well-organized pyogranulomas. By day 22 and beyond, significant lesions in the lung were completely lacking in C57BL/6 mice. This could be attributed to the purposefully low dose of bacteria used in this study, and it is possible that such a resolution of lung lesions would eventually have occurred in BALB/c mice; however we were unable to evaluate this as none of the mice of this strain survived beyond day 28.

In BALB/c mice, the spleen was another common location for development of acute suppurative and chronic granulomatous inflammatory lesions, affecting 12/29 mice. Early lesions starting on day 2 consisted of small foci of neutrophilic/suppurative inflammation with necrosis of adjacent red pulp elements and occasional fibrin thrombi. By day 15, inflammation progressed to histiocytic or pyogranulomatous inflammation, often with organized pyogranuloma formation similar to that seen in the lung (Figure 11). No such inflammatory lesions were noted in any of the C57BL/6 mice examined in this study.

In both strains of mice, liver involvement was not nearly as extensive as observed in the mice exposed via the intraperitoneal route. In fact, none of the aerosol exposed mice (BALB/c or C57BL/6) developed chronic pyogranulomatous lesions in the liver. Liver lesions were limited to small foci of neutrophilic inflammation with or without hepatocyte necrosis were scattered throughout the liver. Based on immunohistochemistry of the mice, it is likely that at least a portion of these lesions can be attributed to *Burkholderia*; however, the remainder of these lesions likely represent inflammation and necrosis secondary to other enterohepatic bacteria, commonly seen in mice.

None of the aerosol exposed mice from either strain developed debilitating/paralytic lesions in the spine and rear legs as was seen frequently with IP exposure; however three BALB/c mice did develop pyogranulomas in the tail. These certainly represent lesions that developed from secondary embolic spread of the *Burkholderia*. One BALB/c mouse developed pyogranulomas in the pancreas, also likely a sequel to embolic spread of the bacteria. All mice from both strains developed hyperplasia of the myeloid component of the bone marrow, as well as variable amounts of extramedullary hematopoiesis in the liver and spleen, representing increased tissue demand for leukocytes; however, these lesions were not nearly as intense as those seen in mice exposed via the IP route.

Immunological response associate with mice exposed to aerosolized bacteria.

We then examined the levels of cytokines/chemokines present in the sera of aerosol exposed BALB/c and C57BL/6 mice (Table S5). In Figure S4, we showed the changes in the cytokines/chemokines in sera for this study up to 22 days PI for C57BL/6 because there were no BALB/c survivors after that time for comparison, and there were not many significant changes in the cytokine/chemokine levels in sera from C57BL/6 mice after 22 days PI. The amount of cytokines/chemokines in sera after 28, 59, and 90 days after exposure to bacteria in C57BL/6 mice can be seen in Table S5. Immediately after the mice were exposed to *B. pseudomallei* K96243 (0 days) we detected a significant rise in IFN-γ [68.6 (1.06) pg/ml, $P<0.05$], IL-4 [134.4 (1.14) pg/ml, $P<0.05$], IL-10 [85.4 (1.13) pg/ml, $P<0.01$], FGFb [507.2 (1.03) pg/ml, $P<0.05$] and MIG [133.6 (1.22) pg/ml, $P<0.01$] in sera from C57BL/6mice (Table S5). After 2 days PI, we saw a significant increase in more cytokines/chemokines in sera from both mouse strains (Table S5, Figure 12). Overall, from 4 days to 22 days PI, we detected an increase in more cytokines/chemokines in sera from BALB/c mice than from C57BL/c (Table S5, Figure 8).

Those would include IFN-γ, IL-1α, IL-1β, IL-6, IP-10, and MIG. We did not show the fold-change of the chemokine MIG in sera from C57BL/6 in Figure 8 because it was very high at 2 days PI (235-fold), and it would make it difficult to see the changes in the amounts of the other cytokines/chemokines in the same figure. From day 28 to 90 days PI, we saw significant levels of IL-2 and MIG in sera from C57BL/6 mice although we detected the presence of many other cytokines/chemokines (Table S5).

We also examined the cytokines/chemokines present in the spleen extracts from the BALB/c and C57BL/6 mice that were exposed to *B. pseudomallei* K96243 by aerosol (Table S6, and Figure 13). We saw many more immediate (0 day PI) increases in cytokines/chemokines levels in the spleen extract of both stains of mice than we saw in sera (Table S6). We saw a significant increase in the expression of many of the cytokines/chemokines after 2 days PI in both mouse strains, but the fold-change was more apparent in spleen extracts from BALB/c mice (Figure 13). MIG levels again showed the largest and rapid changes early after infection in spleen extracts from both mice. In BALB/c mice we detected a rapid rise up to 2 days PI [3494 (1.36) pg/ml, $P \leq 0.001$] before it decreased at day 4 PI [1813 (1.19) pg/ml, $P \leq 0.001$), and MIG levels peaked at 7 days PI [4313 (1.16) pg/ml, $P \leq 0.001$) before there was a gradual decrease to 22 days PI [1905 (1.50) pg/ml, $P < 0.01$) after which all BALB/c mice perished. We also detected a large increase in the inflammatory cytokines IL-1a and IL-1B that peaked at 15 PI [1963 (3.28) pg/ml and 1296 (1.45) pg/ml ($P \leq 0.001$), respectively] before gradually decreasing to day 22 PI (Table S6 and Figure 13). Although we saw increases in these two inflammatory cytokines in spleen extracts from C57BL/6 mice, they did not reach levels seen in BALB/c mice. One cytokine that we found high levels present in spleen extracts from both mice was IL-4, which is a

T-helper type 2 (Th2) cytokine, although more was present in C57BL/c spleen extracts where levels peaked at 28 days PI [522.2 (1.07) pg/ml, $P \leq 0.001$] before it decreased to basal levels at 59 and 90 days PI (Table S6). We also saw high levels of IFN-γ in spleen extracts from BALB/c mice at 2 and 7-22 days PI, but at 2 and 15 – 28 days PI in extracts from C57BL/6. IL-2 had the second highest fold-change in spleen extracts from C57BL/c mice that peaked at 15 days PI. Both IFN-γ and IL-2 are considered Th1-type cytokines. Overall, we detected more cytokines/chemokines in spleen extracts from BALB/c mice than from C57BL/6 mice by 15 day PI and generally at higher levels (Table S6, Figure 9). Before the remaining BALB/c mice expired at 22 days PI there were high levels of IL-1α, IL-1β, IL-2, IL-4, IL-12, IFN-γ, MIG, and TNF-α that were present in their spleen extracts. In addition, there were at least two general peaks of cytokines/chemokines activity in spleen extracts from both mice that occurred at 2 days and 15 days PI. Finally, we saw a mixed Th1- and Th2-like cytokine production in spleen extracts from both BALB/c and C57BL/6 aerosol infected mice.

We also examined the cellular immune response in both BALB/c and C57BL/6 mice that were exposed to *B. pseudomallei* K96243 by aerosol. We examined cellular changes that occurred in spleens from aerosol infected mice and cytokines/chemokines present in serum and expressed in spleen extracts from the same mice. Table S4 and Figure 14 show the results of the analysis of the changes in cell composition of the spleens from the infected mice. However, unlike the IP exposure study described previously, no *B. pseudomallei* K96243 aerosol exposed BALB/c mice survived after 22 days PI. As we saw in the IP challenge study, granulocytes (Ly6G+/CD44) were the predominant host cell that accumulated in the mouse spleen after aerosol exposure up to 22 days PI. At 2 days PI we saw a small but significant transient increase in the granulocyte cell population that decreased on day 4 PI, and then they increased to a

maximum on day 15 PI in spleens from both BALB/c *(*P<0.01) and C57BL/6 (*P*<0.05) *exposed* mice, although we detected more granulocytes in the former mice [25.8 (5.21) %] than in the latter mice [10.0 (2.91) %](Table S4 and Figure 14). After this peak period, the number of granulocytes decreased in spleens from both mouse strains [15.7 (2.58) % and 2.00 (0.34) %], respectively, at day 22 PI. We also saw a significant increase in the other two types of inflammatory cells [monocytes/macrophages (CD11b+/CD14) and NK cells (CD49b/CD69)] in spleens at the same time in both strains of mice, except they did not reach as high a percentage as the granulocytes (Table S4 and Figure 14). In spleens from C57BL/6 mice at day 15 PI the number of NK cells rose to 25.5 (1.62) % (*P*≤0.001) and in BALB/c we saw an increase in numbers up to 29.7 (1.37) % (*P*≤0.001). In Figure 7 the fold changes in the number of monocytes/macrophages and NK cells were lower than that of the granulocytes because the initial amount of granulocytes in naïve mice were much lower than that of monocytes/macrophages and NK cells. We detected very little numbers of granulocytes in naïve mouse spleens (~1.0% in BALB/c and ~0.58% in C57BL/6) compared to the other inflammatory cells (see Table S4).

The presence of multi-nucleated giant cells (MNGCs) is appreciable in mice exposed to aerosolized bacteria.

MNGCs were not readily observed in the animals challenged by the intraperitoneal route in this study. This was in contrast to data presented by Chirakul et al. that indicated that MNGCs were present in the spleens of BALB/c mice challenged intraperitoneally with *B. pseudomallei* K96243 [58]. Previous reports of multinucleated giant cell macrophages in chronic melioidosis

suggest that these cells may be seen in a second wave of inflammation, perhaps from a recrudescence of *Burkholderia* infection [58, 60]. It is possible that if mice were sacrificed at later time points (>60 days post infection), such lesions might be more prominent in the mice challenged via the IP route. We did observe MNGCs in the lungs of 3/28 C57BL/6 mice and both the lungs and spleens of 9/29 BALB/c mice challenged with aerosolized bacteria (Figure 15).

DISCUSSION

We have systematically characterized the disease progression after introduction of *B. pseudomallei* K96243 into either BALB/c or C57BL/6 mice. The mice were challenged with these bacteria by either IP injection or by exposure to aerosolized bacteria. Our data support other work [27, 30, 35-44, 46-50] suggesting that each strain of mouse has strengths and weaknesses when studying the pathogenesis of *B. pseudomallei* and as models for the human responses to infection. To our knowledge, this is one of the most comprehensive reports of these murine disease models. While the ultimate goal of biodefense research is to elucidate therapies and vaccines to treat inhalational forms of these diseases, it is important to also have a well-characterized alternate model due to logistic and financial constrains when dealing with aerosol exposure studies. We chose to pursue the IP model as an alternate for several reasons; including, ease and reproducibly of exposure methodology, and the fact that many of the clinical signs may be potentially mimicking some of those observed in human cases of melioidosis [40, 50]. As illustrated in Figure 2, the dissemination patterns after IP injection of the bacteria were fairly similar between BALB/c and C57BL/6 mice in spite of the disparity between the numbers of bacteria administered to achieve comparable LD_{50} equivalents in each mouse strain. While the amount of bacteria used to challenge the C57BL/6 mice was approximately 30 times greater than

678 the challenge dose used for BALB/c mice, the resulting levels of bacteremia were similar. This
679 clearly demonstrates that the C57BL/6 immune response is better suited to combat this infection.
680 Interestingly, the bacteria can disseminate to the lungs very early after injection, but by day 4
681 post-infection the majority of lungs were free of bacteria.

682 These data collected from mice exposed to aerosolized bacteria demonstrated a similar
683 trend. We attempted to deliver comparable LD_{50} equivalents by exposing mice to aerosolized
684 bacteria. However, due to the difficulty associated with reproducibly delivering very low doses
685 of bacteria (i.e. >20 CFU), the BALB/c mice received approximately 0.5 LD_{50} equivalent
686 whereas the C57BL/6 mice received approximately 0.02 LD_{50} equivalents. This difference in
687 achieved delivered LD_{50} equivalents may account for some of the differences we observed.
688 When mice were exposed to aerosolized bacteria, there was an increase in bacterial burdens in
689 either strain of mouse; however the extent and duration of detectable bacteria in tissues were
690 appreciably greater and longer in BALB/c as compared to C57BL/6 mice. C57BL/6 mice were
691 never observed to be bacteremic, whereas BALB/c mice were demonstrably bacteremic from day
692 4 through day 15. In the case of lung bacterial burden, C57BL/6 mice experienced bacterial
693 replication through day 4, followed by a decline, and then plateau of bacterial growth. The
694 BALB/c mice exhibited a greater and longer lived bacterial replication cycle in the lungs, and
695 unfortunately, there were no survivors beyond day 28 to analyze and compare with the C57BL/6
696 mice. Of note were the results obtained from the spleen homogenates. The BALB/c mice
697 exposed to aerosolized bacteria had rapid and robust dissemination to and replication within the
698 spleen, peaking at approximately day 7 but remained significant throughout the entire study (day
699 22 for BALB/c mice). The C57BL/6 mice exposed to aerosolized bacteria, however,
700 demonstrated rapid dissemination, but replication peaked at day 2 and then bacterial growth was

not observed in the spleen tissues after day 7. Interestingly, however, bacteria were detected in samples collected on day 91 post exposure to aerosolized bacteria, lending further support to the concept that C57BL/6 mice may represent an appropriate chronic disease model. In our studies, particles containing aerosolized bacteria were approximately 1-3 μm in diameter. There is evidence that different particle sizes can lead to different disease progression. Thomas et al. demonstrated that *B. pseudomallei* delivered in larger droplets (i.e. 12 μm in diameter) resulted in a greater involvement in the nasal tissues, olfactory mucosa, olfactory nerve, olfactory bulb and brain tissue [68]. Similar results have been demonstrated when mice were exposed to *B. pseudomallei* via intranasal instillation which inherently delivers large droplets of bacteria [69]. This was in contrast to pathology observed when mice were exposed to 1 μm sized particles of aerosolized bacteria which displayed more significant lung pathology, as well as involvement of the mediastinal lymph nodes [68]. The impact of particle size on *B. pseudomallei* pathogenesis has also been established in intratracheal instillation of *B. pseudomallei* when separate laboratories utilized similar techniques but their respective equipment yielded differing particle sizes [70, 71].

Interestingly, we observed MNGCs in both the spleen and lungs of BALB/c and in lungs of C57BL/6 mice after exposure to aerosolized bacteria (Figure 15). We were unable to identify MNGCs in either mouse strain following the introduction of bacteria via IP injection. Again, these differences underscore the importance of bacterial strain, delivered dose, and delivery route. There have been reports suggesting a correlation of MNGC formation with other virulence attributes [72], and our previous work has proposed an inverse correlation between MNGC formation in vitro with virulence in mouse models of infection [40]. Chirakul et al.

reported differences in the inflammatory response observed in BALB/c mice compared to C57BL/6 mice when infected with either wild-type K96243 or a mutant strain with altered type III secretion system expression [58]. These authors readily found MNGC formation in BALB/c mice infected with either strain of *B. pseudomallei* and demonstrated that bacterial genes (i.e. *bprD*) may be expressed differentially in BALB/c mice compared to C57BL/6 mice [58]. Why the MNGCs were encountered in the aerosol challenged mice, and not the intraperitoneally exposed mice is unclear; perhaps initial passage through alveolar macrophages early in the disease process enhances the ability of the bacterial to induce MNGC formation or perhaps the IP exposure in some way reduces this ability. Further studies specifically examining MNGC prevalence in vivo and potential significance of such cellular morphologies are warranted.

Although histochemical analysis of infected tissue identified the infiltrating granulocytes were predominately neutrophils, we also used flow cytometry to identify that the major infiltrating cells into the infected spleens were Ly6G+, infiltrating monocytes/macrophages and NK cells. Although there were similarities in the temporal pattern and the amount of infiltrating inflammatory cells into the spleens in these two mouse strains after IP infection, there were some differences in the overall immune response and susceptibility of BALB/c mice to *B. pseudomallei* K96243 infection compared to the more resistant C57BL/6 mice. In the cellular innate immune response in the IP challenge study, there was a transitory increase in Ly6G+ granulocytes, monocytes/macrophages, and NK cells between 2-7 days after infection in C57BL/6 mice that was not evident in BALB/c mice that were infected by the same route. In the aerosol challenge study, there was a very minor but noticeable transitory increase in granulocytes

in both mouse strains but not the other inflammatory cells two days after infection. It is not clear at this time if the early transitory peak of granulocytes reflects an initial response to CFU appearing in the spleen or an initial infiltration of granulocytes that contain *B. pseudomallei* that appear in the spleen within 1-2 days after infection, although this early association with Ly6G+ neutrophils was also previously observed in lungs of BALB/c mice [73]. Although we cannot discount the influence of the number of CFU used between the IP and aerosol challenge study, one of the major differences between the two routes of infection was the larger number of Ly6G+ granulocytes that infiltrated the spleens of the two mouse strains by the IP route over that by the aerosol route of infection. This occurred even though eventually the CFU in the spleen, lung, and liver reached similar levels in the aerosol challenged mice when compared with the IP challenged mice which occurred almost immediately. At the same time, the number of the other innate immune inflammatory cells (monocytes/macrophages and NK cells) did not appear to appreciably change over the same period. There have been a number of reports noting the importance of neutrophils in the response to or required for clearance of *B. pseudomallei* in BALB/c or C57BL/6 mice [41, 50, 73-75]. The peak level of Ly6G+ granulocytes present in spleens of both BALB/c and C57BL/6 mice that were challenged by the IP route was between 15 to 22 days PI with the maximum at 22 days PI (36.6- and 39-fold increase, respectively), which was also similar with the peak levels that occurred for monocytes/macrophages and NK cells in the same spleens, but they were present in much lower amounts. At the same time, the CFU load in the various organs and blood was decreasing or close to the limit of detection. At the end of the IP challenge study (59 days PI) we saw a significant fold increase in monocytes/macrophages, granulocytes, and NK cells, with former cells being the most abundant at 59 days PI. In the aerosol challenged mice, however, the maximum level of Ly6G+

granulocytes in spleens was detected at 15 days PI in both BALB/c and C57BL/6 mice (25.5- and 17.2-fold increase, respectively), but the peak amounts were lower than detected in the IP challenged mice. After 22 days PI in the spleens of aerosol infected BALB/c mice, the amount of Ly6G+ granulocytes was still 15.5-fold over the control naïve mice levels, while in the spleens of C57BL/6 mice 22 days PI they were down to 3.4-fold over the control mice. This may be because the spleens of the same BALB/c mice 22 days PI had still a modest amount of CFU (geometric mean >100 CFU/g), while spleens from C57BL/6 mice had barely detectable numbers of CFU at the same time.

Besides the differences that we noted in the expression of cytokines/chemokines between BALB/c and C57BL/6 mice there were some differences in the expression of cytokines/chemokines that we detected between mice challenged by either the IP or aerosol route. In serum of BALB/c mice that were challenged by aerosol, we detected more cytokines/chemokines present for up to 22 days PI than we do in sera from mice that were infected by the IP route. We saw heightened levels of IFN-γ, IP-10, IL-1B, IL-6, and we detected longer expression of MIG over the period measured in the aerosol exposed BALB/c mice. In the sera of IP infected BALB/c mice, we detected a more defined peak of cytokines 2 days PI than in the sera of aerosol exposed mice. In the latter case, we saw a broader peak of cytokines/chemokines, which might be because of the more gradual increase in CFU in organs of the aerosol challenged mice. We detected some cytokines/chemokines in the sera of BALB/c mice infected by the IP route, such as KC and IL-1a that appeared to be immediately expressed upon exposure to *B. pseudomallei* K96243. KC is a chemokine that is a major chemoattractant for neutrophils, and it has been suggested that it may be a homolog of the human IL-8 from its ability to bind to a murine IL8 type B receptor [76]. IL-1α and IL-1β are proinflammatory

cytokines that are the host's innate immune response to exposure to the pathogen. One common phenomenon we observed in sera from C57BL/6 mice that were challenged by either IP or aerosol at day 2 PI was an enormous, transient increase of MIG that we did not observe in sera of *B. pseudomallei* K96243 infected BALB/c mice by either route. It went up to 230-fold above what was normally seen in naïve mice in both cases. MIG and IP-10, the latter which was also elevated, belong to the CXCL family of chemokines, CXCL9 and CXCL10, respectively, which are both induced by IFN-γ and share the same receptor CXCR3 (as well as CXCL11 or I-TAC) [77]. The expression of CXCL9 (MIG) can be detected in many antigen presenting cells, and the receptor CXCR3 is present on activated T cells and B cells that may influence both cellular immunity and antibody responses to the presence of a pathogen [78, 79]. The expression of IP-10, in addition, can also be induced by IFN-α and IFN-β [78], and it can be secreted by monocytes, endothelial cells, fibroblasts, and keratinocytes [80]. In our present study, we observed more IFN-γ in serum from both BALB/c and C57BL/6 mice that were exposed to *B. pseudomallei* K96243 by aerosol than the IP infected mice, and although we saw a higher peak of MIG in sera (at day 2 PI) from IP infected BALB/c mice, the elevated levels of MIG and IP-10 in sera from pathogen aerosol exposed were observed for a longer period after infection. Elevated levels of IP-10 and MIG have been observed in severe human melioidosis cases previously on admission in a clinical setting and during antibiotic treatment [81].

When we compared the cytokines/chemokines in spleen extracts from IP infected mice with that from the aerosol infected mice, we saw many more elevated levels of cytokines/chemokines that we were able to detect for a longer period of time in spleen extracts from both BALB/c and C57BL/6 mice exposed to *B. pseudomallei* by aerosol compared to that in spleen extracts from mice exposed to the pathogen by IP injection. In the spleen extracts from

BALB/c IP exposed mice we saw 6 cytokines/chemokines that were elevated (MIG, IP-10, IFN-γ, IL-1α, and IL-1β) early in the study (0 – 22 days PI). In spleen extracts from C57BL/6 IP exposed mice, we detected the same cytokines/chemokines in addition to the chemokine KC. The peak level of several of the cytokines/chemokine detected in spleen extracts in both cases occurred at 15-22 days PI (excluding the immediate expression that occurred at 0 days PI) where IL-1α, IL-1β, and MIG were the primary elevated cytokines/chemokine at that time. The number and amount of cytokines/chemokines in the aerosol challenged mice were higher until the end of the study (22 days and 90 days PI for BALB/c and C57BL/6 mice, respectively) which might reflect the CFU recovered from the aerosol infected mice. In lungs, spleens, and livers from C57BL/6 mice, the peak of CFU recovered (geometric mean) occurred at 2 days PI, while in the same organs from BALB/c mice the peak of CFU (geometric mean) occurred approximately 7 days PI. In spleen extracts from the aerosol infected mice, there were two peaks in the amount of cytokines/chemokines in both mouse species: one at 2 days PI, and another at approximately 15 days PI. Up to 22 days PI (after that period there were not enough BALB/c mice left to examine) we saw at least elevated amounts of 12 cytokines/chemokines: IFN-γ, MIG, IP-10, FGFb, IL-1α, IL-1β, IL-2, IL-4, IL-12, and VEGF. In spleen extracts from BALB/c mice we also saw elevated levels of TNF-α but not in spleen extracts from C57BL/6 mice. There was a noticeable decrease in the level of cytokines/chemokines at 59 days PI in spleen extracts from aerosol infected C57BL/6 mice, but there was still a modest amount of some of these (Figure S4: IL-1α, IL-1β, IL-2, IL-12, MIG, FGFb, VEGF, MIP-1α) at the end of the study.

In conclusion, Ly6G+ granulocytes were the major infiltrating cells in both IP and aerosol infected mice, but they reached higher levels and reached a maximum period PI around 22 days in IP infected mice, while in aerosol challenged mice they peaked approximately 15 days

PI. The next most prevalent infiltrating cells in the infected spleen were the monocytes/macrophages and NK cells in both mouse strains and by either infection route. We saw more cytokines/chemokines in aerosol infected mice in serum and spleen extracts than in IP infected mice. MIG, IP-10, KC, as well as IFN-g appeared to play a dominate role in the early response period to *B. pseudomallei* in both mouse models, but in aerosol infected mice they were also present after 4-7 days PI. Because of the abundance of MIG and IP-10 which are chemoattractants of activated T-cells [78, 82], it may suggest that T-cells are involved in the infection, pathogenesis, and immunity to *B. pseudomallei*, although in this study we did not examine the activity of T cells [78, 82-86]. In IP infected mice IL-1a and IL-1B were the predominate innate immune inflammatory cytokines that were more apparent than in aerosol infected mice, with IL-1B which appears to be generated by a special cytosolic inflammasome and a deleterious cytokine the more prevalent of the two [74, 87, 88]. Finally, there appeared to be a mixed cytokine response with Th1- and Th2-like cytokines expressed in response to *B. pseudomallei* in the murine models even in the Th-1-like C57BL/6 mouse after aerosol infection. This immune response by the host may be partly responsible for the inability of the host to completely resolve the infection and could lead to a fatal outcome in both acute and chronic infections by *B. pseudomallei*.

The differences and similarities we highlighted here are important; however, we do not want to oversimplify or understate the complex process of selecting the appropriate model for melioidosis. Inherent differences between BALB/c and C57BL/6 mice are numerous and well documented. Whereas BALB/c mice mount a rapid and robust TH-2 like response, their adaptive Th-1 response is not as efficient nor long lasting when compared to that of C57BL/6 mice [89-94]. The differential immune responses have been observed to include cellular

recruitment kinetics and downstream cellular functionality (i.e. cytokine and chemokine expression) [30, 38, 95]. Accordingly, BALB/c mice are known to be more susceptible to autoimmune disease [96-98] and are more susceptible to tumor proliferation in certain models [99-101]. BALB/c mice and macrophages derived from these mice are also well documented to be more susceptible to infectious diseases (to include bacteria, intracellular bacteria/parasites, and viruses) [36, 45, 92, 94, 102-112]. Thus, there are many factors that need to be taken into account when determining applicability of a mouse model and subsequently how to analyze these data from said models [91, 104, 113]. Additionally, when specifically examining *B. pseudomallei* the bacterial strain selection and route of infection are of the utmost importance. The virulence of the bacterial strains are known to vary substantially [40, 45, 50, 94, 102-104, 114], and the route of infection can significantly alter the disease pathogenesis as well. In conclusion, the BALB/c and C57BL/6 mouse each model different parameters of melioidosis. BALB/c mice may be more appropriate for virulence testing/classification of bacterial strains, and C57BL/6 may be best suited for vaccine or therapeutic testing, and perhaps when taken together represent the best approach for understanding bacterial pathogenesis and efficacy testing of medical counter-measures.

ACKNOWLEDGEMENTS

This research was funded by the Medical Biological Defense Research Program; Defense Threat Reduction Agency (DTRA). The authors would like to thank Dr. David DeShazer for their critical review of this manuscript. Opinions, interpretations, conclusions and recommendations are those of the authors and are not necessarily endorsed by the U.S. Army.

883 **FIGURE LEGENDS**

884

885 **Figure 1. Analyses of daily recorded temperatures (A) and daily recorded weights (B) for**
886 **mice challenged with *B. pseudomallei* K96243 delivered via the IP route.**

887

888 **Figure 2. Bacterial burden determined in mice challenged with *B. pseudomallei* K96243**
889 **delivered via the IP route.** CFU/g for spleen (A), lungs (B), liver (C) and CFU/ml for blood (D)
890 are depicted. The geometric mean for each group is indicated. BALB/C mice are depicted with
891 open circles and C57BL/6 mice are depicted with filled squares. 5 mice were euthanized at each
892 time point.

893

894 **Figure 3. Histopathology observed in mice with rear leg clinical signs assocaited with**
895 **intraperitoneal challenge with *B. pseudomallei* K96243. A.** C57BL/6 euthanized on day 22
896 post-infection showing clinical signs in the hind-end and tail. Tail, transverse section: Multiple
897 pyogranulomas partially effacing vertebral body and associated soft tissues. H&E, 20X. B.
898 BALB/c mouse euthanized on day 25 post-infection with rear-leg paralysis and labored
899 breathing. Lumbar spine, longitudinal section: Pyogranulomatous inflammation partially
900 effacing vertebral body and associated soft tissues. H&E, 40X.

901

902 **Figure 4. Histopathology observed in mice following intraperitoneal challenge with *B.***
903 ***pseudomallei* K96243. A.** C57BL/6 mouse euthanized on day 2 post-infection Liver: Random
904 foci of neutrophilic inflammation with individual hepatocyte necrosis/apoptosis (arrow). H&E,
905 400X. **B.** C57BL/6 mouse euthanized on day 22 post-infection. Femoral bone marrow: Myeloid

hyperplasia with predominance of neutrophils. H&E, 400X. C. BALB/c mouse euthanized on day 20 post-infection with rear-leg paralysis. Spleen: Multiple pyogranulomas effacing red and white pulp. H&E, 40X.

Figure 5. Cellular changes in spleens occurring in BALB/c and C57BL/6 mice after intraperitoneal infection with *B. pseudomallei* K96243. Spleen homogenates were prepared from infected (A) BALB/c and (B) C57BL/6 mice over time, and the percent of each cell type examined was determined as described in the Material and Methods. For each mouse strain n was equal to 5 at each time point. The fold-change for each cell type was determined by dividing the percent of the cell type at each time point (reported in Table S1) by the percent of the cell type present in normal, naïve mice, where n was 10 for BALB/c and 4 for C57BL/6 mice

Figure 6. Changes in the amount of cytokines/chemokines in spleen extracts from BALB/c and C57BL/6 mice after intraperitoneal infection with *B. pseudomallei* K96243. The amount of cytokines/chemokines present in spleen extracts (shown in Table S3) was determined as described in the Material and Methods. Only fold-changes in ten of the cytokines/chemokines are shown for (A) BALB/c and (B) C57BL/6 because they showed the most changes from normal levels after infection or were known to be important for host immunity, such as TNF-α. For each time point, n was equal to five for BALB/c and C57BL/6 mice. Fold-changes in cytokines/chemokines was determined by dividing the amount (pg/ml) present in the spleen extract by the amount present in normal, naïve mice, where n was 10 for BALB/c and 4 for C57BL/6 mice.

Figure 7. Analyses of daily recorded temperatures (A) and daily recorded weights (B) for mice exposed to aerosolized *B. pseudomallei* K96243.

Figure 8. Bacterial burden determined in mice exposed to aerosolized *B. pseudomallei*. CFU/g for spleen (A), Lungs (B), Liver (C) and CFU/ml for blood (D) are depicted. The geometric mean for each group is indicated. BALB/C mice are depicted with open circles and C57BL/6 mice are depicted with filled squares. 5 mice were euthanized at each time point through day 22, after which the surviving BALB/c were used to perform histopathological analyses. N = 12 for C57BL/6 mice on day 91.

Figure 9. Cranial histopathology observed in mice following exposure to aerosolized *B. pseudomallei* K96243. A. BALB/c mouse euthanized on day 4 post-infection. Nasal cavity: Epithelial and subepithelial suppurative inflammation and necrosis. H&E, 100X. **B.** BALB/c mouse euthanized on day 10 when early endpoint-euthanasia criteria were met. Nasal cavity and calvarium: Suppurative inflammation arising in the nasal cavity (N) and extending through the cribriform plate (arrow) into the olfactory bulb and cerebrum (C). H&E 20X. **C.** BALB/c mouse euthanized on day 7 post-infection with clinical signs indicative of an inner ear-infection Middle ear: Suppurative inflammation and necrosis of epithelium (suppurative otitis media). H&E 200X

Figure 10. Lung histopathology observed in mice following exposure to aerosolized *B. pseudomallei* K96243. A. C57BL/6 mouse euthanized on day 2 post-infection. Lung: Multifocal random (embolic) suppurative pneumonia. H&E 20X. **B.** BALB/c mouse euthanized on day 4 post-infection. Lung: Suppurative inflammation and alveolar necrosis with numerous

short bacilli (arrow). H&E 600X. **C.** BALB/c mouse euthanized on day 7 post-infection. Lung: Focally extensive pyogranuloma. H&E 40X. **D.** Lung: Periphery of pyogranuloma with multinucleate giant cell macrophage formation. H&E 600X.

Figure 11. Spleen histopathology observed in mice following exposure to aerosolized *B. pseudomallei* K96243. BALB/c mouse euthanized on day 15 post-infection and displayed ruffled apperance at that time. Spleen: Multiple distinct pyogranulomas. H&E 20X.

Figure 12. Changes in the amount of cytokines/chemokines in sera from BALB/c and C57BL/6 mice after aerosol exposure to *B. pseudomallei* K96243. The amount of cytokines/chemokines present in sera (shown in Table S5) was determined as described in the Material and Methods section. For changes in cytokine/chemokine levels in sera from BALB/c mice (A), we show changes in levels up to 22 days PI because there were no survivors after that period. We also show changes in cytokine/chemokine levels in sera for C57BL/6 mice (B) up to 22 days PI for comparison and not many significant changes occurred after 22 days PI in sera from C57BL/6 mice. For each mouse strain n was equal to 5 at each time point. Fold-changes in cytokines/chemokines were determined by dividing the amount (pg/ml) present in sera of exposed mice (Table S5) by the mount present in normal, naïve mice, where n was 10 for BALB/c and 4 for C57BL/6 mice. For C57BL/6 mice fold-change for MIG was not shown because it was very high (235-fold), and it would make it difficult to see the changes in the levels of the other cytokines/chemokines at the same time.

Figure 13. Changes in the amount of cytokines/chemokines in spleen extracts from BALB/c and C57BL/6 mice after aerosol exposure to *B. pseudomallei* K96243. The amount

974 of cytokines/chemokines present in spleen extracts (shown in Table S6) was determined as
975 described in the Material and Methods section. For changes in cytokine/chemokine levels in
976 spleen extracts from BALB/c mice (A), we show changes in levels up to 22 days PI because
977 there were no survivors after that period. We also show changes in cytokines/chemokine levels
978 in spleen extracts for C57BL/6 mice (B) for comparison although they were determined to 90
979 days PI (see Table S6). For each time point, n was equal to five for BALB/c and C57BL/6 mice.
980 Fold-changes in cytokines/chemokines was determined by dividing the amount (pg/ml shown in
981 Table S6) present in the spleen extract by the amount present in normal, naïve mice, where n was
982 10 for BALB/c and 4 for C57BL/6 mice.

983 **Figure 14. Cellular changes in spleens occurring in BALB/c and C57BL/6 mice after**
984 **aerosol exposure to *B. pseudomallei* K96243.** Spleen homogenates were prepared from
985 infected (A) BALB/c and (B) C57BL/6 mice over time, and the percent of each cell type
986 examined was determined as described in the Material and Methods. After 22 days PI there were
987 no BALB/c mice survivors. For each mouse strain n was equal to 5 at each time point. The
988 fold-change for each cell type was determined by dividing the percent of the cell type at each
989 time point (found in Table S4) by the percent of the cell type present in normal, naïve mice,
990 where n was 10 for BALB/c and 4 for C47BL/6 mice.

991 **Figure 15. Representative micrographs demonstrating the presence of MNGC in mice**
992 **exposed to aersolized bacteria.** MNGCs (arrows) were observed in lungs (A) and spleens (B)
993 in BALB/c mice and in lungs (C) of C57BL/6 mice.
994
995

996

997

998 **Supporting Information**

999

1000 **Figure S1. Spleen weights of mice following intraperitoneal challenge with *B. pseudomallei***
1001 **K96243.** As observed previously, spleen weight can be indicative of intrinsic diffrences in host
1002 immune response or bacterial replications [40, 50]. After IP infection with realtive LD_{50}
1003 equivalents, trends in spleen weight in both BALB/c and C57BL/6 mice were comparable,
1004 except on day 4 where C57BL/6 mice spleens were significantly larger than BALB/c mice mice
1005 ($P = 0.0122$).

1006

1007 **Figure S2. Spleen weights of mice following exposre to aerosolized *B. pseudomallei* K96243.**
1008 As observed previously, spleen weight can be indicative of intrinsic diffrences in host immune
1009 response or bacterial replications [40, 50]. After exposre to low doses the spleens harvested
1010 from BALB/c mice were signifcantly larger on days 15 and 22 post exposure ($P = 0.0324$ and
1011 0.0007, respectively).

1012

1013 **Figure S3. Changes in the amount of cytokines/chemokines in sera from BALB/c and**
1014 **C57BL/6 mice after intraperitoneal infection with *B. pseudomallei* K96243.** The amount of
1015 cytokines/chemokines present in sera (shown in Table S2) from infected (A) BALB/c and (B)
1016 C57BL/6 mice was determined as described in the Material and Methods. The fold-change in
1017 MIG levels in sera was not shown for C57BL/6 because it was very high at 2 days PI (231-fold),
1018 and it would make it difficult to see changes in other cytokines/chemokines for comparison. For

each time point, n was equal to 5 for BALB/c and C57BL/6 mice. Fold-change in cytokines/chemokines was determined by dividing the amount (pg/ml) present in sera after infection by the amount present in normal, naïve mice, where n was 10 for BALB/c and 4 for C57BL/6 mice.

Figure S4. Changes in the amount of cytokines/chemokines in sera and spleen from C57BL/6 mice after aerosol exposure to *B. pseudomallei* K96243 through day 91 post exposure to aerosolized bacteria. The amount of cytokines/chemokines present in sera (shown in Table S5) was determined as described in the Material and Methods section. For changes in cytokine/chemokine levels in sera from C57BL/6 mice (A), we show changes in levels up to 91 days PI. We also show changes in cytokine/chemokine levels in spleen extracts for C57BL/6 mice (B) up to 91 days PI for comparison. For each mouse strain n was equal to 5 at each time point. Fold-changes in cytokines/chemokines were determined by dividing the amount (pg/ml) present in sera of exposed mice (Table S5) by the mount present in normal, naïve mice, where n was 10 for BALB/c and 4 for C57BL/6 mice. For C57BL/6 mice fold-change for MIG was not shown because it was very high (235-fold), and it would make it difficult to see the changes in the levels of the other cytokines/chemokines at the same time.

Table S1. Cellular changes in spleen composition in BALB/c and C57BL/6 mice after IP challenge with *B. pseudomallei* K96243.

Table S2. Cytokines/chemokines in serum from BALB/c and C57BL/6 mice after IP challenge with *B. pseudomallei* K96243.

Table S3. Cytokines/chemokines in spleen extracts from BALB/c and C57BL/6 mice after IP challenge with *B. pseudomallei* K96243.

Table S4. Cellular changes in spleen composition in BALB/c and C57BL/6 mice after aerosol exposure to *B. pseudomallei* K96243.

Table S5. Cytokines/chemokines in sera from BALB/c and C57BL/6 mice after aerosol exposure to *B. pseudomallei* K96243.

Table S6. Cytokines/chemokines in spleen extracts from BALB/c and C57BL/6 mice after aerosol exposure to *B. pseudomallei* K96243.

REFERENCES

1. Cheng, A.C. and B.J. Currie, *Melioidosis: epidemiology, pathophysiology, and management.* Clin Microbiol Rev, 2005. **18**(2): p. 383-416.
2. Churuangsuk, C., et al., *Characteristics, clinical outcomes and factors influencing mortality of patients with melioidosis in southern Thailand: A 10-year retrospective study.* Asian Pac J Trop Med, 2016. **9**(3): p. 256-60.
3. Limmathurotsakul, D., et al., *Melioidosis caused by Burkholderia pseudomallei in drinking water, Thailand, 2012.* Emerg Infect Dis, 2014. **20**(2): p. 265-8.
4. Limmathurotsakul, D., et al., *Burkholderia pseudomallei is spatially distributed in soil in northeast Thailand.* PLoS Negl Trop Dis, 2010. **4**(6): p. e694.
5. Kaestli, M., et al., *Out of the ground: aerial and exotic habitats of the melioidosis bacterium Burkholderia pseudomallei in grasses in Australia.* Environ Microbiol, 2012. **14**(8): p. 2058-70.
6. Currie, B.J., *Melioidosis: an important cause of pneumonia in residents of and travellers returned from endemic regions.* Eur Respir J, 2003. **22**(3): p. 542-50.
7. Currie, B.J. and S.P. Jacups, *Intensity of rainfall and severity of melioidosis, Australia.* Emerg Infect Dis, 2003. **9**(12): p. 1538-42.
8. Aardema, H., et al., *Changing epidemiology of melioidosis? A case of acute pulmonary melioidosis with fatal outcome imported from Brazil.* Epidemiol Infect, 2005. **133**(5): p. 871-5.
9. Dance, D.A., *Melioidosis as an emerging global problem.* Acta Trop, 2000. **74**(2-3): p. 115-9.
10. Gee, J.E., et al., *Burkholderia pseudomalle type G in Western Hemisphere.* Emerg Infect Dis, 2014. **20**(4): p. 682-684.
11. Hassan, M.R., et al., *Incidence, risk factors and clinical epidemiology of melioidosis: a complex socio-ecological emerging infectious disease in the Alor Setar region of Kedah, Malaysia.* BMC Infect Dis, 2010. **10**: p. 302.
12. Limmathurotsakul, D., et al., *Predicted global distribution of and burden of melioidosis.* Nat Microbiol, 2016. **1**(1).
13. Lo, T.J., et al., *Melioidosis in a tropical city state, Singapore.* Emerg Infect Dis, 2009. **15**(10): p. 1645-7.
14. Rammaert, B., et al., *Pulmonary melioidosis in Cambodia: a prospective study.* BMC Infect Dis, 2011. **11**: p. 126.
15. Zehnder, A.M., et al., *Burkholderia pseudomallei isolates in 2 pet iguanas, California, USA.* Emerg Infect Dis, 2014. **20**(2): p. 304-6.
16. O'Sullivan, B.P., et al., *Burkholderia pseudomallei infection in a child with cystic fibrosis: acquisition in the Western Hemisphere.* Chest, 2011. **140**(1): p. 239-42.
17. Doker, T.J., et al., *Contact Investigation of Melioidosis Cases Reveals Regional Endemicity in Puerto Rico.* Clin Infect Dis, 2014.
18. Hogan, C., et al., *Melioidosis in Trinidad and Tobago.* Emerg Infect Dis, 2015. **21**(5): p. 902-4.
19. Sanford, J.P., *Melioidosis and Glanders*, in *Harrison's Principles of Internal Medicine*, W. J.D., B. E., and I. K.J., Editors. 1991, McGraw-Hill, Inc.: New York, NY. p. 606-609.
20. Vietri, N.J. and D. DeShazer, *Melioidosis*, in *Textbook of Military Medicine: Medical Aspect of Biological Warfare*, Z. Dembek, Editor. 2007, Borden Institute Walter Reed Army Medical Center: Washington, D.C. p. 147-166.

21. Wiersinga, W.J., B.J. Currie, and S.J. Peacock, *Melioidosis.* N Engl J Med, 2012. **367**(11): p. 1035-44.
22. Yabuuchi, E. and M. Arakawa, *Burkholderia pseudomallei and melioidosis: be aware in temperate area.* Microbiol Immunol, 1993. **37**(11): p. 823-36.
23. Hatcher, C.L., L.A. Muruato, and A.G. Torres, *Recent Advances in Burkholderia mallei and B. pseudomallei Research.* Curr Trop Med Rep, 2015. **2**(2): p. 62-69.
24. Ngauy, V., et al., *Cutaneous melioidosis in a man who was taken as a prisoner of war by the Japanese during World War II.* J Clin Microbiol, 2005. **43**(2): p. 970-2.
25. Nandi, T. and P. Tan, *Less is more: Burkholderia pseudomallei and chronic melioidosis.* MBio, 2013. **4**(5): p. e00709-13.
26. Suputtamongkol, Y., et al., *Risk factors for melioidosis and bacteremic melioidosis.* Clin Infect Dis, 1999. **29**(2): p. 408-13.
27. Tamrakar, S.B. and C.N. Haas, *Dose-response model for Burkholderia pseudomallei (melioidosis).* J Appl Microbiol, 2008. **105**(5): p. 1361-71.
28. Liu, X., et al., *Association of melioidosis incidence with rainfall and humidity, singapore, 2003-2012.* Emerg Infect Dis, 2015. **21**(1): p. 159-62.
29. Chen, P.S., et al., *Airborne Transmission of Melioidosis to Humans from Environmental Aerosols Contaminated with B. pseudomallei.* PLoS Negl Trop Dis, 2015. **9**(6): p. e0003834.
30. Titball, R.W., et al., *Burkholderia pseudomallei: animal models of infection.* Trans R Soc Trop Med Hyg, 2008. **102 Suppl 1**: p. S111-6.
31. van Schaik, E., et al., *Development of novel animal infection models for the study of acute and chronic Burkholderia pseudomallei pulmonary infections.* Microbes Infect, 2008. **10**(12-13): p. 1291-9.
32. DeShazer, D., et al., *Mutagenesis of Burkholderia pseudomallei with Tn5-OT182: isolation of motility mutants and molecular characterization of the flagellin structural gene.* J Bacteriol, 1997. **179**(7): p. 2116-25.
33. Kaufmann, A.F., et al., *Melioidosis in imported non-human primates.* J Wildl Dis, 1970. **6**(4): p. 211-9.
34. Sprague, L.D. and H. Neubauer, *Melioidosis in animals: a review on epizootiology, diagnosis and clinical presentation.* J Vet Med B Infect Dis Vet Public Health, 2004. **51**(7): p. 305-20.
35. Barnes, J.L. and N. Ketheesan, *Route of infection in melioidosis.* Emerg Infect Dis, 2005. **11**(4): p. 638-9.
36. Hoppe, I., et al., *Characterization of a murine model of melioidosis: comparison of different strains of mice.* Infect Immun, 1999. **67**(6): p. 2891-900.
37. Conejero, L., et al., *Low-dose exposure of C57BL/6 mice to burkholderia pseudomallei mimics chronic human melioidosis.* Am J Pathol, 2011. **179**(1): p. 270-80.
38. Leakey, A.K., G.C. Ulett, and R.G. Hirst, *BALB/c and C57Bl/6 mice infected with virulent Burkholderia pseudomallei provide contrasting animal models for the acute and chronic forms of human melioidosis.* Microb Pathog, 1998. **24**(5): p. 269-75.
39. Tan, G.Y., et al., *Burkholderia pseudomallei aerosol infection results in differential inflammatory responses in BALB/c and C57Bl/6 mice.* J Med Microbiol, 2008. **57**(Pt 4): p. 508-15.
40. Welkos, S.L., et al., *Characterization of Burkholderia pseudomallei strains using a murine intraperitoneal infection model and in vitro macrophage assays.* PLoS One, 2015. **pii: S0882-4010(15)00104-7. doi: 10.1016/j.micpath.2015.07.004. [Epub ahead of print] PMID: 26162294**
41. West, T.E., et al., *Murine pulmonary infection and inflammation induced by inhalation of Burkholderia pseudomallei.* Int J Exp Pathol, 2012. **93**(6): p. 421-8.

42. West, T.E., et al., *Pathogenicity of high-dose enteral inoculation of Burkholderia pseudomallei to mice.* Am J Trop Med Hyg, 2010. **83**(5): p. 1066-9.
43. Lever, M.S., et al., *Experimental acute respiratory Burkholderia pseudomallei infection in BALB/c mice.* Int J Exp Pathol, 2009. **90**(1): p. 16-25.
44. Jeddeloh, J.A., et al., *Biodefense-driven murine model of pneumonic melioidosis.* Infect Immun, 2003. **71**(1): p. 584-7.
45. Challacombe, J.F., et al., *Interrogation of the Burkholderia pseudomallei Genome to Address Differential Virulence among Isolates.* PLoS One, 2014. **9**(12): p. e115951.
46. Welkos, S.L., et al., *Characterization of Burkholderia pseudomallei Strains Using a Murine Intraperitoneal Infection Model and In Vitro Macrophage Assays.* PLoS One, 2015. **10**(4): p. e0124667.
47. Chua, K.L., Y.Y. Chan, and Y.H. Gan, *Flagella are virulence determinants of Burkholderia pseudomallei.* Infect Immun, 2003. **71**(4): p. 1622-9.
48. Dannenberg, A.M., Jr. and E.M. Scott, *Melioidosis: pathogenesis and immunity in mice and hamsters. I. Studies with virulent strains of Malleomyces pseudomallei.* J Exp Med, 1958. **107**(1): p. 153-66.
49. Nieves, W., et al., *A Burkholderia pseudomallei outer membrane vesicle vaccine provides protection against lethal sepsis.* Clin Vaccine Immunol, 2014. **21**(5): p. 747-54.
50. Amemiya, K., et al., *Comparison of the early host immune response to two widely diverse virulent strains of Burkholderia pseudomallei that cause acute and chronic infections in BALB/c mice.* Microb Pathog, 2015.
51. Massey, S., et al., *Comparative Burkholderia pseudomallei natural history virulence studies using an aerosol murine model of infection.* Sci Rep, 2014. **4**: p. 4305.
52. Horton, R.E., et al., *Quorum sensing negatively regulates multinucleate cell formation during intracellular growth of Burkholderia pseudomallei in macrophage-like cells.* PLoS One, 2013. **8**(5): p. e63394.
53. Pegoraro, G., et al., *A high-content imaging assay for the quantification of the Burkholderia pseudomallei induced multinucleated giant cell (MNGC) phenotype in murine macrophages.* BMC Microbiol, 2014. **14**: p. 98.
54. Wand, M.E., et al., *Macrophage and Galleria mellonella infection models reflect the virulence of naturally occurring isolates of B. pseudomallei, B. thailandensis and B. oklahomensis.* BMC Microbiol, 2011. **11**(1): p. 11.
55. Kespichayawattana, W., et al., *Burkholderia pseudomallei induces cell fusion and actin-associated membrane protrusion: a possible mechanism for cell-to-cell spreading.* Infect Immun, 2000. **68**(9): p. 5377-84.
56. Harley, V.S., et al., *Effects of Burkholderia pseudomallei and other Burkholderia species on eukaryotic cells in tissue culture.* Microbios, 1998. **96**(384): p. 71-93.
57. Mulye, M., et al., *Delineating the importance of serum opsonins and the bacterial capsule in affecting the uptake and killing of Burkholderia pseudomallei by murine neutrophils and macrophages.* PLoS Negl Trop Dis, 2014. **8**(8): p. e2988.
58. Chirakul, S., et al., *Characterization of BPSS1521 (bprD), a regulator of Burkholderia pseudomallei virulence gene expression in the mouse model.* PLoS One, 2014. **9**(8): p. e104313.
59. Fisher, N.A., et al., *The Madagascar hissing cockroach as a novel surrogate host for Burkholderia pseudomallei, B. mallei and B. thailandensis.* BMC Microbiol, 2012. **12**: p. 117.
60. Wong, K.T., S.D. Puthucheary, and J. Vadivelu, *The histopathology of human melioidosis.* Histopathology, 1995. **26**(1): p. 51-5.

61. Zumbrun, E.E., et al., *Development of a murine model for aerosolized ebolavirus infection using a panel of recombinant inbred mice.* Viruses, 2012. **4**(12): p. 3468-93.
62. Davis, K.J., et al., *Bacterial filamentation of Yersinia pestis by beta-lactam antibiotics in experimentally infected mice.* Arch Pathol Lab Med, 1997. **121**(8): p. 865-8.
63. Amemiya, K., et al., *Interleukin-12 induces a Th1-like response to Burkholderia mallei and limited protection in BALB/c mice.* Vaccine, 2006. **24**(9): p. 1413-20.
64. Patil, H.G., et al., *Musculoskeletal melioidosis: An under-diagnosed entity in developing countries.* J Orthop, 2016. **13**(1): p. 40-2.
65. Raja, N.S. and C. Scarsbrook, *Burkholderia Pseudomallei Causing Bone and Joint Infections: A Clinical Update.* Infect Dis Ther, 2016.
66. McInnes, E.F., *Background Lesions in Laboratory Animals: A Color Atlas*. 2012, New York, NY: Saunders Elsevier. 48-53.
67. Allwood, E.M., et al., *Strategies for Intracellular Survival of Burkholderia pseudomallei.* Front Microbiol, 2011. **2**: p. 170.
68. Thomas, R.J., et al., *Particle-size dependent effects in the Balb/c murine model of inhalational melioidosis.* Front Cell Infect Microbiol, 2012. **2**: p. 101.
69. St John, J.A., et al., *Burkholderia pseudomallei penetrates the brain via destruction of the olfactory and trigeminal nerves: implications for the pathogenesis of neurological melioidosis.* MBio, 2014. **5**(2): p. e00025.
70. Lafontaine, E.R., et al., *Use of a safe, reproducible, and rapid aerosol delivery method to study infection by Burkholderia pseudomallei and Burkholderia mallei in mice.* PLoS One, 2013. **8**(10): p. e76804.
71. Revelli, D.A., J.A. Boylan, and F.C. Gherardini, *A non-invasive intratracheal inoculation method for the study of pulmonary melioidosis.* Front Cell Infect Microbiol, 2012. **2**: p. 164.
72. Suparak, S., et al., *Multinucleated giant cell formation and apoptosis in infected host cells is mediated by Burkholderia pseudomallei type III secretion protein BipB.* J Bacteriol, 2005. **187**(18): p. 6556-60.
73. Laws, T.R., et al., *Neutrophils are the predominant cell-type to associate with Burkholderia pseudomallei in a BALB/c mouse model of respiratory melioidosis.* Microb Pathog, 2011. **51**(6): p. 471-5.
74. Ceballos-Olvera, I., et al., *Inflammasome-dependent pyroptosis and IL-18 protect against Burkholderia pseudomallei lung infection while IL-1beta is deleterious.* PLoS Pathog, 2011. **7**(12): p. e1002452.
75. Easton, A., et al., *A critical role for neutrophils in resistance to experimental infection with Burkholderia pseudomallei.* J Infect Dis, 2007. **195**(1): p. 99-107.
76. Bozic, C.R., et al., *The murine interleukin 8 type B receptor homologue and its ligands. Expression and biological characterization.* J Biol Chem, 1994. **269**(47): p. 29355-8.
77. Nomiyama, H., N. Osada, and O. Yoshie, *Systematic classification of vertebrate chemokines based on conserved synteny and evolutionary history.* Genes Cells, 2013. **18**(1): p. 1-16.
78. Farber, J.M., *Mig and IP-10: CXC chemokines that target lymphocytes.* J Leukoc Biol, 1997. **61**(3): p. 246-57.
79. Park, M.K., et al., *The CXC chemokine murine monokine induced by IFN-gamma (CXC chemokine ligand 9) is made by APCs, targets lymphocytes including activated B cells, and supports antibody responses to a bacterial pathogen in vivo.* J Immunol, 2002. **169**(3): p. 1433-43.
80. Luster, A.D. and J.V. Ravetch, *Biochemical characterization of a gamma interferon-inducible cytokine (IP-10).* J Exp Med, 1987. **166**(4): p. 1084-97.

81. Lauw, F.N., et al., *The CXC chemokines gamma interferon (IFN-gamma)-inducible protein 10 and monokine induced by IFN-gamma are released during severe melioidosis.* Infect Immun, 2000. **68**(7): p. 3888-93.
82. Loetscher, M., et al., *Chemokine receptor specific for IP10 and mig: structure, function, and expression in activated T-lymphocytes.* J Exp Med, 1996. **184**(3): p. 963-9.
83. Barnes, J.L., et al., *Adaptive immunity in melioidosis: a possible role for T cells in determining outcome of infection with Burkholderia pseudomallei.* Clin Immunol, 2004. **113**(1): p. 22-8.
84. Haque, A., et al., *Role of T cells in innate and adaptive immunity against murine Burkholderia pseudomallei infection.* J Infect Dis, 2006. **193**(3): p. 370-9.
85. Jenjaroen, K., et al., *T-Cell Responses Are Associated with Survival in Acute Melioidosis Patients.* PLoS Negl Trop Dis, 2015. **9**(10): p. e0004152.
86. Wiersinga, W.J., et al., *Melioidosis: insights into the pathogenicity of Burkholderia pseudomallei.* Nat Rev Microbiol, 2006. **4**(4): p. 272-82.
87. Bast, A., et al., *Caspase-1-dependent and -independent cell death pathways in Burkholderia pseudomallei infection of macrophages.* PLoS Pathog, 2014. **10**(3): p. e1003986.
88. Rathinam, V.A., et al., *TRIF licenses caspase-11-dependent NLRP3 inflammasome activation by gram-negative bacteria.* Cell, 2012. **150**(3): p. 606-19.
89. Chen, X., J.J. Oppenheim, and O.M. Howard, *BALB/c mice have more CD4+CD25+ T regulatory cells and show greater susceptibility to suppression of their CD4+CD25- responder T cells than C57BL/6 mice.* J Leukoc Biol, 2005. **78**(1): p. 114-21.
90. Kuroda, E., T. Kito, and U. Yamashita, *Reduced expression of STAT4 and IFN-gamma in macrophages from BALB/c mice.* J Immunol, 2002. **168**(11): p. 5477-82.
91. Sellers, R.S., et al., *Immunological variation between inbred laboratory mouse strains: points to consider in phenotyping genetically immunomodified mice.* Vet Pathol, 2012. **49**(1): p. 32-43.
92. Wakeham, J., J. Wang, and Z. Xing, *Genetically determined disparate innate and adaptive cell-mediated immune responses to pulmonary Mycobacterium bovis BCG infection in C57BL/6 and BALB/c mice.* Infect Immun, 2000. **68**(12): p. 6946-53.
93. Watanabe, H., et al., *Innate immune response in Th1- and Th2-dominant mouse strains.* Shock, 2004. **22**(5): p. 460-6.
94. Watkiss, E.R., et al., *Innate and adaptive immune response to pneumonia virus of mice in a resistant and a susceptible mouse strain.* Viruses, 2013. **5**(1): p. 295-320.
95. Depke, M., et al., *Bone marrow-derived macrophages from BALB/c and C57BL/6 mice fundamentally differ in their respiratory chain complex proteins, lysosomal enzymes and components of antioxidant stress systems.* J Proteomics, 2014. **103**: p. 72-86.
96. Caspi, R.R., et al., *T cell mechanisms in experimental autoimmune uveoretinitis: susceptibility is a function of the cytokine response profile.* Eye (Lond), 1997. **11 (Pt 2)**: p. 209-12.
97. Graus, Y.M., P.J. van Breda Vriesman, and M.H. de Baets, *Characterization of anti-acetylcholine receptor (AChR) antibodies from mice differing in susceptibility for experimental autoimmune myasthenia gravis (EAMG).* Clin Exp Immunol, 1993. **92**(3): p. 506-13.
98. Sun, B., et al., *Genetic susceptibility to experimental autoimmune uveitis involves more than a predisposition to generate a T helper-1-like or a T helper-2-like response.* J Immunol, 1997. **159**(2): p. 1004-11.
99. Kuraguchi, M., et al., *Differences in susceptibility to colonic stem cell somatic mutation in three strains of mice.* J Pathol, 2001. **193**(4): p. 517-21.
100. Medina, D., *Mammary tumorigenesis in chemical carcinogen-treated mice. I. Incidence in BALB-c and C57BL mice.* J Natl Cancer Inst, 1974. **53**(1): p. 213-21.

101. Ullrich, R.L., et al., *Strain-dependent susceptibility to radiation-induced mammary cancer is a result of differences in epithelial cell sensitivity to transformation.* Radiat Res, 1996. **146**(3): p. 353-5.
102. Jiang, X., et al., *Differences in innate immune responses correlate with differences in murine susceptibility to Chlamydia muridarum pulmonary infection.* Immunology, 2010. **129**(4): p. 556-66.
103. Reiner, S.L. and R.M. Locksley, *The regulation of immunity to Leishmania major.* Annu Rev Immunol, 1995. **13**: p. 151-77.
104. Stundick, M.V., et al., *Animal models for Francisella tularensis and Burkholderia species: scientific and regulatory gaps toward approval of antibiotics under the FDA Animal Rule.* Vet Pathol, 2013. **50**(5): p. 877-92.
105. Weening, E.H., et al., *The dependence of the Yersinia pestis capsule on pathogenesis is influenced by the mouse background.* Infect Immun, 2011. **79**(2): p. 644-52.
106. Breitbach, K., et al., *Role of inducible nitric oxide synthase and NADPH oxidase in early control of Burkholderia pseudomallei infection in mice.* Infect Immun, 2006. **74**(11): p. 6300-9.
107. Brenner, G.J., N. Cohen, and J.A. Moynihan, *Similar immune response to nonlethal infection with herpes simplex virus-1 in sensitive (BALB/c) and resistant (C57BL/6) strains of mice.* Cell Immunol, 1994. **157**(2): p. 510-24.
108. Hancock, G.E., R.W. Schaedler, and T.T. MacDonald, *Yersinia enterocolitica infection in resistant and susceptible strains of mice.* Infect Immun, 1986. **53**(1): p. 26-31.
109. Heinzel, F.P., R.M. Rerko, and A.M. Hujer, *Underproduction of interleukin-12 in susceptible mice during progressive leishmaniasis is due to decreased CD40 activity.* Cell Immunol, 1998. **184**(2): p. 129-42.
110. Kohler, J., et al., *NADPH-oxidase but not inducible nitric oxide synthase contributes to resistance in a murine Staphylococcus aureus Newman pneumonia model.* Microbes Infect, 2011. **13**(11): p. 914-22.
111. Tabel, H., R.S. Kaushik, and J.E. Uzonna, *Susceptibility and resistance to Trypanosoma congolense infections.* Microbes Infect, 2000. **2**(13): p. 1619-29.
112. Kaushik, R.S., et al., *Innate resistance to experimental African trypanosomiasis: differences in cytokine (TNF-alpha, IL-6, IL-10 and IL-12) production by bone marrow-derived macrophages from resistant and susceptible mice.* Cytokine, 2000. **12**(7): p. 1024-34.
113. Limmathurotsakul, D., et al., *Consensus on the development of vaccines against naturally acquired melioidosis.* Emerg Infect Dis, 2015. **21**(6).
114. Sahl, J.W., et al., *Genomic characterization of Burkholderia pseudomallei isolates selected for medical countermeasures testing: comparative genomics associated with differential virulence.* PLoS One, 2015. **10**(3): p. e0121052.

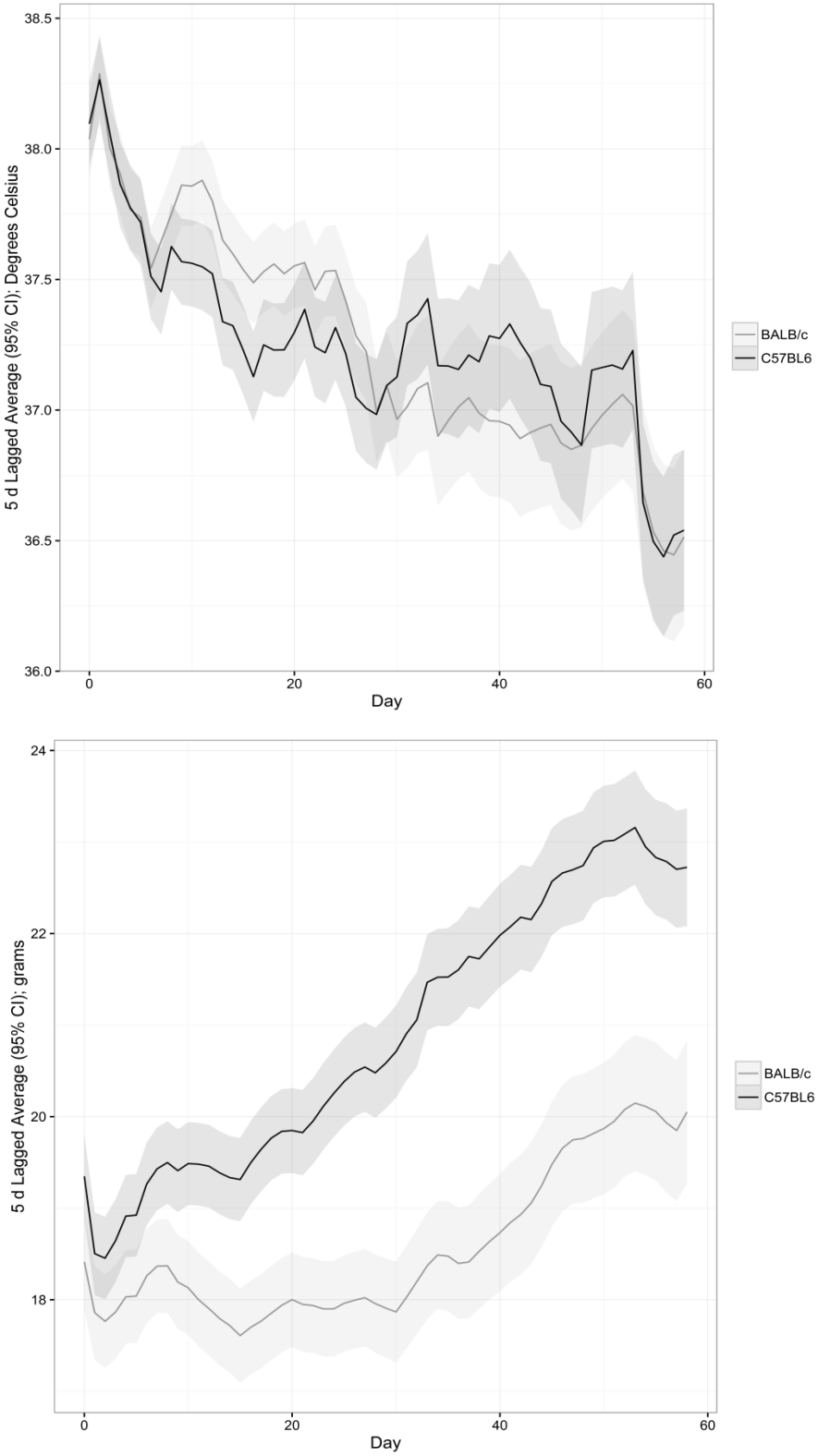
38.5
38.0
37.5
37.0
36.5
36.0
5 d Lagged Average (95% CI); Degrees Celsius
0
20
40
60
Day
BALB/c
C57BL6
24
22
20
18
5 d Lagged Average (95% CI); grams
0
20
40
60
Day
BALB/c
C57BL6

Figure 1

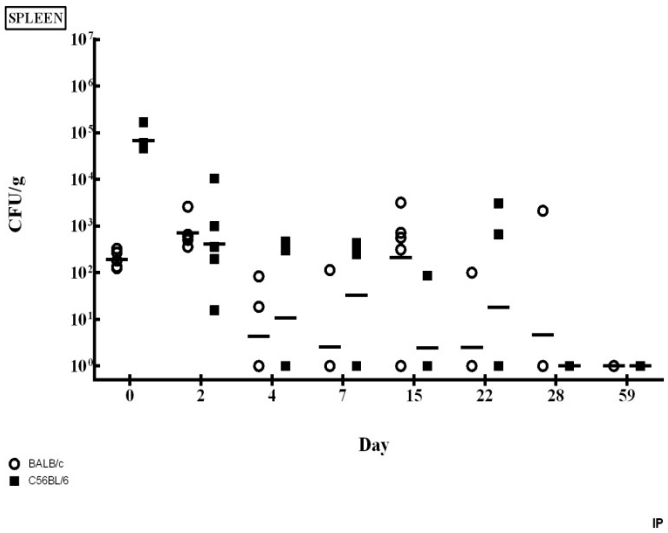
SPLEEN
CFU/g
Day
BALB/c
C56BL/6
IP

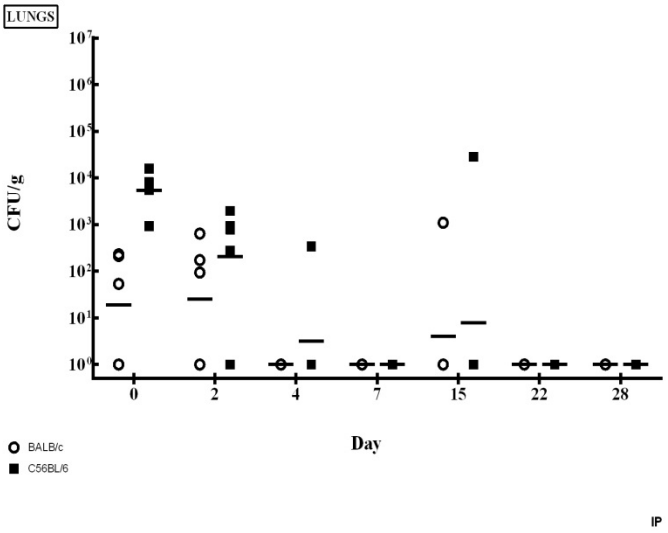
LUNGS
CFU/g
Day
BALB/c
C56BL/6
IP

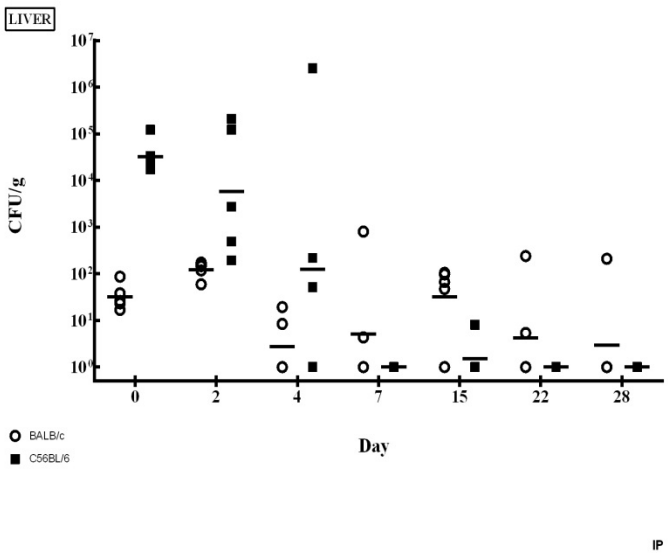
LIVER
CFU/g
Day
BALB/c
C56BL/6
IP

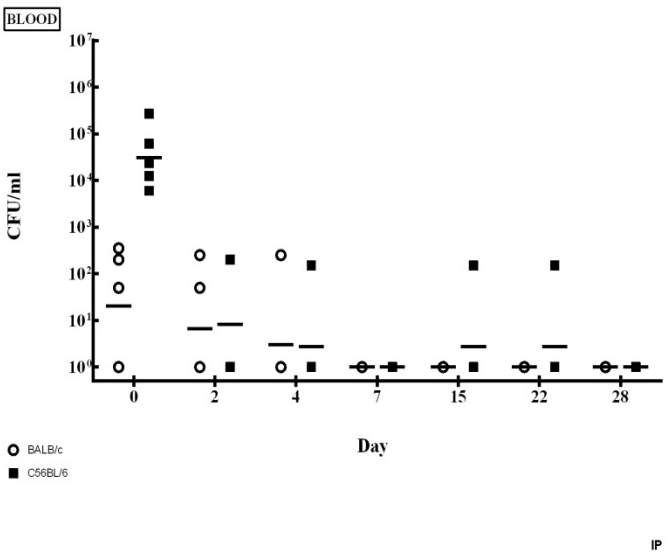
BLOOD
CFU/ml
Day
BALB/c
C56BL/6
IP

Figure 2

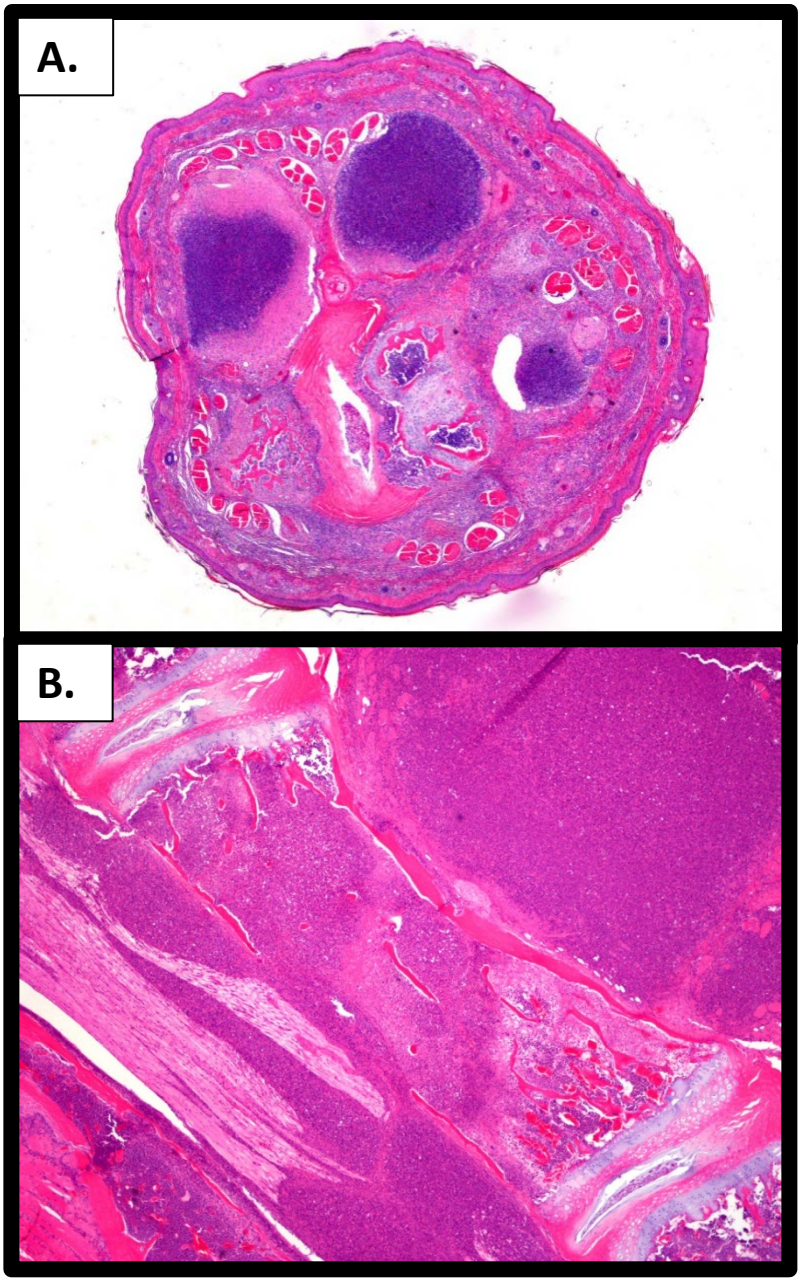

Figure 3

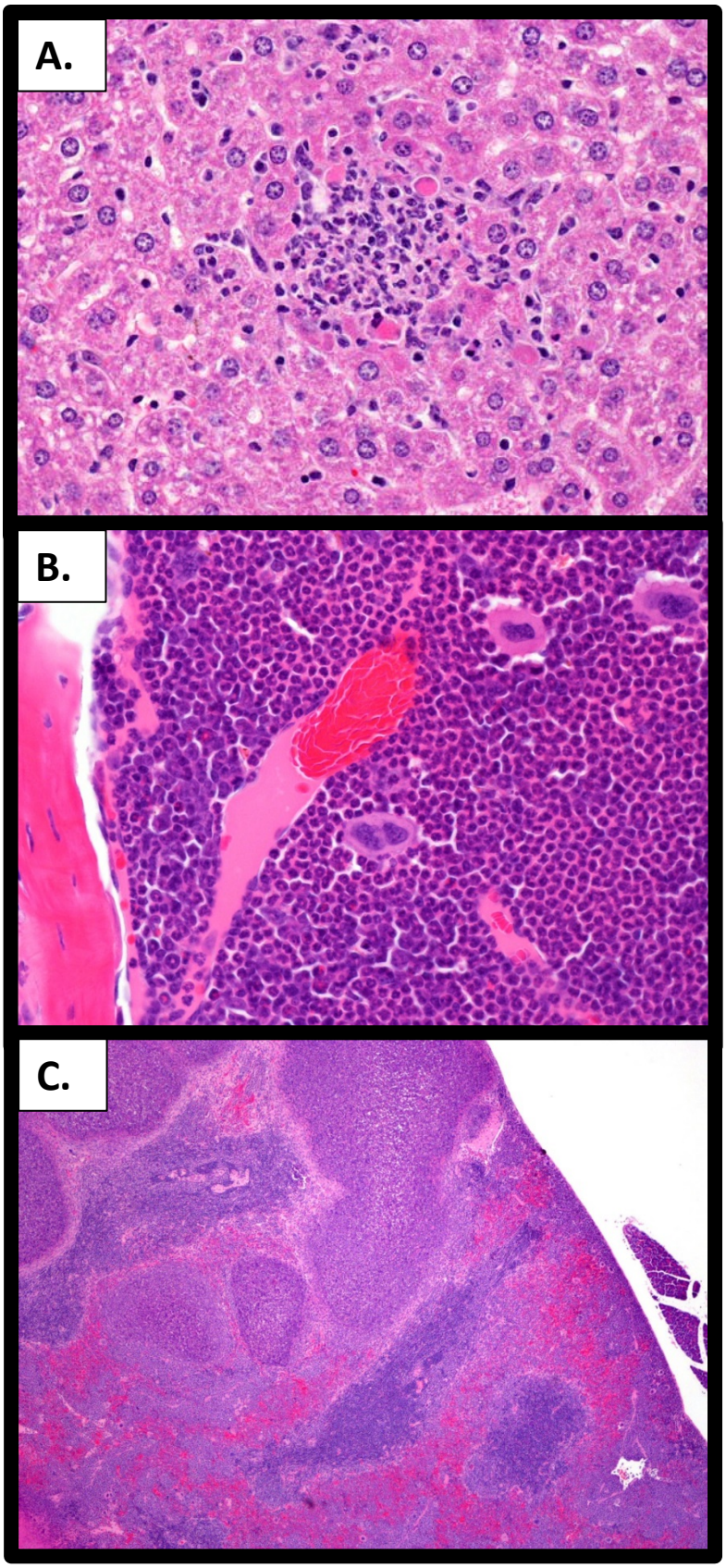

Figure 4

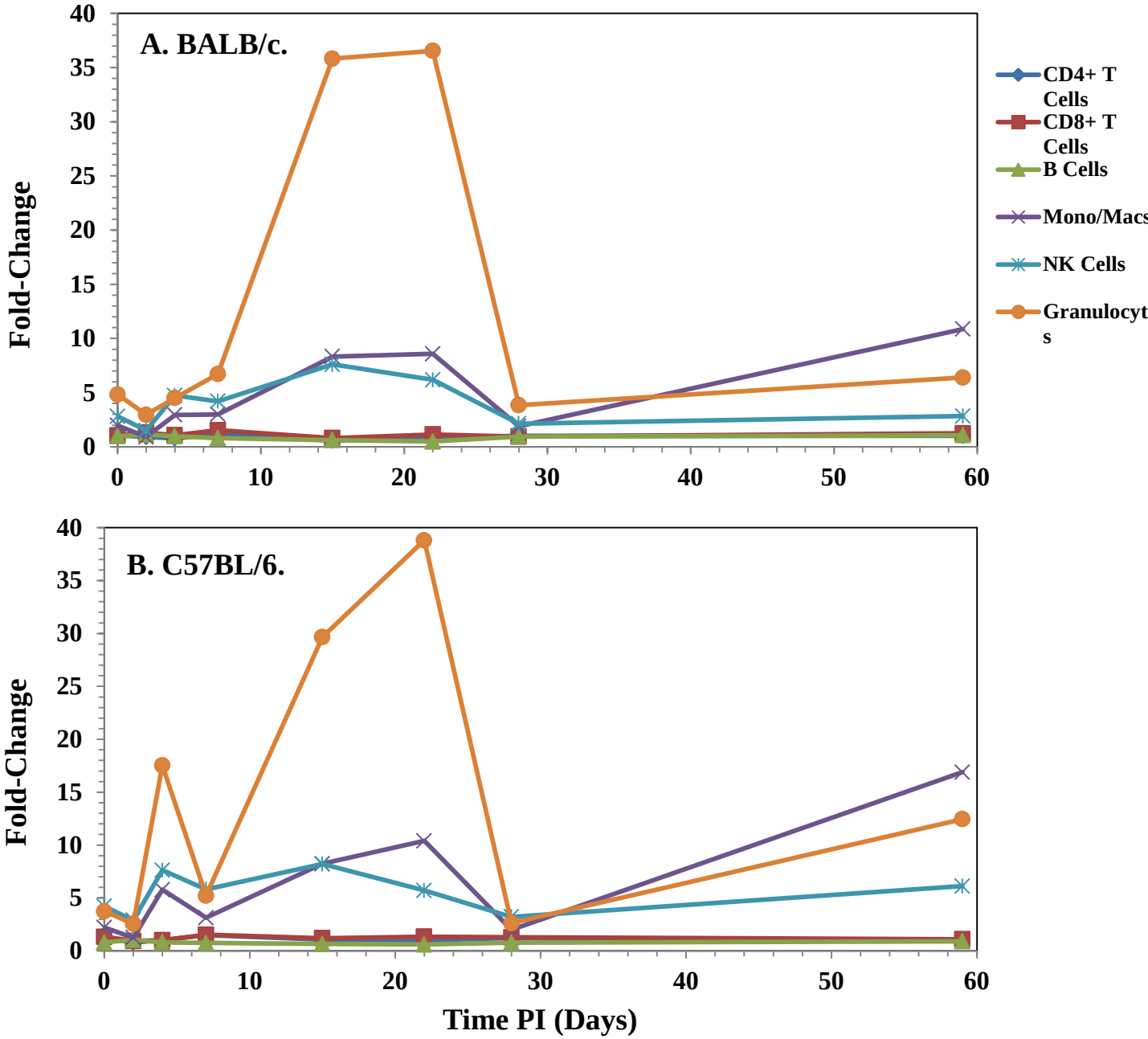

Figure 5 cell distribution after IP infection

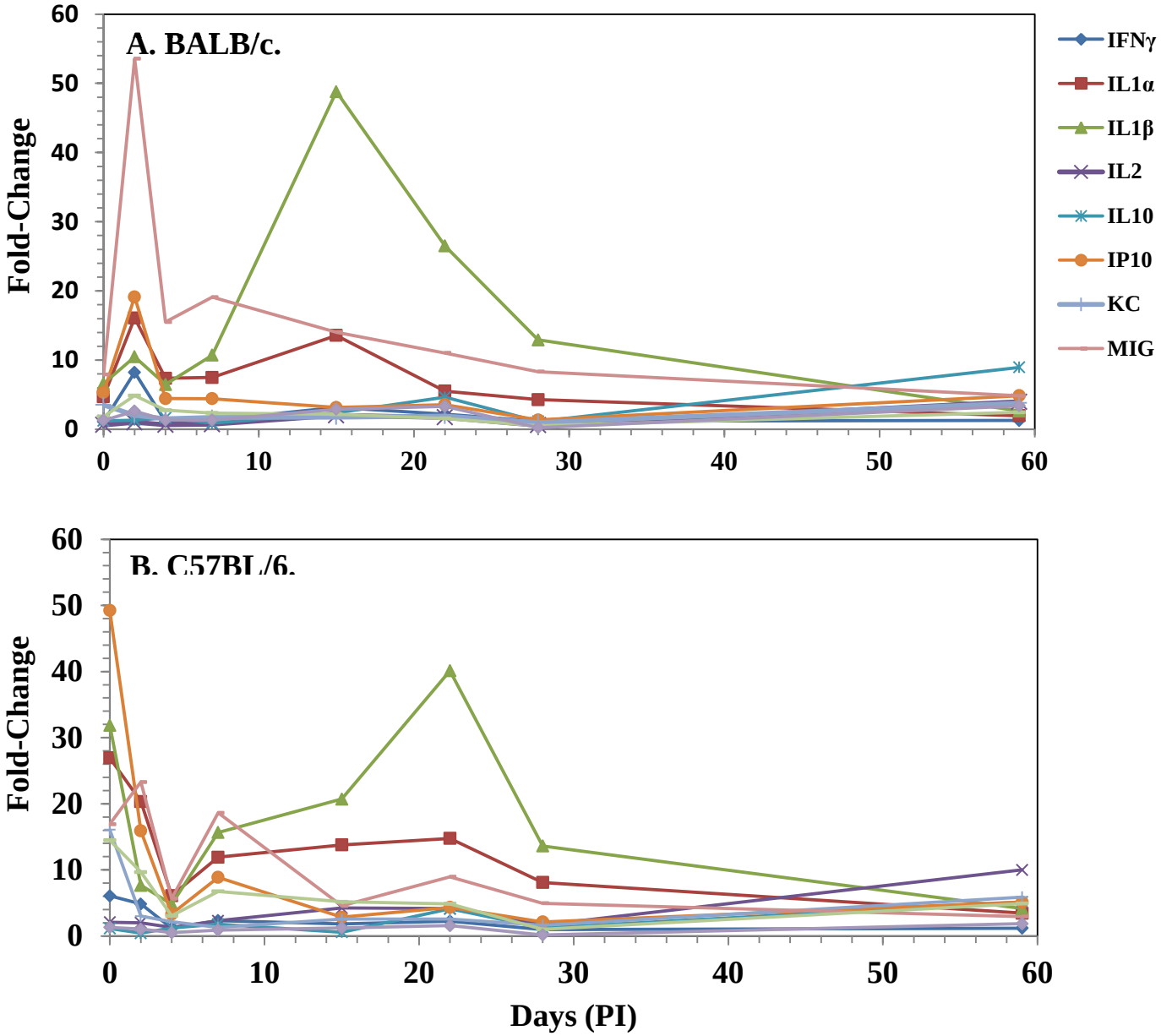

Figure 6-cytokine panel from spleen extracts after IP challenge

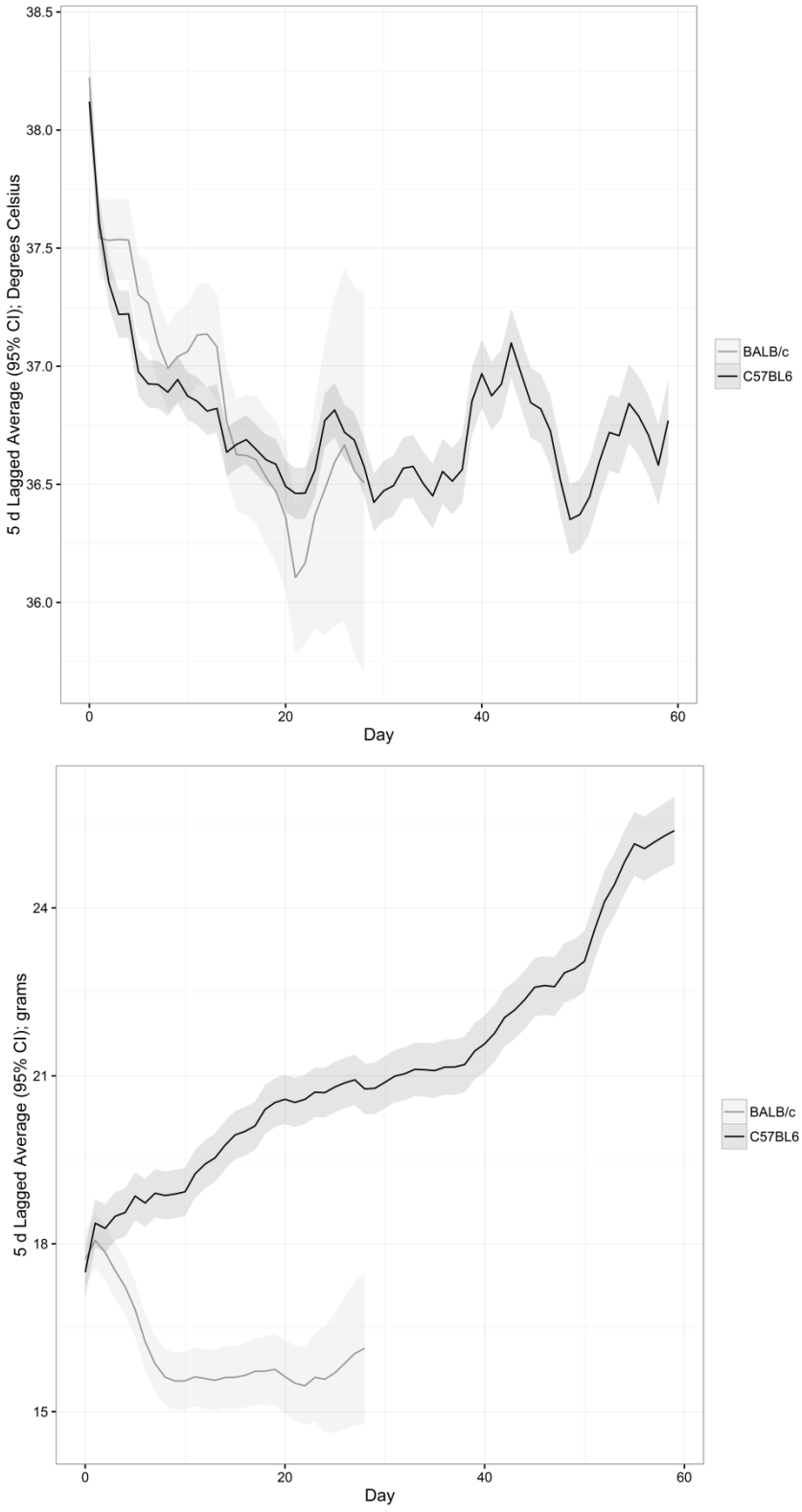
38.5
38.0
37.5
37.0
36.5
36.0
5 d Lagged Average (95% CI); Degrees Celsius
0
20
40
60
Day
BALB/c
C57BL6
24
21
18
15
5 d Lagged Average (95% CI); grams
0
20
40
60
Day
BALB/c
C57BL6

Figure 7

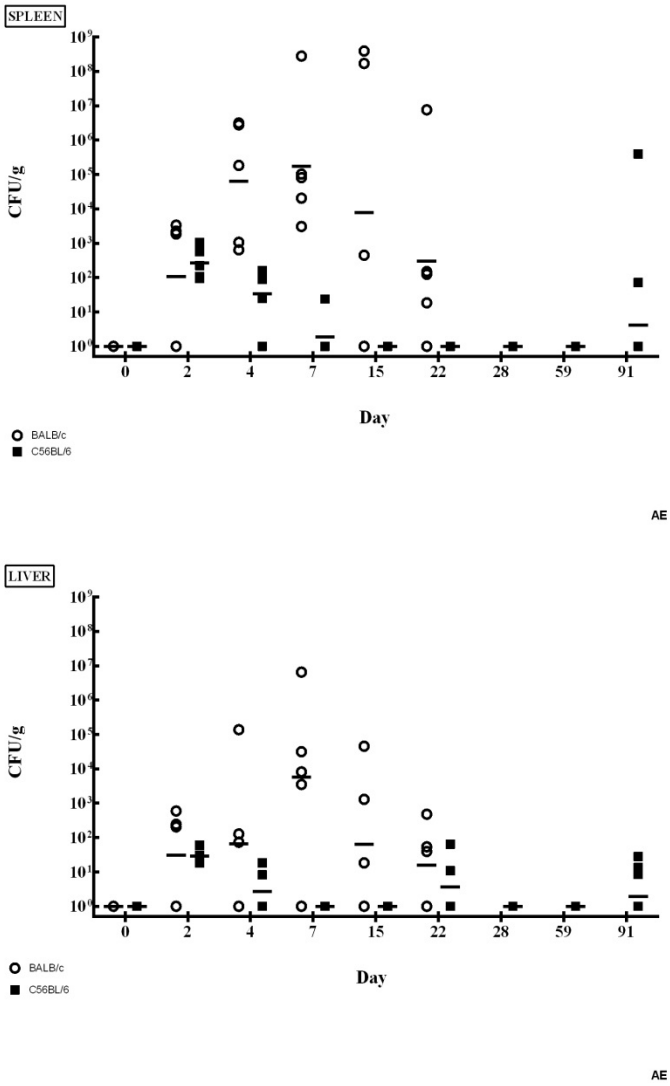
SPLEEN
CFU/g
Day
0
2
4
7
15
22
28
59
91
BALB/c
C56BL/6
AE

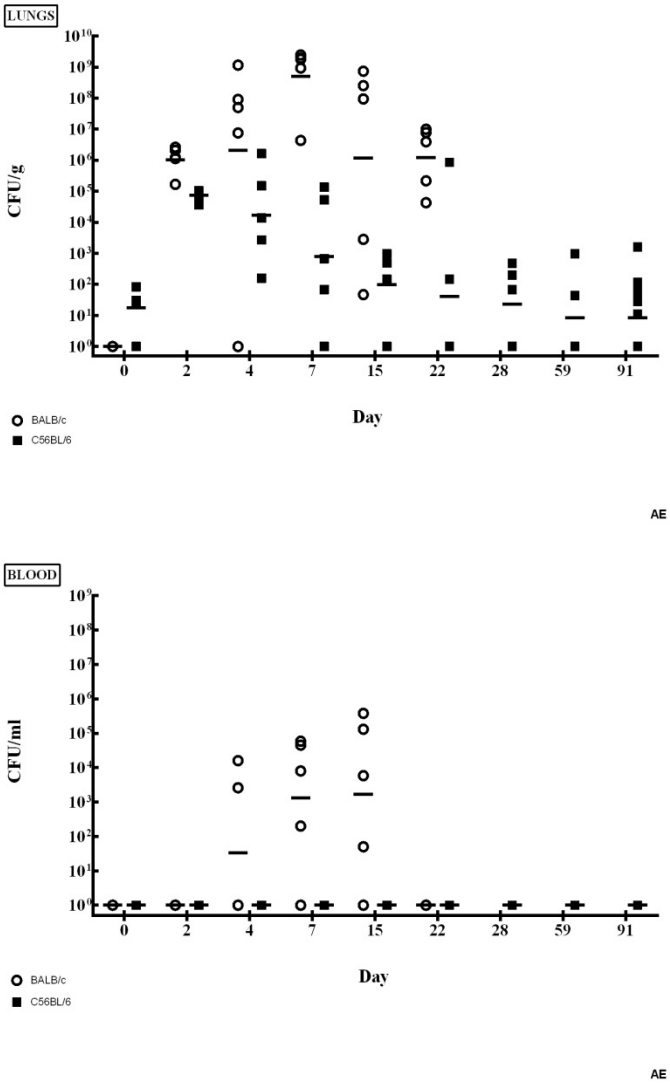
LUNGS
CFU/g
Day
0
2
4
7
15
22
28
59
91
BALB/c
C56BL/6
AE

LIVER
CFU/g
Day
0
2
4
7
15
22
28
59
91
BALB/c
C56BL/6
AE

BLOOD
CFU/ml
Day
0
2
4
7
15
22
28
59
91
BALB/c
C56BL/6
AE

Figure 8

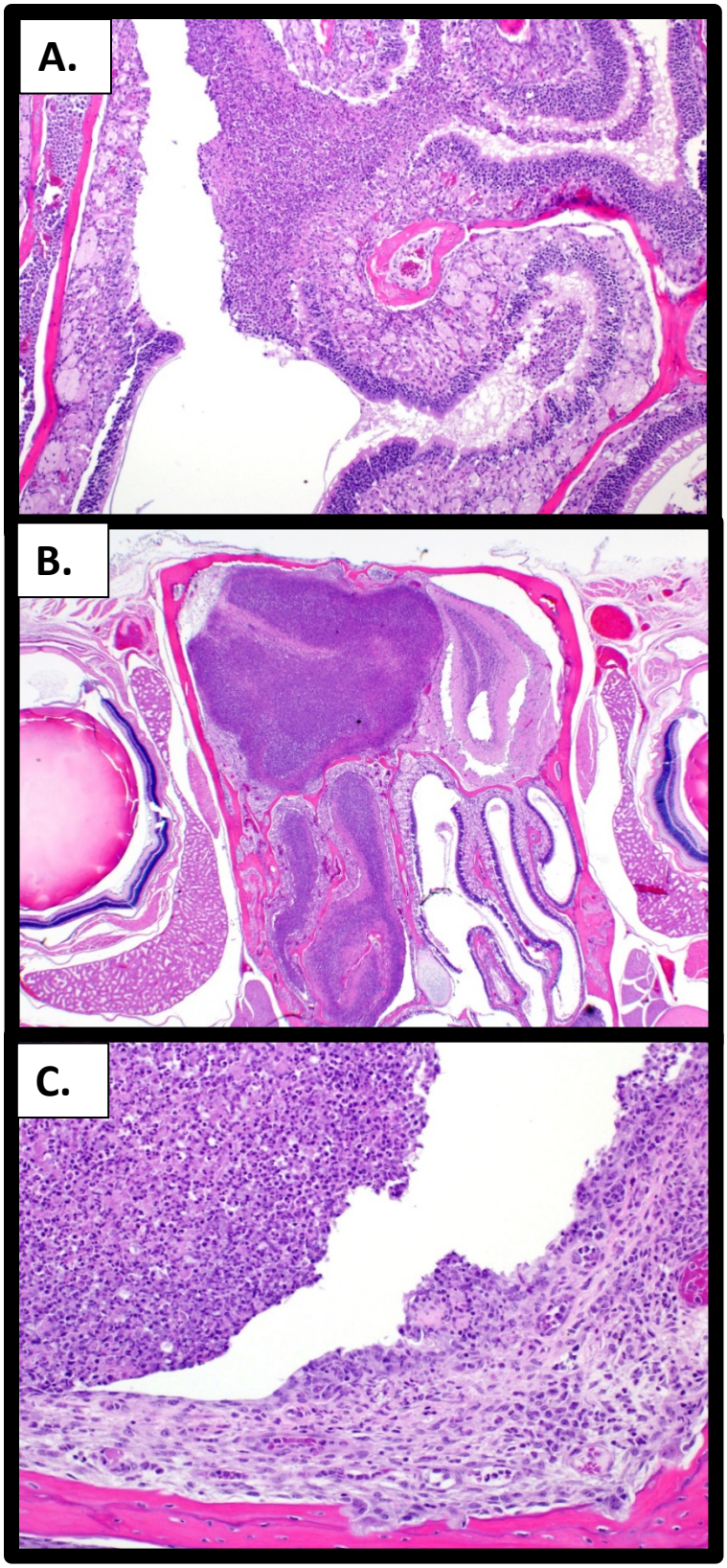

Figure 9

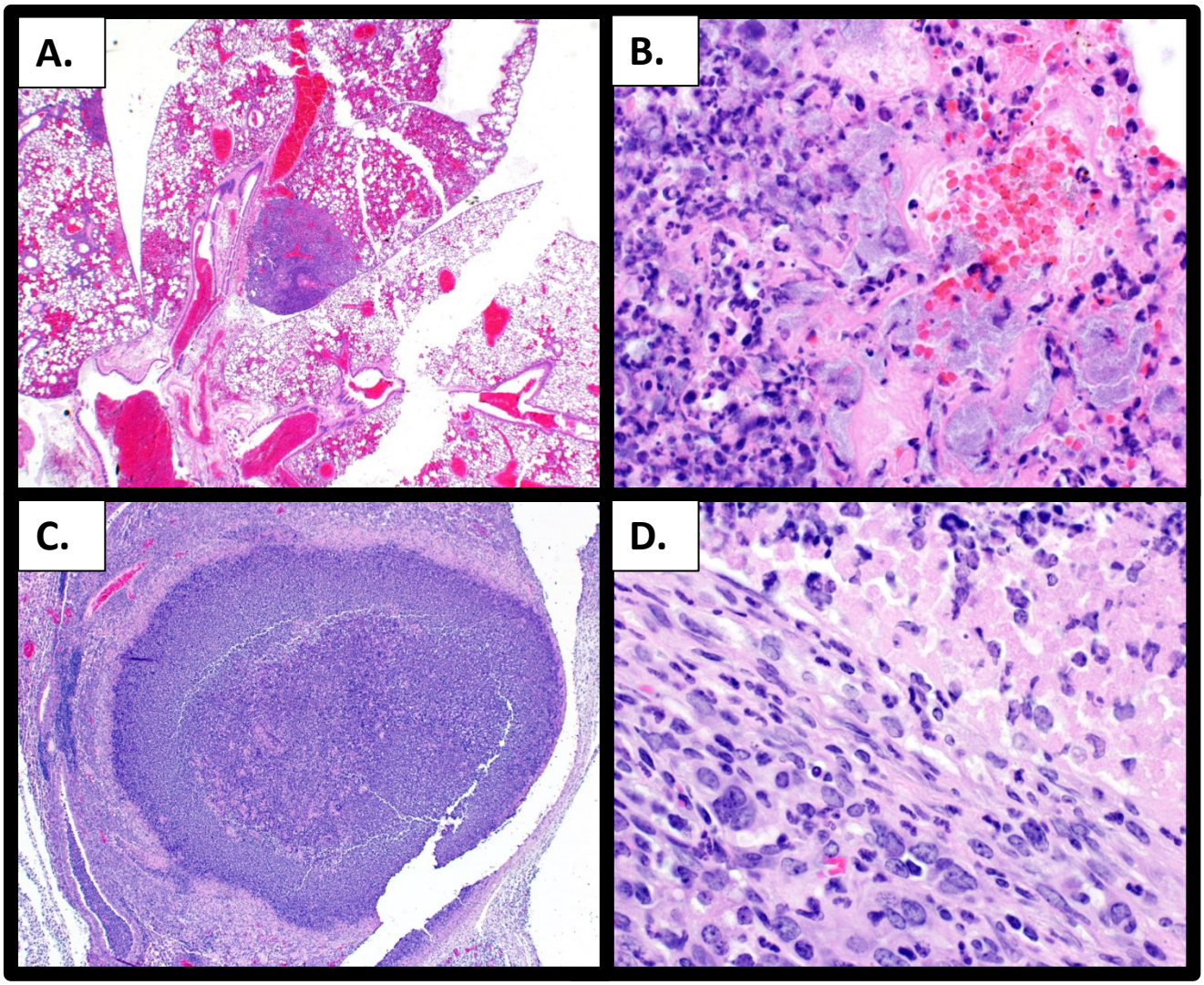

Figure 10

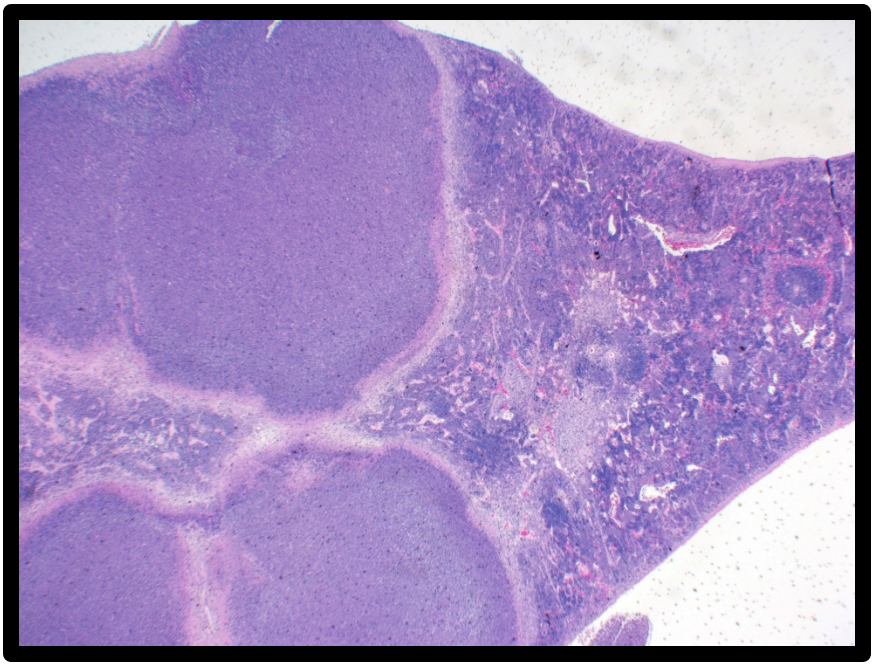

Figure 11

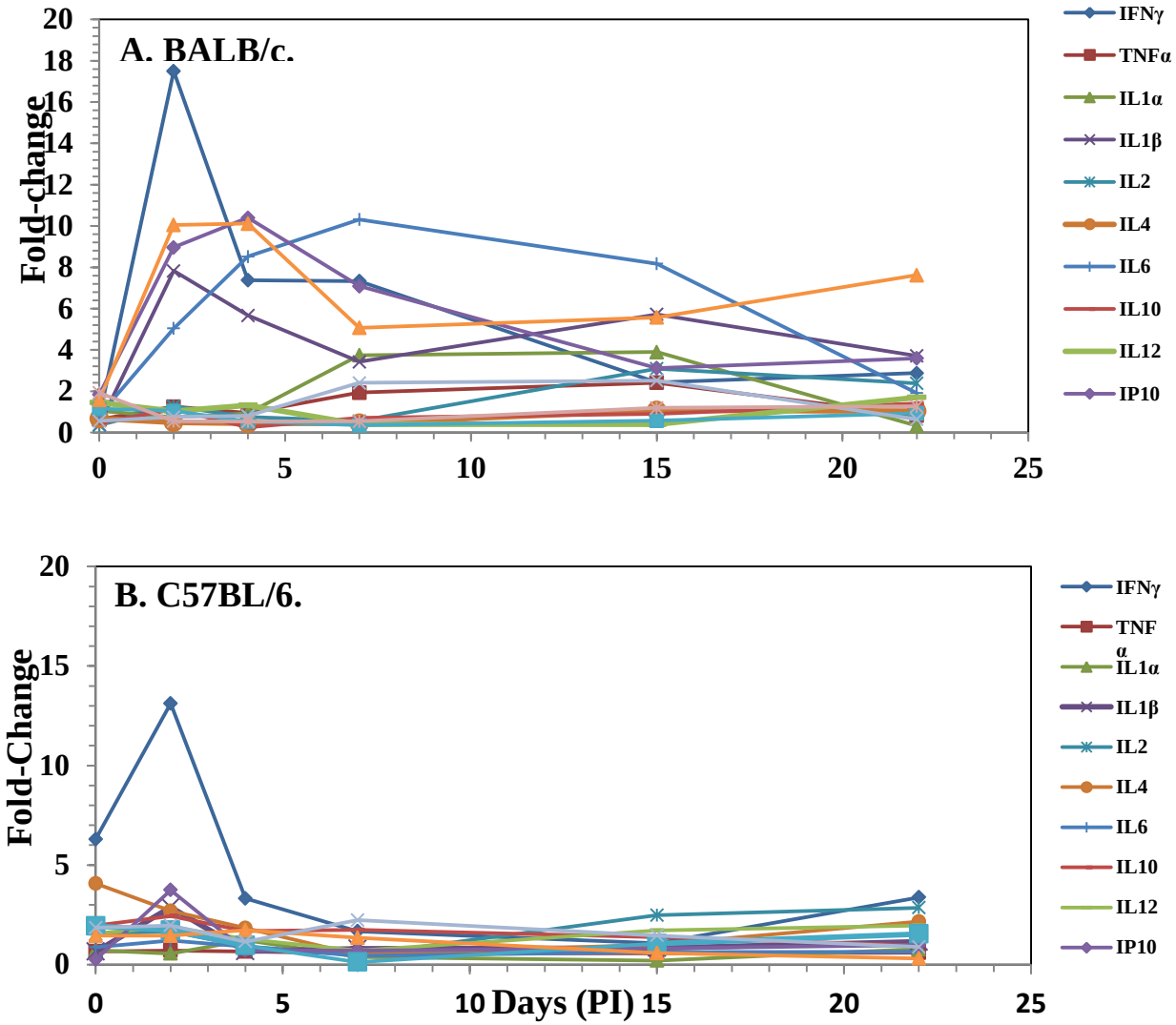

Figure 12-cytokine panel-sera after exposure to aerosolized bacteria-through day 22

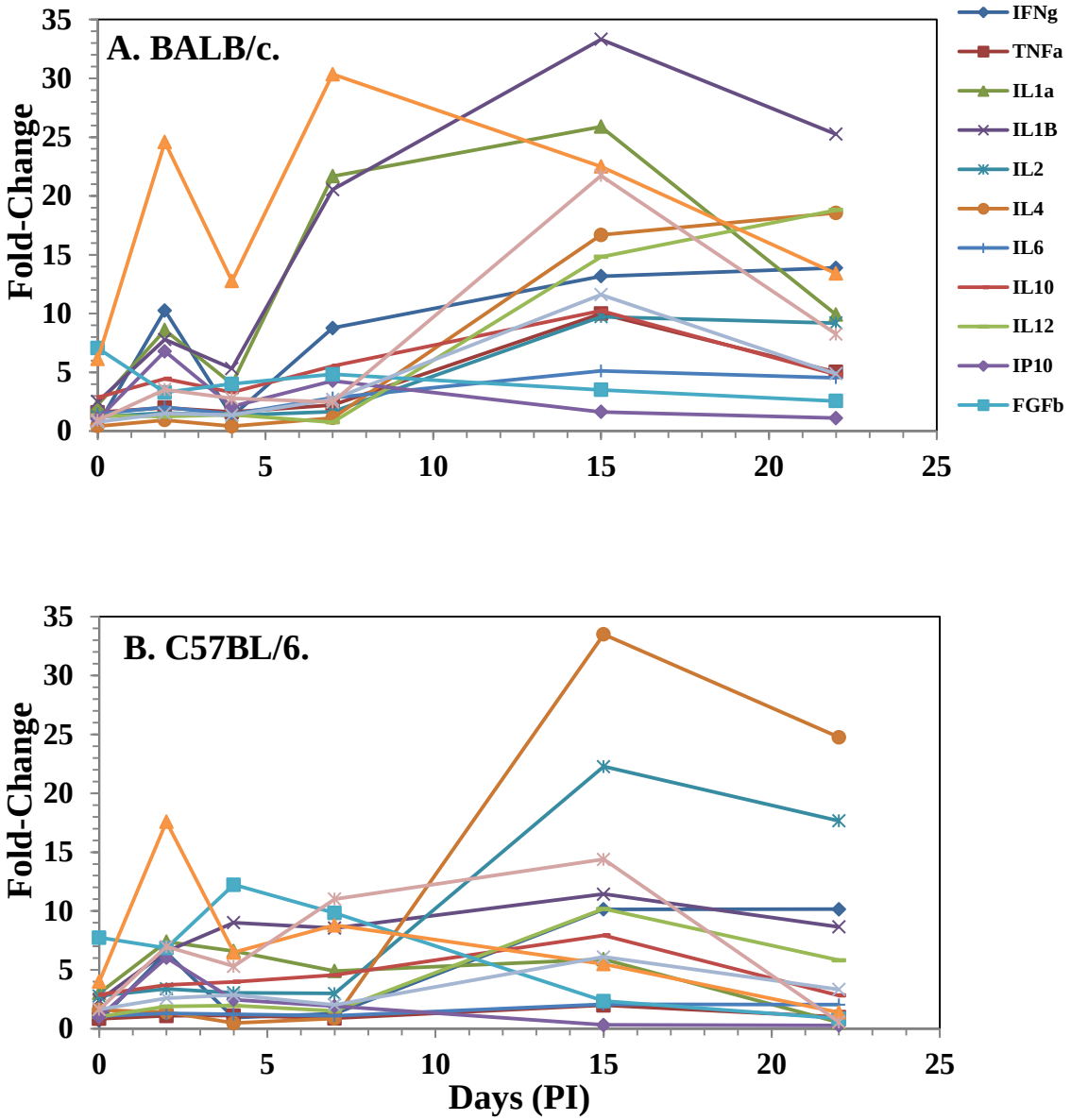

Figure 13-cytokine panel spleen extract after expose to aerosolized bacteria

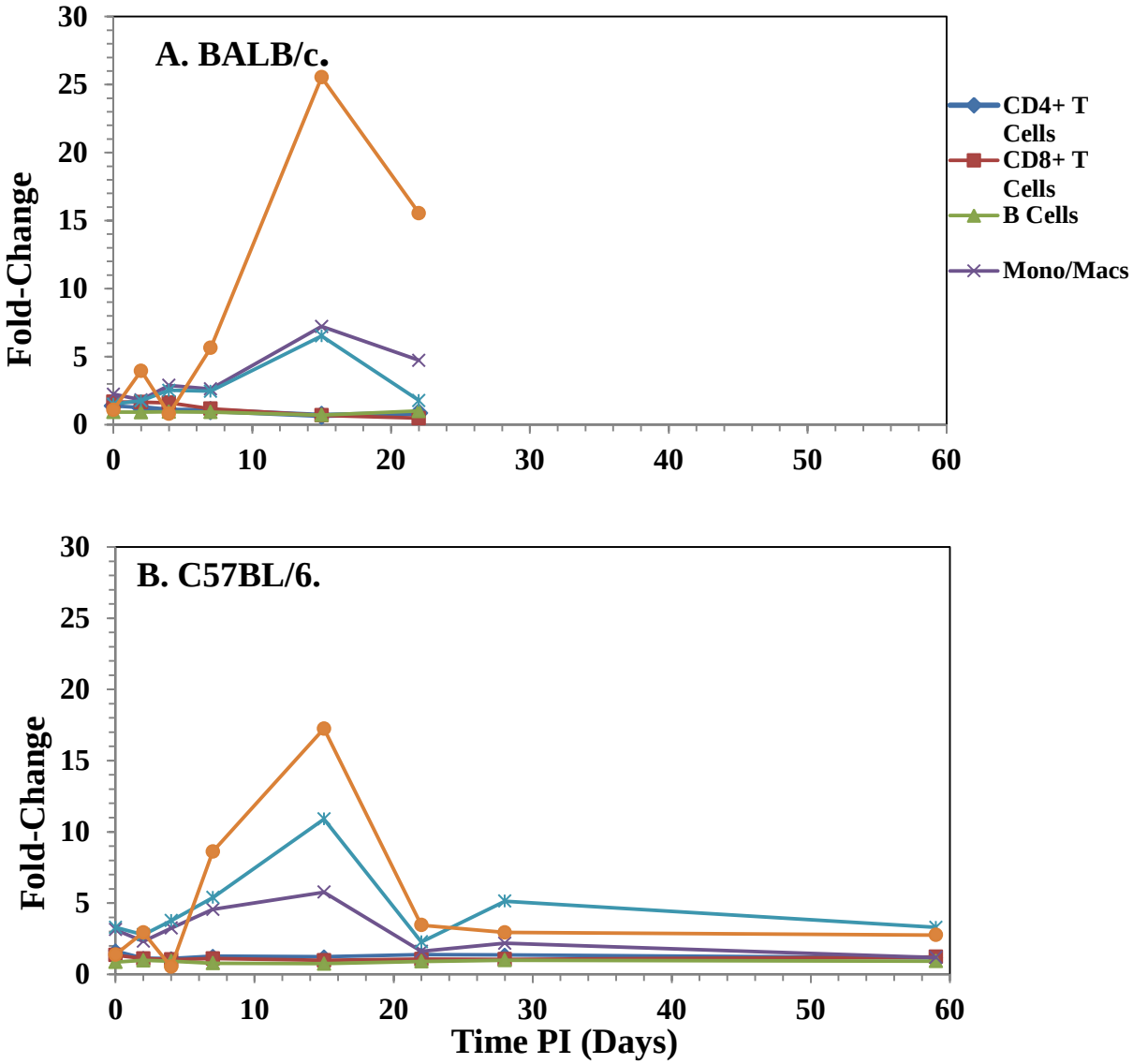

Figure 14-cell distribution spleen extract after expose to aerosolized bacteria

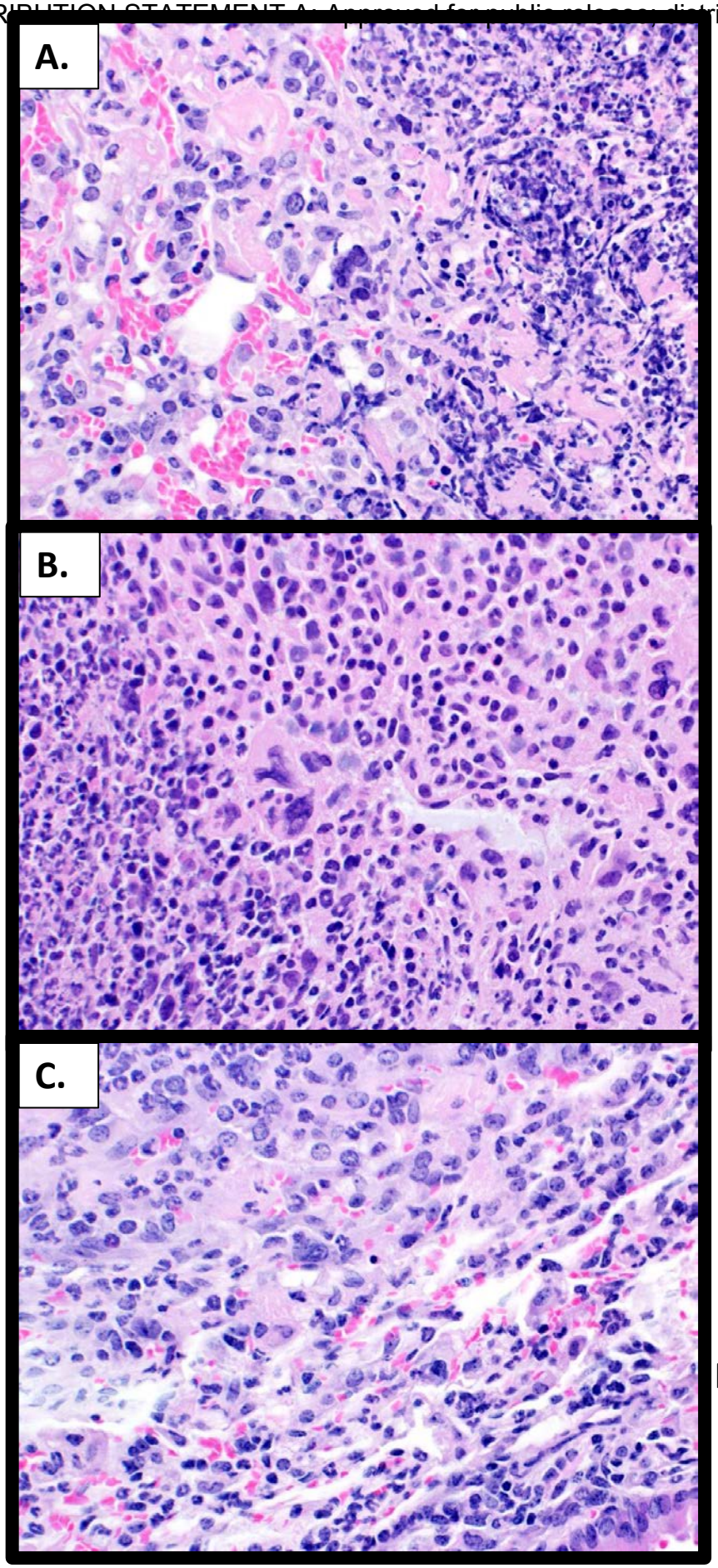

Figure 15-MNG

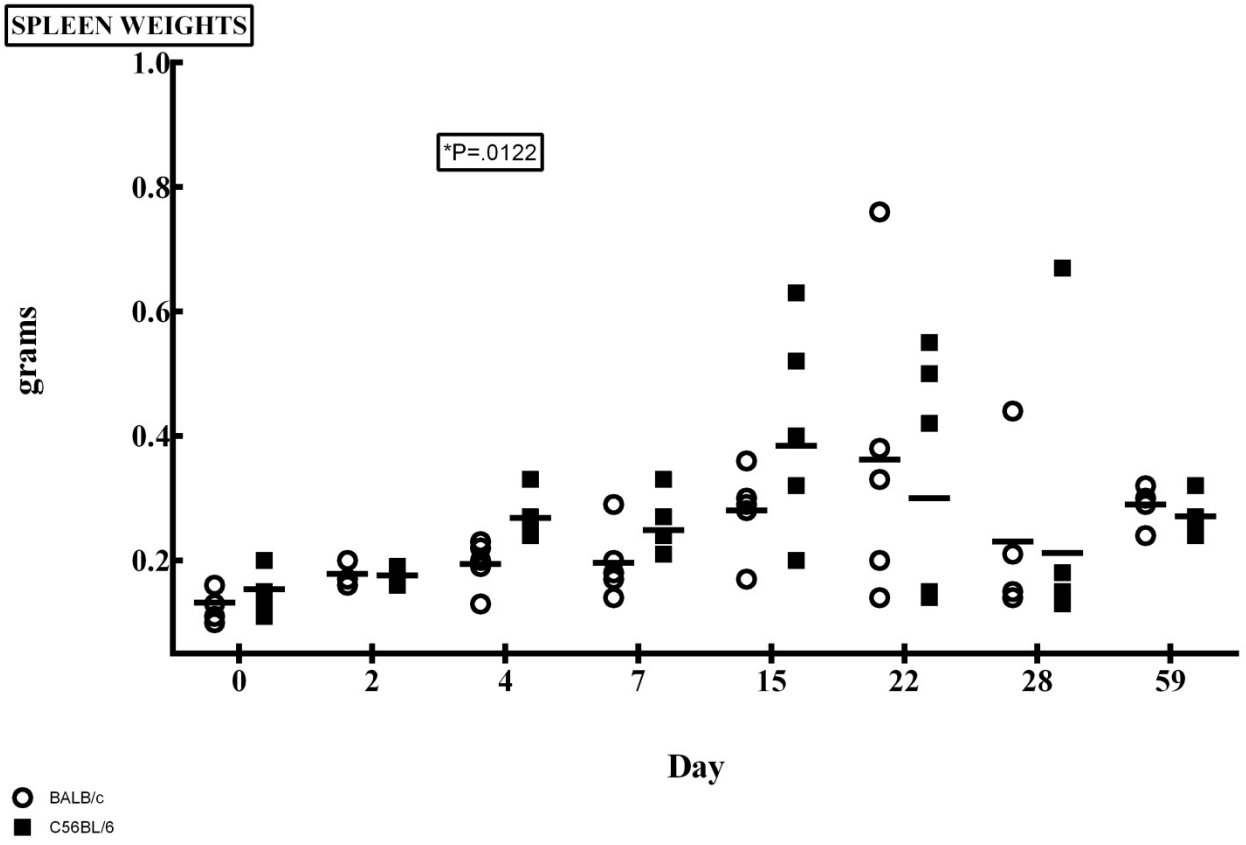

Figure S1-spleen weights after IP infection

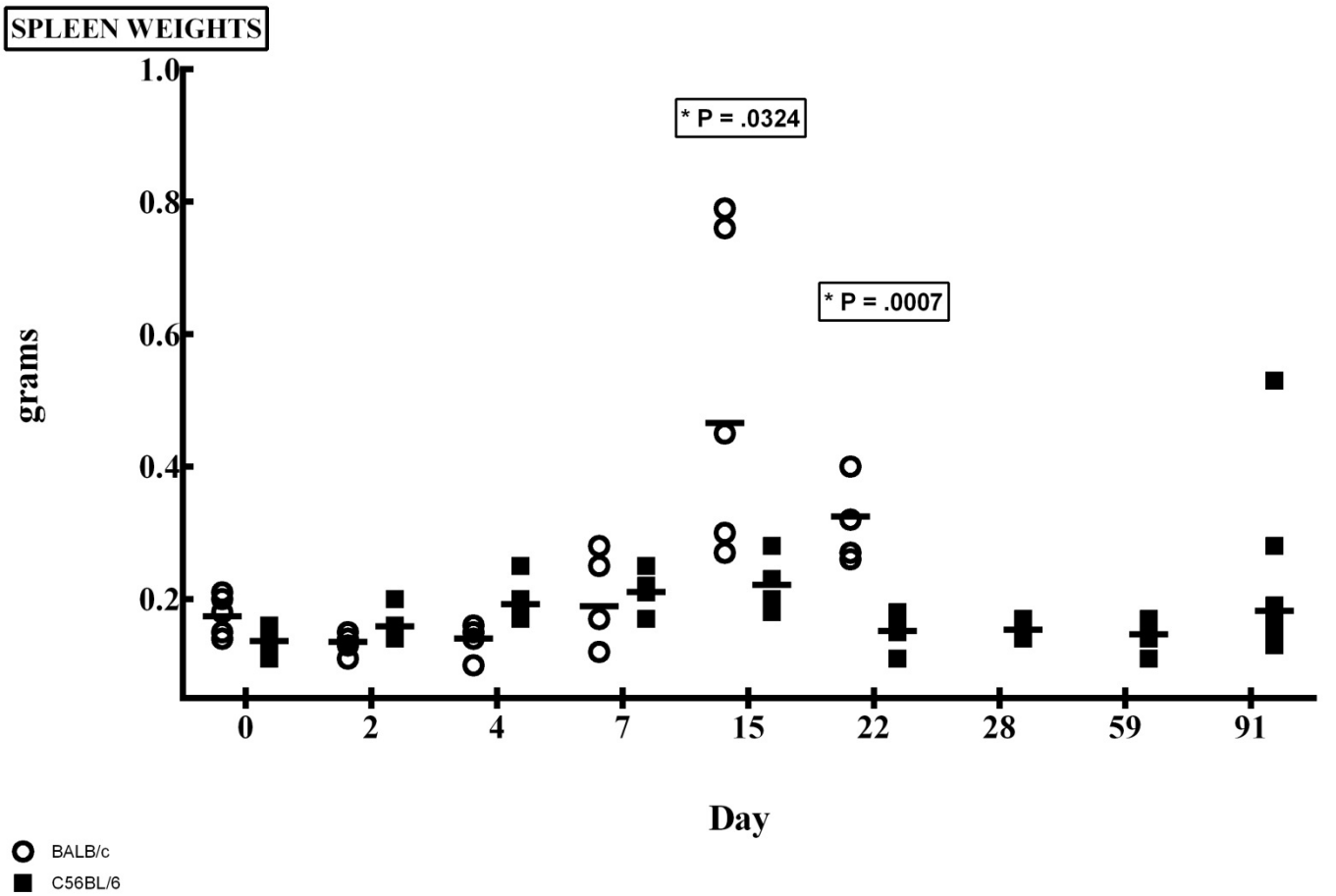

Figure S2-spleen weights after exposure to aerosolized bacteria

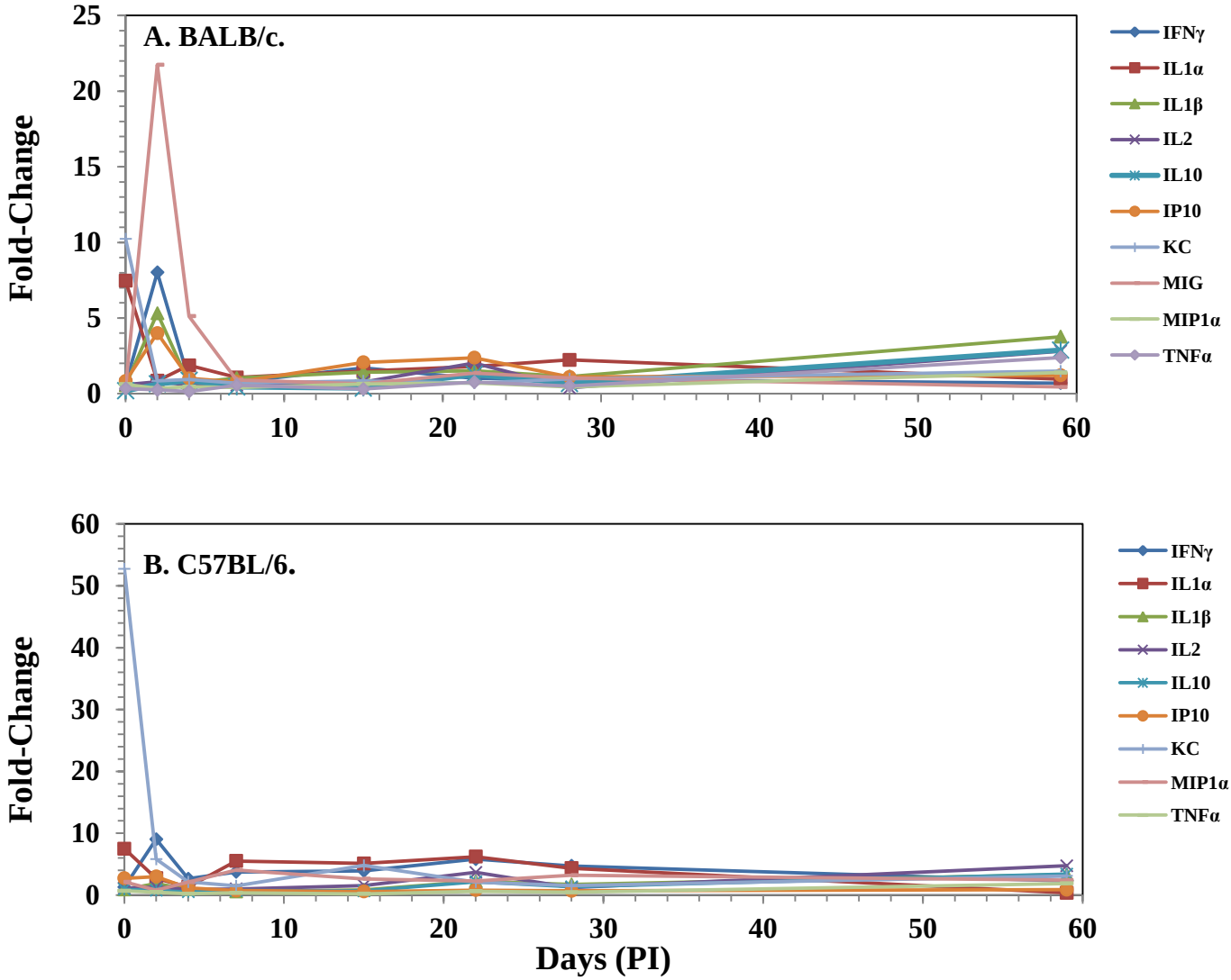

Table S3- cytokine panel sera after IP injections

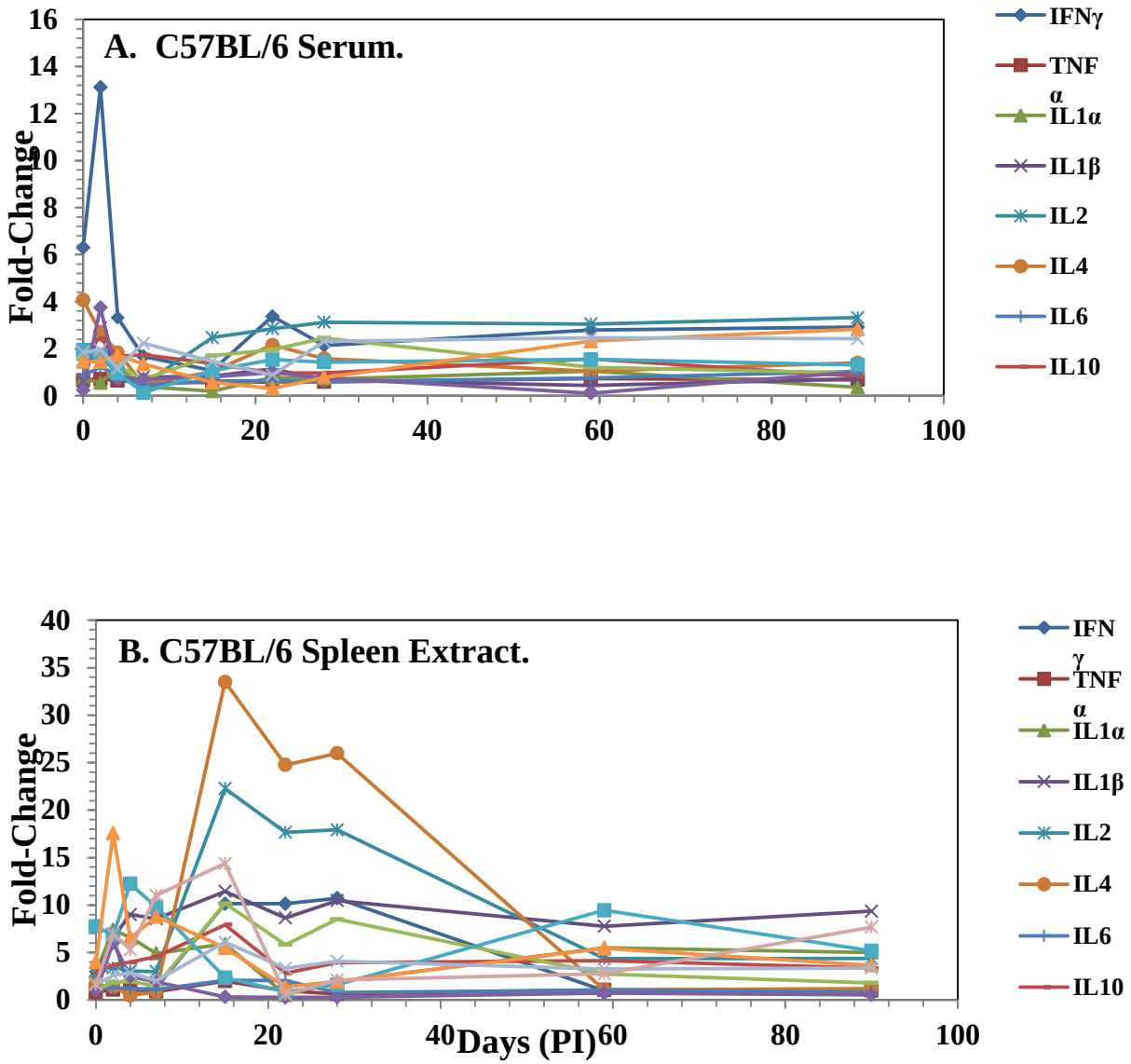

Figure s4 Cytokine Panel in both sera and spleen extract in C57Bl/6 mice exposed to aerosolized bacteria through day 90

Table S1. Cellular changes in spleen composition in BALB/c and C57BL/6 mice after IP challenge with *B. pseudomallei* K96243.

Mouse Strain	Cell type	% Cell Type[a]								
			Days (PI)							
		Normal, naïve mice[b]	0[c,d]	2	4	7	15	22	28	59
A. BALB/c.										
	CD4+ T Cells	**23.6(0.60)**	**24.5(4.28)**	**21.70.47)**	**18.4(0.80)**	**27.2(1.88)**	**13.4(3.43)**	**19.5(4.71)**	**24.2(4.25)**	**23.9(1.29)**
	CD8+ T Cells	**10.0(0.39)**	**10.5(1.97)**	**13.1(0.44)**	**10.8(0.69)**	**15.4(0.95)§**	**8.07(2.04)**	**12.0(2.55)**	**10.0(1.92)**	**13.1(1.30)†**
	B Cells	**51.1(2.03)**	**50.0(0.82)**	**57.6(1.52)†**	**49.8(1.81)**	**40.6(0.89)**	**31.5(5.69)**	**24.8(6.52)**	**48.2(0.63)**	**54.6(1.70)**
	Monocyte/Macrophages	**4.61(0.53)**	**9.10(4.65)**	**4.22(0.24)**	**13.6(1.67)§**	**13.8(2.57)§**	**38.4(8.70)§**	**39.6(13.9)†**	**8.73(4.52)**	**50.1(4.50)§**
	NK Cells	**4.55(0.58)**	**12.8(3.39)†**	**6.85(0.60)¶**	**21.6(1.79)§**	**19.2(1.93)§**	**34.6(9.46)¶**	**28.1(7.00)¶**	**9.71(2.78)**	**12.9(1.68)§**
	Granulocytes	**1.01(0.16)**	**4.88(3.77)**	**2.99(0.21)§**	**4.56(1.61)†**	**6.79(1.80)¶**	**36.2(7.96)§**	**36.9(13.9)†**	**3.89(3.36)**	**6.46(0.66)¶**
B. C57BL/6.										
			0	**2**	**4**	**7**	**15**	**22**	**28**	**59**
	CD4+ T Cells	**16.2(0.64)**	**20.0(2.41)**	**12.7(0.66)**	**16.4(0.40)**	**23.8(1.67)§**	**17.3(1.81)**	**16.2(2.39)**	**19.7(2.40)**	**16.9(0.85)**
	CD8+ T Cells	**10.8(0.35)**	**14.4(1.25)¶**	**10.1(0.41)**	**10.8(0.50)**	**16.5(1.42)§**	**12.9(2.96)**	**14.6(2.44)**	**13.9(1.12)¶**	**11.8(0.31)†**
	B Cells	**65.1(0.55)**	**52.0(4.86)**	**67.6(0.75)¶**	**52.6(3.19)**	**48.6(1.61)**	**42.4(3.34)**	**38.7(5.99)**	**50.1(4.96)**	**59.2(1.49)**
	Monocyte/Macrophages	**2.81(0.30)**	**6.18(2.70)**	**3.51(0.30)**	**16.2(4.59)†**	**8.78(1.97)¶**	**23.1(4.56)§**	**29.2(6.93)§**	**5.62(2.64)**	**47.5(3.52)§**
	NK Cells	**2.34(0.24)**	**9.85(2.54)¶**	**6.78(0.49)§**	**17.8(2.09)§**	**13.6(0.76)§**	**19.2(1.84)§**	**13.4(2.57)§**	**7.53(2.66)**	**14.3(1.98)§**
	Granulocytes	**0.58(0.90)**	**2.17(1.40)**	**1.48(0.22)§**	**10.2(4.59)†**	**3.03(1.18)†**	**17.2(4.45)§**	**22.5(7.79)¶**	**1.52(1.18)**	**7.22(0.57)§**

[a] % Cell type were reported as geometric means with the geometric standard error of the means.

[b] N was 10 for normal naïve BALB/c mice, and N was 4 for normal naïve C57BL/6 mice.

[c] N was equal to 5 for each mouse strain at each time point post-infection (PI).

[d] For significant levels compared to the naïve, control mice: † $P < 0.05$; ¶ $P < 0.01$; § $P \leq 0.001$.

Table S2. Cytokines/chemokines in serum from BALB/c and C57BL/6 mice after IP challenge with *B. pseudomallei* K96243.

Cytokine/ Chemokine	Mouse Strain[b]	Amount Cytokine/Chemokine Expressed (pg/ml)[a]								
		Time (Days PI)								
		Naïve[c], Control	0[d]	2	4	7	15	22	28	59
IFN-γ	BALB/c	21.0(1.13)	12.9(1.27)	168.3(1.11)§	18.6(1.49)	16.2(1.03)	35.8(1.33)	21.5(1.42)	20.3(1.42)	14.6(1.05)
	C57BL/6	10.8(1.47)	13.9(1.21)	97.6(1.11)¶	28.6(1.49)	40.3(1.16)†	42.2(1.33)†	62.7(1.09)†	51.0(1.20)†	24.8(1.28)
TNF-α	BALB/c	23.0(1.01)	7.7(1.67)	5.7(1.14)	3.3(1.65)	12.9(1.78)	7.1(1.33)	17.5(1.12)	11.7(1.27)	55.0(1.30)†
	C57BL/6	24.0(1.03)	16.6(1.22)	11.3(1.40)	5.3(1.87)	8.6(1.99)	4.6(1.17	15.0(1.03)	10.7(1.09)	44.8(1/11)¶
IL-1α	BALB/c	25.9(1.01)	196.2(1.16)§	22.4(1.65)	49.1(1.52)	27.8(1.25)	39.4(1.95)	47.1(2.07)	58.8(1.64)	25.3(1.12)
	C57BL/6	30.9(1.18)	235.3(1.15)§	85.3(1.33)†	41.2(1.30)	172.9(1.21)§	160.9(1.11)§	194.7(1.47)¶	136.5(1.27)¶	11.0(2.03)
IL-1β	BALB/c	22.2(1.01)	11.8(1.69)	113.9(1.12)§	14.4(1.31)	21.9(1.01)	30.5(1.41)	32.3(1.25)	24.2(1.24)	80.5(1.43)†
	C57BL/6	21.8(1.01)	19.7(1.44)	40.1(1.36)	19.9(1.45)	12.4(1.42)	18.1(1.17)	47.7(1.23)†	36.8(1.14)†	70.3(1.55)
IL-2	BALB/c	5.8(1.07)	3.5(1.04)	4.6(1.04)	3.3(1.01)	3.2(1.03)	4.5(1.27)	11.8(1.21)†	2.2(1.15)	16.3(1.02)§
	C57BL/6	4.0(1.04)	4.4(1.07)	5.2(1.03)	3.7(1.07)	4.0(1.06)	6.2(1.37)	14.7(1.07)§	4.8(1.28)	19.0(1.03)§
IL-5	BALB/c	19.8(1.02)	36.7(1.21)†	10.7(1.34)	10.2(1.55)	19.7(1.02)	22.5(1.10)	12.6(1.41)	10.3(1.33)	13.8(1.19)
	C57BL/6	15.8(1.27)	96.5(1.19)¶	37.2(1.20)†	19.7(1.02)	19.0(1.18)	19.3(1.02)	8.3(1.50)	13.8(1.35)	21.3(1.39)
IL-6	BALB/c	24.7(1.05)	49.6(1.29)	34.3(1.20)	8.5(1.50)	7.1(2.34)	40.3(1.46)	52.2(1.46)	16.3(1.97)	16.4(1.02)
	C57BL/6	29.1(1.01)	60.6(1.36)	18.2(1.18)	22.2(1.93)	12.1(1.53)	24.5(1.26)	26.0(1.24)	18.7(1.35)	17.9(1.17)
IL-10	BALB/c	50.8(1.16)	9.5(1.70)	32.6(1.38)	44.0(1.01)	22.5(1.95)	18.5(2.34)	64.3(1.24)	33.8(1.32)	146.1(1.13)§
	C57BL/6	43.5(1.01)	41.3(1.34)	33.1(1.19)	22.6(1.44)	31.9(1.33)	29.8(1.25)	93.9(1.25)	58.1(1.26)	147.9(1.07)§
FGFb	BALB/c	216.8(1.12)	389.8(1.28)	288(1.05)†	335.2(1.11)†	188.6(1.07)	194.5(1.05)	226(1.19)	216.6(1.06)	176.7(1.30)
	C57BL/6	262.4(1.19)	419.9(1.12)	516.9(1.05)†	464.2(1.14)†	527.4(1.14)†	424.2(1.11)	564.9(1.07)†	414.5(1.12)	318.0(1.31)
IP10	BALB/c	23.3(1.21)	19.3(1.06)	93.3(1.16)§	23.5(1.22)	18.1(1.09)	48.1(1.47)	55.3(1.36)†	25.7(1.50)	28.2(1.57)
	C57BL/6	26.1(1.30)	70.9(1.45)	78.0(1.43)†	29.8(1.34)	19.2(1.02)	14.6(1.19)	21.1(1.20)	17.9(1.05)	22.8(1.28)
KC	BALB/c	260.7(1.40)	2668(1.15)§	218.4(1.70)	243.2(1.94)	182.0(2.15)	219.7(1.39)	182.6(1.50)	255.0(1.80)	386.7(1.43)
	C57BL/6	73.0(1.06)	3848(1.08)§	424.4(1.68)†	155.5(1.39)	108.5(1.33)	350.1(1.87)	154.3(1.65)	111.3(2.21)	225.4(1.38)†
MCP-1	BALB/c	21.2(1.01)	43.4(1.53)	37.2(1.16)†	20.7(1.01)	24.9(1.14)	19.3(1.08)	20.0(1.15)	11.7(1.06)	19.3(1.63)
	C57BL/6	20.4(1.02)	247.5(1.29)§	118.0(1.54)†	21.4(1.03)	19.7(1.21)	21.5(1.05)	28.7(1.20)	21.6(1.32)	25.9(1.48)
MIG	BALB/c	184.4(1.16)	70.3(1.47)	4009(1.11)§	943.7(1.06)§	167.2(1.14)	120.2(2.13)	251.8(1.36)	192(1.50)	81.2(1.54)
	C57BL/6	9.1(1.14)	493.7(1.33)§	2107(1.13)§	491.8(1.27)§	90.7(1.42)¶	183.4(1.39)§	136.9(1.23)§	98.0(1.33)§	77.3(1.15)§
MIP-1α	BALB/c	38.4(1.01)	23.8(1.35)	13.5(1.08)	17.8(1.30)	15.7(1.31)	24.5(1.99)	27.5(1.07)	17.2(1.28)	53.5(1.16)
	C57BL/6	18.3(1.55)	39.1(1.09)	14.8(1.29)	38.4(1.31)	73.9(1.57)	48.1(1.53)	41.6(1.10)	58.6(1.26)	44.2(1.18)
VEGF	BALB/c	12.2(1.31)	5.4(1.99)	4.1(1.45)	7.3(1.52)	4.1(1.71)	9.0(1.52)	15.3(1.26)	7.9(1.57)	13.8(1.41)
	C57BL/6	2.6(2.32)	2.0(1.34)	2.1(1.63)	3.6(1.68)	3.8(1.69)	6.4(1.21)	9.1(1.15)	3.6(1.56)	8.5(1.19)

[a] Cytokine/chemokines were reported as geometric means with the geometric standard error of the means.

[b] N was equal to 5 for each mouse strain at each time point after infection (PI).

[c] For geometric means for the naïve mice, n was equal to 10 for BALB/c mice, and n was equal to 4 for C57BL/6 mice.

[d] For significant levels compared to the naïve, control mice: †P<0.05; ¶P<0.01; §P≤0.001.

Table S3. Cytokines/chemokines in spleen extracts from BALB/c and C57BL/6 mice after IP challenge with *B. pseudomallei* K96243.

			Amount Cytokine/Chemokine Expressed (pg/ml)[a]							
			Time (Days PI)							
Cytokine/ Chemokine	Mouse Strain[b]	Naïve[c], Control	0[d]	2	4	7	15	22	28	59
IFN-γ	BALB/c	20.8(1.08)	23.0(1.14)	171.4(1.16)§	24.0(1.11)	27.9(1.06)†	65.6((1.48)†	45.7(1.39)	24.3(1.50)	26.7(1.26)
	C57BL/6	16.5(1.03)	100.3(1.35)¶	79.8(1.11)§	19.6(1.33)	38.6(1.24)†	30.2(1.07)§	37.1(1.25)†	15.7(1.02)	19.7(1.230
TNF-α	BALB/c	12.6(1.17)	16.3(1.05)	33.2(1.06)§	17.1(1.05)	16.9(1.08)	36.5(1.12)§	42(1.55)†	3.2(2.58)	43.1(1.01)§
	C57BL/6	23.3(23.3)	30.3(1.19)	24.1(1.10)	11.7(1.07)	21.0(1.14)	28.4(1.06)†	36.9(1.41)	3.6(1.62)	43.2(1.01)§
IL-1α	BALB/c	75.8(1.10)	356.8(1.09)§	1220(1.14)§	559.2(1.09)§	568.1(1.19)§	1029(1.27)§	418.8(1.27)§	325.8(1.15)§	148.5(1.12)†
	C57BL/6	45.9(1.19)	1237(1.25)§	934.2(1.10)§	281(1.13)§	547.4(1.17)§	632.4(1.25)§	677.8(1.28)§	371.9(1.34)§	159.0(1.17)†
IL-1β	BALB/c	38.9(1.23)	256.8(1.06)§	407.5(1.07)§	252.1(1.14)§	417(1.33)§	1898(1.80)¶	1030(1.79)¶	502.5(1.69)¶	102.8(1.45)
	C57BL/6	21.1(1.10)	672.7(1.10)§	162(1.10)§	101.3(1.28)¶	330.7(1.28)§	437.2(1.40)§	846.5(1.67)¶	287.4(1.51)¶	87.5(1.41)†
IL-2	BALB/c	7.3(1.15)	4.6(1.04)	7.3(1.02)	4.8(1.03)	5.3(1.05)	14.8(1.03)¶	12.7(1.24)	4.3(1.26)	29.1(1.09)§
	C57BL/6	3.3(1.08)	6.9(1.08)§	6.6(1.05)§	4.3(1.04)†	7.6(1.08)§	14.0(1.02)§	13.7(1.20)§	5.5(1.28)	33.0(1.07)§
IL-5	BALB/c	24.7(1.10)	19.6(1.06)	42.3(1.14)†	10.8(1.11)	14.0(1.45)	40.1(1.12)†	24.5(1.30)	14.2(1.38)	14.4(1.43)
	C57BL/6	20.1(1.04)	81.7(1.23)¶	45.3(1.22)†	4.8(1.43)	34.7(1.24)	35.2(1.11)¶	34.0(1.23)	19.2(1.04)	5.7(1.33)
IL-6	BALB/c	22.4(1.10)	23.1(1.09)	48.1(1.08)§	27.3(1.07)	22.5(1.22)	43.6(1.10)§	33.8(1.20)	11.3(2.22)	16.5(1.02)
	C57BL/6	29.5(1.01)	60.6(1.35)	35.3(1.09)	9.7(1.75)	57.5(1.24)§	32.4(1.08)	41.8(1.22)	8.2(2.16)	15.8(1.04)
IL-10	BALB/c	26.2(1.07)	31.9(1.37)	35.2(1.07)†	43.4(1.01)§	23.4(1.48)	62.2(1.10)§	121.7(1.16)§	30.1(1.44)	235.0(1.28)§
	C57BL/6	35.6(1.14)	41.1(1.21)	15.5(1.74)	44.0(1.01)	63.9(2.41)	20.7(1.28)	146.0(1.16)§	43.8(0.204)	183.3(1.18)§
IL-12	BALB/c	19.1(1.23)	63.8(1.03)§	95.1(1.09)§	70.5(1.04)§	93.7(1.10)§	44.3(1.07)¶	65.1(1.23)¶	37.0(1.13)†	61.3(1.15)§
	C57BL/6	28.5(1.19)	111.2(1.26)¶	76.6(1.14)¶	39.4(1.23)	97.2(1.13)¶	89.6(1.12)¶	111.0(1.07)¶	74.9(1.05)¶	77.0(1.07)¶
FGFb	BALB/c	489.4(1.21)	2908(1.13)§	2175(1.02)§	2484(1.07)§	1491(1.05)§	4466(1.06)§	5571(1.25)§	4298(1.28)§	1523(1.15)§
	C57BL/6	313.8(1.02)	2074(1.05)§	1860(1.11)§	1592(1.07)§	1646(1.10)§	2475(1.23)§	4335(1.33)§	2811(1.16)§	949.2(1.09)§
IP10	BALB/c	19.5(1.05)	103.8(1.08)§	373.3(1.18)§	86.6(1.12)§	86.2(1.09)§	61.4(1.11)§	69.7(1.11)§	26.4(1.53)	94.9(1.52)†
	C57BL/6	24.8(1.33)	1221(1.25)§	394.4(1.23)§	82.6(1.21)†	220.1(1.21)¶	70.6(1.15)†	107.3(1.04)†	52.9(1.16)	127.2(1.11)¶
KC	BALB/c	350.8(1.04)	1237(1.21)¶	713.8(1.04)§	535.4(1.07)§	598.9(1.20)†	619.6(1.23)†	666.8(1.23)†	349.5(1.22)	1331(1.14)§
	C57BL/6	206.5(1.07)	3320(1.12)§	622.1(1.08)§	442.4(1.10)§	266.7(1.40)	529.5(1.25)†	533.7(1.08)§	331.9(1.16)†	1216(1.15)§
MCP-1	BALB/c	18.2(1.12)	41.2(1.15)¶	68.5(1.18)§	16.1(1.16)	17.5(1.39)	34.0(1.11)¶	27.0(1.31)	20.6(1.01)	33.4(1.37)
	C57BL/6	13.3(1.08)	182.1(1.20)§	80.7(1.26)§	21.1(1.02)¶	30.7(1.37)	31.0(1.11)§	30.6(1.29)†	21.2(1.01)¶	18.1(1.36)
MIG	BALB/c	142.1(1.09)	1122(1.10)§	7612((1.14)§	2203(1.14)§	2713(1.07)§	1996(1.42)¶	1567(1.29)§	1184(1.58)¶	687.7(1.09)§
	C57BL/6	216(1.41)	3653(1.21)§	5032(1.12)¶	1223(1.25)¶	4024(1.33)§	984.8(1.08)†	1935(1.40)¶	1071(1.26)¶	634.9(1.14)†
MIP-1α	BALB/c	59.3(1.12)	108.9(1.06)§	289.2(1.07)§	164.21.06)§	140.3(1.10)§	129.2(1.08)§	93.2(1.18)	29.2(1.21)	145.1(1.14)§
	C57BL/6	26.4(1.23)	382.4(1.25)§	255.3(1.07)§	80.2(1.09)¶	177.9(1.09)¶	136.5(1.08)¶	128.3(1.12)¶	26.4(1.35)	129.8(1.12)¶
VEGF	BALB/c	13.5(1.05)	58.8(1.06)§	67.5(1.04)§	33.9(1.10)§	35.3(1.37)†	495.3(2.10)¶	363.5(3.03)†	40.2(2.58)	34.9(1.23)¶
	C57BL/6	4.6(1.07)	34(1.27)§	33.2(1.10)§	20.4(1.59)†	26.3(1.33)¶	118.5(1.61)¶	140.1(1.94)¶	54.2(1.93)†	20.1(1.47)†

[a] Cytokine/chemokines were reported as geometric means with the geometric standard error of the means.

[b] N was equal to 5 for each mouse strain at each time point after infection (PI).

[c] For geometric means for the naïve mice, n was equal to 10 for BALB/c mice, and n was equal to 4 for C57BL/6 mice.

[d] For significant levels compared to the naïve, control mice: †P<0.05; ¶P<0.01; §P≤0.001.

Table S4. Cell distribution of spleens from aerosol infected BALB/c or C57BL/6 mice with *B. pseudomallei* K96243.

		% Cell Distribution[a]								
			Time (Days PI)							
Cell Type	Mouse Strain[b]	Naïve Control[c]	0[d]	2	4	7	15	22	28	59
CD4+ T Cells	BALB/c	23.6 (0.60)	32.4(0.56)§	29.3(1.63)†	24.9(2.02)	24.1(1.30)	15.8(2.21)	19.9(1.28)	---	---
	C57BL/6	16.1(0.64)	26.4(1.39)§	18.1(1.44)	17.7(0.63)	20.5(1.39)†	19.8(1.10)†	22.2(0.98)¶	21.9(0.64)§	18.5(0.88)
CD8+ T Cells	BALB/c	10.0(0.38)	16.8(0.27)§	16.6(0.97)¶	16.1(1.43)†	11.7(0.66)	6.90(0.97)	8.0(0.40)	---	---
	C57BL/6	10.8(0.35)	14.5(0.68)¶	11.9(0.42)	11.1(0.45)	11.9(0.78)	10.5(0.75)	11.5(0.69)	11.3(0.40)	13.2(0.36)¶
B Cells	BALB/c	51.1(2.03)	47.4(0.67)	46.7(2.07)	48.3(3.39)	47.4(3.08)	36.0(2.89)	51.2(1.74)	---	---
	C57BL/6	65.1(0.55)	56.0(1.86)	63.2(1.88)	59.9(1.97)	50.6(1.32)	48.2(4.56)	58.9(0.75)	64.2(0.76)	60.4(0.57)
Monocytes/Macrophages	BALB/c	4.60(0.53)	10.3(0.45)§	8.40(0.40)§	13.3(1.25)§	12.1(0.83)§	33.3(5.95)§	21.8(3.09)¶	---	---
	C57BL/6	2.80(0.30)	8.80(0.27)§	6.50(1.22)†	9.10(0.62)§	12.8(2.11)¶	16.2(3.92)†	4.50(0.71)	6.10(0.63)¶	3.30(0.45)
NK Cells	BALB/c	4.60(0.58)	6.90(0.52)†	8.00(0.59)¶	11.5(1.37)¶	11.2(0.61)§	29.7(1.37)§	8.10(0.92)†	---	---
	C57BL/6	2.30(0.23)	7.70(0.51)§	6.50(1.12)†	8.80(0.60)§	12.6(0.85)§	25.5(1.62)§	5.30(0.55)¶	12.0(0.58)§	7.70(0.74)¶
Granulocytes	BALB/c	1.00(0.16)	1.10(0.10)	4.00(0.27)§	0.80(0.06)	5.70(1.12)†	25.8(5.21)¶	15.7(2.58)¶	---	---
	C57BL/6	0.60(0.09)	0.80(0.12)	1.70(0.30)†	0.30(0.04)	5.00(1.61)	10.0(2.91)†	2.00(0.34)†	1.70(0.52)	1.60(0.23)†

[a] % Cell distribution is reported as geometric means with the geometric standard error of the means.

[b] N was equal to 5 for each mouse strain at each time point after infection (PI). Dash lines (---) represents no data because mice had expired.

[c] For geometric means for the naïve mice, n was equal to 10 for BALB/c mice, and n was equal to 4 for C57BL/6 mice.

[d] For significant levels compared to the naïve, control mice: †$P < 0.05$; ¶ $P < 0.01$; §$P \leq 0.001$.

Table S5. Cytokines/chemokines in serum from BALB/c and C57BL/6 mice after aerosol challenge with B. pseudomallei K96243.

		Amount Cytokine/Chemokine Expressed (pg/ml)[a]									
			Time (Days PI)								
Cytokine/ Chemokine	Mouse Strain[b]	Naïve[c], Control	0[d]	2	4	7	15	22	28	59	90
IFN-γ	BALB/c	21.2(1.13)	16.0(1.02)	371(1.50)¶	156.4(1.67)†	155.5(1.70)†	51.5(1.94)	61.0(1.57)	---	---	---
	C57BL/6	10.9(1.47)	68.6(1.06)†	143(1.25)¶	36.2(1.47)	18.2(1.14)	11.6(2.01)	36.8(1.15)†	23.3(1.31)	30.5(1.38)	31.8(1.38)
TNF-α	BALB/c	23.4(1.03)	14.7(1.01)	29.3(1.54)	22.2(1.29)	45.2(1.49)	56.5(1.73)	19.0(1.15)	---	---	---
	C57BL/6	23.4(1.06)	15.4(1.09)	16.6(1.05)	15.2(1.08)	13.2(1.01)	13.3(1.01)	13.8(1.03)	13.8(1.09)	17.1(1.12)	15.9(1.04)
IL-1α	BALB/c	25.3(1.03)	26.6(1.02)	18.51.41)	23.7(1.97)	94.7(2.00)	98.5(2.90)	8.1(1.76)	---	---	---
	C57BL/6	30.7(1.18)	22.1(1.77)	17.0(1.39)	37.5(1.51)	11.7(1.46)	6.1(1.60)	23.7(1.23)	21.72.24)	32.1(1.86)	11.1(1.70)
IL-1β	BALB/c	21.6(1.02)	8.0(1.42)	169.1(1.59)†	122.5(1.82)†	74(2.10)	123.6(1.83)†	80.1(1.50)†	---	---	---
	C57BL/6	21.2(1.05)	13.7(1.13)	60.9(1.37)†	14.1(1.46)	16.8(1.31)	17.5(1.21)	24.3(1.15)	14.2(1.18)	9.1(1.60)	15.1(1.41)
IL-2	BALB/c	6.5(1.04)	2.3(1.37)	8.3(1.56)	4.9(1.68)	3.6(1.35)	20.1(1.47)†	15.5(1.16)¶	---	---	---
	C57BL/6	4.0(1.04)	6.1(1.18)	6.7(1.12)¶	3.7(1.40)	1.9(1.05)	9.9(1.11)§	11.4(1.11)§	12.5(1.08)§	12.2(1.02)§	13.3(1.11)§
IL-4	BALB/c	43.1(1.03)	29.0(1.33)	21.0(1.26)	18.8(2.30)	19.3(1.37)	46.4(1.04)	44.7(1.04)	---	---	---
	C57BL/6	33.0(1.43)	134.3(1.14)†	88.9(1.37)	60.6(1.21)	16.0(1.67)	33.5(1.33)	71.2(1.16)	52.1(1.12)	34.5(1.82)	46.0(2.28)
IL-6	BALB/c	24.6(1.05)	20.2(1.12)	124.0(1.16)§	209.6(2.09)	253.8(2.43)	201.0(3.06)	46.9(1.29)	---	---	---
	C57BL/6	30.0(1.06)	26.1(1.14)	36.2(1.23)	27.1(1.37)	13.3(1.24)	18.6(1.23)	19.2(1.10)	17.9(1.06)	22.7(1.21)	31.1(1.51)
IL-10	BALB/c	51.1(1.16)	23.4(1.61)	57(1.35)	12.6(2.06)	36.5(1.57)	45.7(1.03)	71.7(1.63)	---	---	---
	C57BL/6	43.6(1.01)	85.4(1.13)¶	106.2(1.17)¶	73.1(1.22)	75.8(1.14)†	60.0(1.19)	42.1(1.25)	42.3(1.29)	68(1.21)	36.3(1.25)
IL-12	BALB/c	49.1(1.29)	71.3(1.13)	51(1.25)	64.8(1.18)	19.4(1.68)	19.4(1.68)	83.6(1.18)	---	---	---
	C57BL/6	44.6(1.24)	69.6(1.15)	85(1.26)	57.3(1.95)	31.5(1.26)	76.2(1.26)	87.1(1.23)	109.5(1.23)†	53.8(1.14)	43.2(1.40)
FGFb	BALB/c	216.8(1.12)	249.4(1.26)	225.8(1.43)	114.7(1.73)	75.2(1.57)	124.2(1.40)	200.8(1.29)	---	---	---
	C57BL/6	262.4(1.19)	507.2(1.03)†	452.8(1.06)†	250.21.43)	33.3(1.25)	276.61.23)	403.4(1.03)	374(1.05)	406.1(1.08)	343.7(1.11)
IP10	BALB/c	23.4(1.21)	42.9(1.70)	209.8(1.47)¶	243.3(1.88)†	165.9(1.75)†	73.1(1.81)	84.0(1.76)	---	---	---
	C57BL/6	25.1(1.32)	6.1(1.37)	94.0(1.34)†	17.8(1.12)	17.7(1.04)	20.3(1.05)	24.6(1.30)	19.2(1.03)	2.7(3.70)	25.6(1.50)
KC	BALB/c	260.7(1.40)	155.7(2.36)	1501(1.29)¶	1706(1.35)¶	1610(1.72)†	236.3(3.19)	532.8(2.14)	---	---	---
	C57BL/6	73.0(1.06)	96.7(1.18)	188.9(1.55)	282.4(1.58)†	38.6(1.49)	102.7(1.49)	67.9(1.03)	72.6(1.05)	114.0(1.52)	77.5(2.09)
MCP-1	BALB/c	21.5(1.04)	13.3(1.05)	67.0(1.37)†	61.8(1.96)	107.5(1.70)†	53.5(1.35)†	34.9(1.15)†	---	---	---
	C57BL/6	20.6(1.03)	21.1(1.35)	44.6(1.19)†	29.1(1.18)	18.4(1.13)	21.9(1.12)	23.0(1.18)	28.0(1.22)	29.9(1.24)	26.2(1.14)
MIG	BALB/c	184.4(1.16)	291.8(1.21)	1854(1.13)§	1866(1.07)§	934.9(1.31)¶	1027(1.76)†	1405(1.54)¶	---	---	---
	C57BL/6	9.1(1.14)	133.6(1.22)¶	2149(1.02)§	440.8(1.38)	88.4(1.51)¶	147.4(1.28)§	342.5(1.19)§	81.8(1.22)¶	114.5(1.35)§	186.8(1.19)§
MIP-1α	BALB/c	39.6(1.03)	21.9(1.06)	29.6(1.07)	32.1(1.15)	95.1(1.37)†	99.7(1.79)	25.4(1.24)	---	---	---
	C57BL/6	18.3(1.55)	26.6(1.03)	26.5(1.07)	31.6(1.08)	24.6(1.05)	10.5(2.27)	5.7(1.44)	14.3(1.37)	42.5(1.02)	51.8(1.05)
VEGF	BALB/c	12.3(1.31)	23.7(1.41)	6.8(1.72)	6.6(1.87)	6.7(1.22)	14.7(1.80)	15.6(1.65)	---	---	---
	C57BL/6	2.6(2.32)	4.8(1.15)	5.1(1.24)	3.0(1.49)	5.8(1.05)	3.8(1.41)	2.3(1.45)	6.0(1.05)	6.4(1.03)	6.3(1.02)

[a] Cytokine/chemokines were reported as geometric means with the geometric standard error of the means.

[b] N was equal to 5 for each mouse strain at each time point post-infection (PI). Dashes (---) represent no data because no mice were left at that time.

[c] For geometric means for the naïve mice, n was equal to 10 for BALB/c mice, and n was equal to 4 for C57BL/6 mice.

[d] For significant levels compared to the naïve, control mice: †P<0.05; ¶P<0.01; §P£0.001.

Table S6. Cytokines/chemokines in spleen extracts from BALB/c and C57BL/6 mice after aerosol challenge with *B. pseudomallei* K96243.

		Amount Cytokine/Chemokine Expressed (pg/ml)[a]									
				Time (Days PI)							
Cytokine/ Chemokine	Mouse Strain[b]	Naïve[c], Control	0[d]	2	4	7	15	22	28	59	90
IFN-γ	BALB/c	20.2(1.09)	10.4(1.14)	207.1(1.62)¶	25.6(1.40)	177(1.78)†	266.1(1.38)¶	280.4(1.34)§	---	---	---
	C57BL/6	15.2(1.04)	10.7(1.10)	98.5(1.62)†	14.4(1.12)	19.6(1.43)	154.2(1.32)§	154.3(1.19)§	163.1(1.07)§	15.1(1.02)	17.4(1.09)
TNF-α	BALB/c	12.6(1.17)	20.1(1.03)†	25.1(1.10)¶	20.5(1.03)†	28.1(1.07)§	125.9(1.96)†	63.3(1.55)†	---	---	---
	C57BL/6	23.3(23.3)	19.9(1.03)	25.5(1.06)	26.3(1.12)	20.8(1.05)	46.5(1.24)†	23.1(1.06)	15.2(1.36)	24.9(1.03)	23.3(1.05)
IL-1α	BALB/c	75.8(1.10)	170(1.11)§	651.9(1.32)¶	304.9(1.22)¶	1643(1.45)§	1963(3.28)	750.8(1.88)†	---	---	---
	C57BL/6	45.9(1.19)	139.2(1.11)¶	339.6(1.19)§	303.2(1.32)¶	225.4(1.06)¶	271.1(1.42)¶	24.4(1.06)	90.4(1.51)	252.4(1.08)§	230.4(1.45)¶
IL-1β	BALB/c	38.9(1.23)	97.6(1.10)¶	303.2(1.35)§	207.2(1.30)§	798.9(1.26)§	1296(1.45)§	982.3(1.45)§	---	---	---
	C57BL/6	21.1(1.10)	51.1(1.11)§	138.6(1.27)§	190.1(1.62)¶	180.6(1.22)§	241.5(1.85)†	182.7(1.26)§	220.9(1.14)§	164(1.10)§	197.4(1.40)¶
IL-2	BALB/c	7.30(1.15)	8.90(1.02)	11.4(1.07)†	9.90(1.06)	12.1(1.06)¶	71(1.05)§	67.1(1.05)§	---	---	---
	C57BL/6	3.30(1.08)	9.20(1.02)§	11.2(1.05)§	10.1(1.08)§	9.91.03)§	73.5(1.07)§	58.3(1.03)§	59.2(1.03)§	14.4(1.08)§	14.4(1.06)§
IL-4	BALB/c	24.7(1.10)	10.5(1.29)	23.2(1.16)	10.3(1.43)	27.6(1.41)	412.0(1.43)¶	458.2(1.11)§	---	---	---
	C57BL/6	20.1(1.04)	32.0(1.10)†	28.2(1.26)	9.70(1.39)	17.6(1.26)	673.5(1.11)§	497.6(1.09)§	522.2(1.07)§	21.8(1.14)¶	24.1(1.45)
IL-6	BALB/c	22.4(1.10)	33.0(1.02)¶	45.7(1.11)§	32.5(1.01)¶	63.5(1.19)¶	114.5(2.09)	101.6(1.43)†	---	---	---
	C57BL/6	29.5(1.01)	31.7(1.04)	38.6(1.08)†	36.4(1.16)	32.6(1.03)†	61.5(1.35)	60.2(1.26)†	23.8(1.44)	31.3(1.28)	24.8(1.21)
IL-10	BALB/c	26.2(1.07)	75.1(1.35)†	116.7(1.22)§	86.7(1.21)¶	145.0(1.11)§	268.2(1.26)¶	126.2(1.23)§	---	---	---
	C57BL/6	35.6(1.14)	85.3(1.21)¶	109.4(1.23)¶	117.7(1.17)§	134.7(1.19)§	234.2(1.27)§	83.6(1.26)†	116.4(1.30)¶	122.4(1.06)§	99.2(1.07)¶
IL-12	BALB/c	19.1(1.23)	25.2(1.23)	23.7(1.29)	26.9(1.45)	14.3(1.99)	283.0(1.26)§	359.0(1.08)§	---	---	---
	C57BL/6	28.5(1.19)	29.1(1.21	54.0(1.20)†	56.2(1.45)	42.8(1.36)	290.1(1.24)§	166.0(1.20)§	242.4(1.09)§	77.8(1.10)¶	51.4(1.15)†
FGFb	BALB/c	489.4(1.21)	3456(1.06)§	1613(1.12)§	1964(1.34)¶	2363(1.28)§	1719(1.17)§	1254(1.25)†	---	---	---
	C57BL/6	313.8(1.02)	2431(1.17)§	2152(1.06)§	3841(1.22)§	3086(1.19)§	739(1.39)	272.0(1.10)	503.8(1.28)	2967(1.06)§	1629(1.15)§
IP10	BALB/c	19.5(1.05)	41.4(1.07)§	281.1(1.43)¶	86.3(1.10)§	177.0(1.24)§	67.9(2.12)	45.8(1.77)	---	---	---
	C57BL/6	24.8(1.33)	62.5(1.13)†	377.2(1.39)§	154.5(1.26)¶	120.1(1.23)¶	20.8(1.06)	18.4(1.03)	19.4(1.04)	45.6(1.06)	34.2(1.16)
KC	BALB/c	350.8(1.04)	243.8(1.11)	372.3(1.10)	303.3(1.05)	573.6(1.25)	1629(1.46)†	970.6(1.45)	---	---	---
	C57BL/6	206.5(1.07)	243.1(1.04)	260.5(1.09)	357.6(1.13)¶	351.4(1.14)†	707.6(1.12)§	174.5(1.32)	256.9(1.30)	230.0(1.17)	277.1(1.18)
MCP-1	BALB/c	18.2(1.12)	14.7(1.04)	25.9(1.18)	16.31.02)	30.8(1.20)†	76.4(1.47)†	51.5(1.63)	---	---	---
	C57BL/6	13.3(1.08)	15.0(1.04)	23.6(1.15)†	22.9(1.18)†	23.1(1.14)¶	28.5(1.08)§	21.5(1.04)¶	20.2(1.02)¶	8.0(1.10)	11.6(1.34)
MIG	BALB/c	142.1(1.09)	871.1(1.17)§	3494(1.36)§	1813(1.19)§	4313(1.16)§	3197(1.25)§	1905(1.50)¶	---	---	---
	C57BL/6	216(1.41)	865.5(1.16)†	3799(1.21)§	1401(1.43)¶	1900(1.26)¶	1189(1.19)¶	299.9(1.31)	421.2(1.30)	1173(1.0)†	789.6(1.24)†
MIP-1α	BALB/c	59.3(1.12)	46.9(1.05)	89.4(1.17)	80.6(1.23)	160.2(1.41)†	688.2(2.46)	288.7(1.46)†	---	---	---
	C57BL/6	26.4(1.23)	43.6(1.05)	68.5(1.10)†	75.6(1.24)†	53.7(1.06)†	161.0(1.14)§	88.2(1.10)¶	108.0(1.10)¶	86.4(1.18)¶	89.1(1.11)¶
VEGF	BALB/c	13.5(1.05)	12.4(1.09)	47.8(1.18)§	37.5(1.25)¶	33.4(1.23)†	293.4(1.98)†	111.4(1.52)¶	---	---	---
	C57BL/6	4.6(1.07)	7.60(1.13)†	32.1(1.21)§	24.4(1.30)¶	50.7(1.45)¶	66.2(1.60)¶	2.70(1.64)	9.70(1.49)	12.7(1.38)†	35.3(2.22)

[a] Cytokine/chemokines were reported as geometric means with the geometric standard error of the means.

[b] N was equal to 5 for each mouse strain at each time point post-infection (PI). Dashes (---) represent no data because no mice were left at that time.

[c] For geometric means for the naïve mice, n was equal to 10 for BALB/c mice, and n was equal to 4 for C57BL/6 mice.

[d] For significant levels compared to the naïve, control mice: †P<0.05; ¶P<0.01; §P£0.001.